Robust and Distributed Model Predictive Control with Application to Cooperative Marine Vehicles

by

Henglai Wei
B.Sc., Northwestern Ploytechnical University, 2014
M.Sc., Northwestern Ploytechnical University, 2017

A Dissertation Submitted in Partial Fulfillment of the
Requirements for the Degree of

DOCTOR OF PHILOSOPHY

in the Department of Mechanical Engineering

Robust and Distributed Model Predictive Control with Application to Cooperative Marine Vehicles

by

Henglai Wei
B.Sc., Northwestern Ploytechnical University, 2014
M.Sc., Northwestern Ploytechnical University, 2017

Supervisory Committee

Dr. Yang Shi, Supervisor
(Department of Mechanical Engineering)

Dr. Daniela Constantinescu, Departmental Member
(Department of Mechanical Engineering)

Dr. Pan Agathoklis, Outside Member
(Department of Electrical and Computer Engineering)

ABSTRACT

Distributed coordination of multi-agent systems (MASs) has been widely studied in various emerging engineering applications, including connected vehicles, wireless networks, smart grids, and cyber-physical systems. In these contexts, agents make the decision locally, relying on the interaction with their immediate neighbors over the connected communication networks. The study of distributed coordination for the multi-agent system (MAS) with constraints is significant yet challenging, especially in terms of ubiquitous uncertainties, the heavy communication burden, and communication delays, to name a few. Hence, it is desirable to develop distributed algorithms for the constrained MAS with these practical issues. In this dissertation, we develop the theoretical results on robust distributed model predictive control (DMPC) algorithms for two types of control problems (i.e., formation stabilization problem and consensus problem) of the constrained and uncertain MAS and apply robust DMPC algorithms in applications of cooperative marine vehicles.

More precisely, **Chapter 1** provides a systematic literature review, where the state-of-the-art DMPC for formation stabilization and consensus, robust MPC, and MPC for motion control of marine vehicles are introduced. **Chapter 2** introduces some notations, necessary definitions, and some preliminaries. In **Chapter 3**, we study the formation stabilization problem of the nonlinear constrained MAS with uncertainties and bounded time-varying communication delays. We develop a min-max DMPC algorithm with the self-triggered mechanism, which significantly reduces the communication burden while ensuring closed-loop stability and robustness. **Chapter 4** investigates the consensus problem of the general linear MAS with input constraints and bounded time-varying delays. We design a robust DMPC-based consensus protocol that integrates a predesigned consensus protocol with online DMPC optimization techniques. Under mild technical assumptions, the estimation errors propagated over prediction due to delay-induced inaccurate neighboring information are proved bounded, based on which a robust DMPC strategy is deliberately designed to achieve robust consensus while satisfying control input constraints. **Chapter 5** proposes a Lyapunov-based DMPC approach for the formation tracking control problem of cooperative autonomous underwater vehicles (AUVs) subject to environmental disturbances. A stability constraint leveraging the extended state observer-based auxiliary control law and the associated Lyapunov function is incorporated into the optimization problem to enforce the stability and enhance formation tracking performance. A

collision-avoidance cost is designed and employed in the DMPC optimization problem to further guarantee the safety of AUVs. **Chapter 6** presents a tube-based DMPC approach for the platoon control problem of a group of heterogeneous autonomous surface vehicles (ASVs) with input constraints and disturbances. In particular, a coupled inter-vehicle safety constraint is added to the DMPC optimization problem; it ensures that neighboring ASVs maintain the safe distance and avoid inter-vehicle collision. Finally, we summarize the main results of this dissertation and discuss some potential directions for future research in **Chapter 7**.

Contents

List of Tables

List of Figures

Preface

The materials presented in this dissertation are part of the research project under the supervision of Dr. Yang Shi, funded by the Natural Science and Engineering Research Council (NSERC). Research reported in this dissertation is also supported by the financial support from the China Scholarship Council (CSC).

Chapter 3 of this dissertation is a revised version of Henglai Wei, Kunwu Zhang and Yang Shi. Self-triggered min-max DMPC for asynchronous multi-agent systems with communication delays. IEEE Transactions on Industrial Informatics, doi: 10.1109/TII.2021.3127197.

Chapter 4 of this dissertation is a revised version of Henglai Wei, Changxin Liu and Yang Shi, A robust distributed model predictive control framework for consensus of multi-agent systems with varying delays and input constraints, which is currently under review.

Chapter 5 of this dissertation is a revised version of Henglai Wei, Chao Shen and Yang Shi. Distributed Lyapunov-based model predictive formation tracking control for autonomous underwater vehicles subject to disturbances. IEEE Transactions on Systems, Man, and Cybernetics: Systems, 51(8), pp. 5198-5208, 2021.

Chapter 6 of this dissertation is a revised version of Henglai Wei, Qi Sun, Jicheng Chen and Yang Shi. Robust distributed model predictive platooning control for heterogeneous autonomous surface vehicles. Control Engineering Practice, 107, p. 104655, 2021.

ACKNOWLEDGEMENTS

First, I would like to express my deepest gratitude to my supervisor Prof. Yang Shi for providing me with the opportunity to study and work at Applied Control and Information Processing Laboratory (ACIPL). During my PhD, his rigorous and enthusiastic academic attitude has greatly influenced me. He opened the window of the academic world and showed me the beauty of research. Moreover, he always encouraged and supported me to continue on my way, even in the most frustrating situation. I am honored to be his student, and thank him for guiding me at UVic.

Thanks to my committee members, Prof. Daniela Constantinescu and Prof. Pan Agathoklis, for their valuable suggestions and insightful comments on improving the dissertation. I also would like to thank the external examiner, Prof. Youmin Zhang, for evaluating this dissertation and providing constructive comments.

I want to thank Prof. Chao Shen, Dr. Jicheng Chen, Dr. Changxin Liu, Dr. Kunwu Zhang, and Dr. Qi Sun for the inspiring discussions and selfless help. And I look forward to continuing these collaborations in the future.

I want to thank the ACIPL members: Prof. Yuanye Chen, Prof. Bingxian Mu, Qian Zhang, Tianyu Tan, Xinxin Shang, Dr. Songlin Zhuang, Yaning Guo, Chen Ma, Zhuo Li, Zhang Zhang, Chonghan Ma, Tianxiang Lu, Binyan Xu, Yufan Dai, and Yue Song. Thanks for the reading club, the group meeting, the coffee breaks, the lake BBQ, and the journey we have traveled together. Without you guys, my time at ACIPL would have been by far less happy and productive.

Finally, my special thanks go to my family, friends my country for their support. I want to thank VC runners for the happy time we ran together. I want to thank my parents and my wife for their love and unconditional support throughout this adventure. I want to thank my brother and sister for their understanding and dedication. And thanks to my niece and nephew for bringing joyful moments to us.

Victoria, BC, Canada
April, 2022

To my beloved parents and wenjing

Acronyms

MAS	multi-agent system
AMV	autonomous marine vehicle
AUV	autonomous underwater vehicle
ASV	autonomous surface vehicle
ISS	input-to-state stable
ISpS	input-to-state practically stable
ESO	extended state observer
LQR	linear quadratic regulator
MPC	model predictive control
DMPC	distributed model predictive control
RMPC	robust model predictive control
LMPC	Lyapunov-based model predictive control
DLMPC	distributed Lyapunov-based model predictive control

Chapter 1

Introduction

1.1 Distributed Coordination of Multi-Agent Systems

1.1.1 Overview

Multi-agent systems (MASs) have received considerable attention in the past two decades, mainly because they play essential roles in broad industrial applications, including connected vehicles, sensor networks, smart grids, and cyber-physical systems. Generally speaking, a multi-agent system (MAS) consists of a team of agents/subsystems, where agents work together to achieve a common objective. In this context, effective coordinated control algorithms are critical for the MAS; the existing algorithms can be classified into two categories, namely, centralized and distributed coordination, as shown in Figure 1.1. In centralized coordination, a central controller collects the information of all agents and computes control inputs of all agents, which has been extensively studied for the MAS [38,144], see Figure 1.1a. These approaches typically have high communication and computational requirements, which are unsuitable for the practical MAS in the real world. In distributed coordination, on the other hand, each agent calculates its control inputs based on the information locally available and the information from its neighbors, where the centralized controller is removed, as demonstrated in Figure 1.1b. In particular, the distributed coordination control problem becomes challenging when the MAS is subject to constraints. However, many large-scale complex systems, such as transportation systems, smart grids, constrained processes systems, wireless sensor networks, and multi-robot sys-

tems, raise computational and communication issues. For such systems, distributed model predictive control (DMPC) is one of the appealing control methods owing to its computational efficiency, superior control performance, and the ability to deal with explicit constraints systematically [119]. Some comprehensive survey papers on DMPC for MASs and their applications have been reported; see [9, 97, 104, 125] and references therein. We provide an overview of DMPC concerning different control tasks as follows.

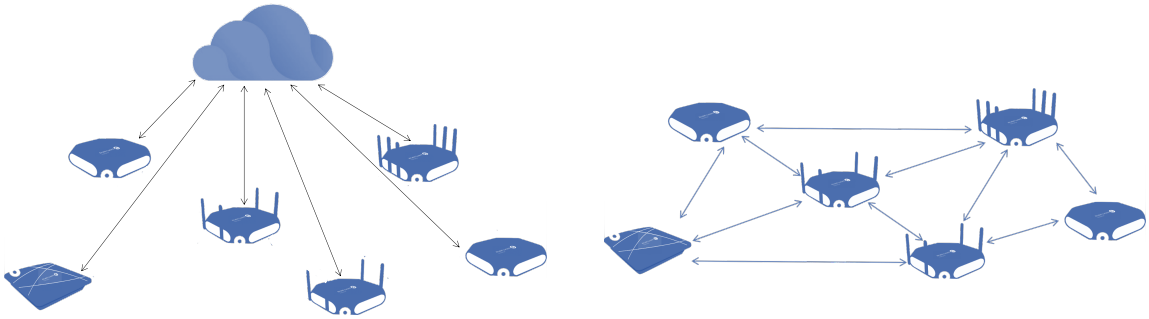

(a) Centralized coordination (b) Distributed coordination

Figure 1.1: Illustration of centralized and distributed coordination for MASs.

1.1.2 DMPC for stabilization of the MAS

The MAS's stabilization (also referred to as formation stabilization) problem is a control problem in which agents are cooperatively controlled to a desired constant setpoint. An extensive literature on DMPC algorithms for solving this problem has emerged in the past twenty years. Loosely speaking, a classification of existing DMPC algorithms can be made according to the coupling source, namely DMPC with coupled cost, coupled constraints, and coupled dynamics.

1.1.2.1 DMPC with coupled cost

In this class, the cooperation component among agents is introduced in an optimization problem via the coupled cost function (1.1), as explored in [19], where each agent optimizes a locally coupled objective function $V_i(x_i, x_j, u_i)$

$$V_i(x_i, x_j, u_i) = \sum_{j \in \mathcal{N}_i} \ell_i(x_i, x_j, u_i) + V_i^f(x_i), \tag{1.1}$$

where x_j denotes the neighboring state information of agent j, $j \in \mathcal{N}_i$, u_i denotes the control input, $\ell_i(x_i, x_j, u_i)$ is the coupled stage cost function and $V_i^f(x_i)$ is the local terminal cost function, with $\mathcal{N}_i$ being the neighbor set of agent i.

Results from the cost-coupled DMPC have been employed to stabilize the constrained MAS. For example, the DMPC approach has been developed for the continuous-time nonlinear MAS [19], where a compatibility constraint is designed to bound the deviation between the actual and assumed states. Consequently, the original optimization problem is decomposed into a set of smaller size optimization problems, and the assumed neighboring state sequence is utilized for solving these optimization problems in parallel. In [123], a similar control problem of dynamically decoupled linear dynamics is formulated. The authors in [102, 153, 182] employ the DMPC framework for the discrete-time nonlinear MAS with dynamically decoupled dynamics and the shared control objective. In addition, DMPC algorithms have been extended to address some practical issues, e.g., the communication delays [26,62], uncertainties [64, 152], and heavy communication load [100, 163]. Particularly, DMPC algorithms find numerous applications of MASs such as connected vehicles [89, 182], cooperative marine vehicles [160], and interconnected microgrids [34].

1.1.2.2 DMPC with coupled constraints

Regarding the system constraints, most of the aforementioned DMPC algorithms may not be feasible for the MAS with global coupled constraints as in (1.2c). However, this type of constraint plays an essential role in many practical applications, including, for instance, controlling a group of vehicles while avoiding collisions and preserving connectivity. It is noted that the main challenge lies in the guarantee of the satisfaction of coupled constraints in a distributed fashion.

$$x_i \in \mathcal{X}_i, \ i = 1, 2, \ldots, M, \tag{1.2a}$$

$$u_i \in \mathcal{U}_i, \ i = 1, 2, \ldots, M, \tag{1.2b}$$

$$\sum_{i=1}^{M} (\Psi_i^x x_i + \Psi_i^u u_i) \leq \mathbf{1}, \tag{1.2c}$$

where x_i and u_i are the system state and the control input, respectively. $\mathcal{X}_i \subset \mathbb{R}^{n_i}$, $\mathcal{U}_i \subset \mathbb{R}^{m_i}$ are the local constraint sets of state and control input of agent i, $i = 1, 2, \ldots, M$, respectively. $\Psi_i^x \in \mathbb{R}^{p \times n_i}$ and $\Psi_i^u \in \mathbb{R}^{p \times m_i}$ are matrices used to define the globally coupled constraints, with $\mathbf{1}$ being the all-one vector of proper dimensions.

In [123], a DMPC algorithm is developed for the dynamically decoupled MAS with coupled constraints; only one agent calculates the locally optimal control inputs and updates the system states at each time instant. As reported in [145, 147], all agents with coupled constraints are optimized jointly in a cooperative set, which may have a strong requirement on the communication networks. Another direction for coupled constraints [158, 159] that achieves global optimality is to distributively solve the dual optimization problem, where dual variables related to the coupled constraints are treated as consensus variables in the distributed optimization problem. In addition, distributed optimization algorithms, such as the alternating direction multiplier method [158] and push-sum dual gradient algorithm [45], are adopted to solve the dual problem of the DMPC optimization problem in a distributed fashion. Considerable efforts have been devoted to exploring more efficient and tractable computation of the solution to the constraint-coupled DMPC optimization problem. For example, accelerated gradient methods using dual decomposition are leveraged to solve the DMPC optimization problem [29, 159]. A recent paper designs the DMPC method for the MAS with stochastic communication noises and global constraints, in which the noisy distributed ADMM strategy is developed to calculate the control inputs within the finite number of iterations [59].

1.1.2.3 DMPC with coupled dynamics

Note that the MAS with coupled system dynamics widely exists in many practical applications, e.g., chemical processes [88]. A DMPC algorithm is developed for the formation stabilization problem of the linear constrained MAS with coupled dynamics in [139]; the DMPC algorithm is extended to control the nonlinear MAS with coupled dynamics [17]. In these implementations, agents solve local optimization problems based on neighbor-to-neighbor communication. In addition to these results, the authors in [86, 87] propose Lyapunov-based iterative DMPC algorithms for the nonlinear MAS with coupled inputs, where a stability constraint derived from an auxiliary control law is imposed on the local DMPC optimization problem to guarantee the closed-loop stability. In [13, 157], the DMPC scheme with a time-varying terminal set is proposed for the dynamically coupled MAS to achieve a less conservative result. For the nonlinear MAS, an event-triggered DMPC method is proposed for the dynamically coupled MAS in [85], in which the coupling term is regarded as bounded external disturbances. Other DMPC methods for the MAS with coupled dynamics

along this line include [10, 42, 90, 93, 124, 162].

1.1.3 DMPC for consensus of the MAS

Compared with the formation stabilization of the MAS, DMPC algorithms for the consensus problem have not been studied extensively. In the consensus problem of the MAS, it is desired that agents agree on a common unknown static or dynamic value. Previous works on DMPC for consensus of the MAS include [7, 11, 23, 28, 37, 47, 49, 66, 68, 71, 102, 154, 155, 174, 175]. In [23], a DMPC-based consensus protocol is proposed for the MAS with single and double integrator dynamics over time-varying networks. The geometric properties of the optimal path for each agent are exploited to analyze the consensus convergence. On the basis of the above technique, a contractive constraint is designed and then incorporated into the MPC problem for the MAS with double integrator dynamics to achieve consensus. The authors of [175] present an analytical DMPC solution to the unconstrained average consensus problem and derive the feasible range of the sampling interval for the sampled-data MAS. In [7], a DMPC-based consensus framework with adjustable prediction horizon is developed to solve the consensus problem of the discrete-time MAS with double integrator dynamics, input constraints, and switching communication topologies. [66, 71] investigate consensus problems for the first-order MAS and general linear MAS. An explicit consensus protocol is derived from the unconstrained DMPC problem based on local and neighboring information, where a necessary and sufficient consensus condition is provided. Later, the work [68] studies the optimal consensus problem for the linear MAS with semi-stable and unstable dynamics and control input constraints. Because of the heavy communication burden and external disturbances, the self-triggered DMPC [174] and output-feedback DMPC [11] are developed for addressing these practical issues of the constrained MAS, respectively. Recently, the unconstrained consensus problem of the asynchronous MAS with single and double integrator dynamics is solved via DMPC in [154]. The control inputs and consensus states are determined by solving the optimization problem in a distributed manner. The authors further extend this method for the general linear MAS in [155]. In this scheme, a consensus manifold is introduced such that the final consensus state and input sequence are regarded as augmented decision variables of the DMPC optimization problem. The output consensus problem of the heterogeneous discrete-time MAS subject to state and control input constraints is considered in [37]. Based on the idea

of tracking MPC in [79], the combination of tracking cost and consensus cost in the overall cost function is beneficial to achieving consensus. It is worth emphasizing that the aforementioned studies either focus on simple integrator dynamics [7, 23, 154] or consider unconstrained consensus problems [66, 71, 175]. A detailed comparison between existing DMPC-based consensus algorithms is summarized in Table 1.1.

Table 1.1: An overview of existing DMPC-based consensus algorithms.

Method	Constraint types	System dynamics	Robustness
[23]	Unconstrained	Single and double integrators	–
[102]	State and input constraints	Linear and nonlinear systems	–
[175]	Unconstrained	Single integrators	–
[7]	Input constraints	Single and double integrators	–
[71]	Unconstrained	Linear system	–
[68]	Input constraints	Linear system	–
[28]	State and input constraints	Nonlinear system	–
[37]	State and input constraints	Linear system	–
[11]	Input constraints	Linear and nonlinear systems	Min-max DMPC
[155]	Unconstrained	Linear system	–

1.2 Robust MPC

1.2.1 Overview

As discussed in the last section, many decent DMPC algorithms have been developed for the constrained MAS. Due to the ubiquitous existence of external disturbances and parametric uncertainties in practice, the closed-loop stability of the systems may not be guaranteed. MPC for the uncertain system aims to steer the states to the neighborhood of the desired setpoint and ensure the satisfaction of state and control constraints for all realizations of uncertainties. Several robust MPC schemes have been proposed to handle this challenging problem, such as min-max MPC and tube-based MPC. The robust stability of such systems has been studied by using the input-to-state stability, and input-to-state practical stability theory [43, 137]. Examples of the use of the input-to-state stability and input-to-state practical stability theory for robust MPC can be found in [55, 94].

Consider a discrete-time nonlinear system with uncertainties

$$x(k+1) = f(x(k), u(k), w(k)), \tag{1.3}$$

where $w(k) \in \mathcal{W} \subseteq \mathbb{R}^w$ denotes the disturbance input. It is assumed that the disturbance $w(k)$ lies in a compact set $\mathcal{W}$ which contains the origin in its interior and may depend on the state and input $\mathcal{W} = \{w \mid \|w\| \leq \gamma(\|x\|) + \rho(\mu)\}$, where $\gamma(\cdot)$ and $\rho(\cdot)$ are $\mathcal{K}$ functions for all $x \in \mathcal{X}$ and $u \in \mathcal{U}$, and the constant μ describes the persistent disturbance. In the following, a brief review of different robust MPC methods is provided.

1.2.2 Nominal MPC with inherent robustness

Typically, nominal MPC ignores the disturbances of the system in the optimization problem. The nominal system is described by

$$\bar{x}(k+1) = f(\bar{x}(k), \bar{\mu}(k), 0), \ k \geq 0, \tag{1.4}$$

in which $\bar{x}^{\bar{\pi}}(k, x(0))$ denotes the solution of the system in (1.4) at time k with the initial state $x(0)$ and the control policy $\bar{\pi} = \{\bar{\mu}(0), \bar{\mu}(1), \ldots, \bar{\mu}(N-1)\}$. And the nominal cost function is defined as

$$V_N(\bar{x}(0), \bar{\pi}) = \sum_{k=0}^{N-1} \ell(\bar{x}(k), \bar{\mu}(k)) + V_f(\bar{x}(N)), \tag{1.5}$$

where N is the prediction horizon, $\ell(\bar{x}(k), \bar{\mu}(k))$ denotes the stage cost function and $V_f(\bar{x}(N))$ denotes the terminal cost function. For the nominal MPC, the optimization problem is formulated as

$$\bar{\mathcal{P}}_N : \quad V_N^0(\bar{x}) = \min_{\bar{\pi} \in \mathcal{U}} V_N(\bar{x}(0), \bar{\pi}), \ \text{s.t. (1.4)}, \ \bar{x}(k) \in \mathcal{X}, \ \bar{\mu}(k) \in \mathcal{U}. \tag{1.6}$$

It is of interest to analyze under which conditions nominal MPC can guarantee the robustness with respect to specific classes of disturbances. Under the optimal control policy $\bar{\pi}^*$, the closed-loop stability of the uncertain system in (1.3) can be obtained if the disturbances are arbitrarily small [31], and the nominal system in (1.4) inherits the robust stability under the fundamental assumption that the presence of the uncertainties does not cause any loss of feasibility [126]. In [173], the authors show that the constrained nonlinear system under nominal MPC is input-to-state stable if the system is subject to sufficiently small additive disturbances. In contrast to the analysis of the inherent robustness of the nominal MPC for linear systems, novel nominal MPC schemes are further extended for hybrid and nonlinear systems [56,115].

1.2.3 Min-max MPC

Under suitable conditions, nominal MPC has inherently robust stability; however, in the presence of state and control input constraint, the robustness margin may be sufficiently small or even nonexistent. Alternatively, min-max MPC can simultaneously handle parametric uncertainties and external disturbances and yield good control performance.

Different from the aforementioned nominal cost function (1.5), the worst case cost function is defined as follows:

$$V_N(x(0),\pi) = \max_{w\in\mathcal{W}}\{\sum_{k=0}^{N-1} \ell(x(k),\mu(k)) + V_f(x(N))\}, \tag{1.7}$$

where $x(k)$ is the system state at time k and $\pi := \{\mu(0),\mu(1),\ldots,\mu(N-1)\}$ is the control policy. The cost function (1.7) is maximized concerning the worst-case realizations of all admissible uncertainties, which yields a min-max optimization problem

$$\mathcal{P}_N: \quad V_N^0(x) = \min_{\pi\in\mathcal{U}} V_N(x(0),\pi),\ \text{s.t. (1.3)},\ x(k)\in\mathcal{X},\ \mu(k)\in\mathcal{U},\ w(k)\in\mathcal{W}. \tag{1.8}$$

The open-loop min-max MPC scheme is proposed in [95] for the nonlinear system. The maximum cost function is further minimized with respect to the control sequence for the worst-case realizations. The open-loop min-max MPC approach is computationally easier than the feedback min-max MPC approach, but the feedback mix-max MPC approach has a larger region of attraction [78]. In [55], the feedback min-max MPC is proposed for the constrained nonlinear systems with parametric uncertainties and external disturbances. It is shown that the nonlinear system under the feedback min-max is input-to-state practical stable (ISpS), and the optimization problem is solved via dynamic programming. The linear system case is considered in [57]. In [116], a novel min-max MPC scheme for the nonlinear system is proposed, where an explicit robustness bound of the closed-loop system is derived based on the ISpS conditions. In [60], the min-max MPC is proposed for the constrained nonlinear networked control systems with uncertainties and network-induced constraints. In [177], a systematic min-max model predictive tracking control strategy is proposed for the industrial processes with actuator saturation and unknown disturbances. To further reduce the communication cost while ensuring the desired level of control performance, a self-triggered min-max MPC is proposed for the constrained nonlinear system with both parametric uncertainties and external disturbances [83].

Compared with the nominal MPC scheme, min-max MPC theoretically has better robustness but is computationally expensive, limiting its application in many practical scenarios. However, the development of the advanced optimization algorithms and the lower cost of the hardware with powerful computation resources may enable the min-max MPC approach to be widely used [170].

1.2.4 Tube-based MPC

The constraint tightening MPC and tube-based MPC are developed in order to achieve a better trade-off between the control performance and the computation complexity. Constraint tightening approaches, as stated in [92, 101, 122], are computationally efficient. Two novel implementable nominal MPC frameworks with tightening robustness constraints are proposed to ensure the robust stability of nonlinear systems in [52, 61]. However, the constraint sets generally shrink drastically due to the uncertainties increasing with the prediction horizon. In contrast, tube-based MPC approaches reduce the online computational burden and exploit both the online control action and the offline feedback control law [8, 99]. The optimal control actions generated by solving a finite-horizon constrained optimization problem steer the nominal system to the origin. The feedback control law keeps the actual system states in a tube that centers on the nominal optimal state.

In contrast to the min-max MPC approach, the conventional nominal cost function and nominal dynamics are used in the tube-based MPC optimization problem. The disturbances are taken into consideration, yielding the tightened state and control input constraints

$$\bar{x}(k) \in \mathcal{X} \ominus \Omega, \ \bar{\mu}(k) \in \mathcal{U} \ominus K\Omega, \tag{1.9}$$

where $\mathcal{X}$ and $\mathcal{U}$ denote the state constraint and control constraint, respectively; $\bar{x}$ is the nominal state, Ω denotes the disturbance invariant set, K is the offline feedback control gain, and $\ominus$ denotes the set subtraction. For the tube-based MPC, the optimization problem is formulated as

$$\mathcal{P}'_N: \quad V_N^0(\bar{x}) = \min_{\bar{\pi} \in \mathcal{U}} V_N(\bar{x}(0), \bar{\pi}), \ \text{s.t. (1.4)}, \ \text{(1.9)}, \tag{1.10}$$

which generates the optimal nominal control sequence $\bar{\pi}^* := \{\bar{\mu}^*(0), \bar{\mu}^*(1), \ldots, \bar{\mu}^*(N-1)\}$, and the control input applied to the actual system (1.3) is designed as $u(k) = \bar{\mu}^*(k) + K(x(k) - \bar{x}(k))$.

Tube MPC that reduces the online computation burden has been widely studied in, for example, [8,54,99,117] for linear systems and in [98,143,150,172] for nonlinear systems. In [54, 99], a tube-based MPC is proposed for the linear systems with additive disturbances, where the rigid tube is calculated offline. The authors in [117,118] develop the homothetic tube and elastic tube-based MPC for the uncertain linear systems to further reduce conservatism by computing the dynamic tube online, thereby enlarging the feasible region. For nonlinear systems, it is challenging to find a local stabilization feedback control law. Tube-based MPC for nonlinear systems with additive disturbances is studied in [98,172], in which the controller has a similar structure as the linear systems, i.e., the optimal nominal control action is generated by calculating the constrained MPC optimization problem and the offline ancillary feedback control law is generated by solving another optimization problem. The extension to the uncertain nonlinear MAS is reported in [106]. Tube-based MPC is also extended to address the tracking control problem of the constrained unicycle robots with additive disturbances in [143].

1.3 Autonomous Marine Vehicles

1.3.1 Overview

The ocean covers about 72% of the earth's surface, but most of the area has not yet been explored. There is an increasing demand for cutting-edge technology and advanced equipment to explore the ocean for different applications, such as ocean transportation, resource exploration, and emergency operation support. These increasing demands have stimulated the research interest in autonomous marine mechanical systems that integrate electronics, mechanics, and control software. A variety of advanced control strategies have been developed for autonomous marine vehicles (AMVs), including autonomous surface vehicles (ASVs) and autonomous underwater vehicles (AUVs) [25,133]. Among these control approaches, MPC is a well-established control scheme, and it has distinct features to cope with physical constraints while optimizing the control performance. In this section, we focus on the motion control problems of AMVs, such as dynamic positioning, and trajectory tracking control from the perspective of MPC. Several representative motion control problems of AMVs are stated as follows.

1) *Dynamic positioning*: The AMV is required to maintain the prespecified posi-

tion and heading autonomously with installed thrusters.

2) *Path following*: The AMV is required to follow a feasible predefined path with desired speed and orientation.

3) *Trajectory tracking*: The AMV is driven to track a spatial and temporal trajectory with a specific time requirement.

4) *Cooperative control*: The AMVs are required to cooperatively complete a specific control task, such as formation tracking control.

1.3.2 MPC for AMVs

1.3.2.1 Dynamic positioning and path following

Dynamic positioning: The dynamic positioning control is a representative control task for marine applications; see the survey paper [138] and the references therein. For the AMV, it is desired to steer the heading to the desired angle and reduce the roll angle under complex marine environments. Early work on MPC for marine vehicles mainly studies the angle stabilization problem and adopts the 1-DoF dynamical system model [114,151]. A novel disturbance compensating MPC method is developed to handle the constraint violation, the disturbances, and the feasibility issues of the ASV heading control problem in [74]. The dynamic positioning using MPC is studied in [148], considering the dynamic thruster capability, the reduction of energy consumption, and the improved control performance. In order to avoid the complex terminal set design, the authors in [130] study dynamic positioning of the AUV and impose a Lyapunov-based constraint into the MPC optimization problem to guarantee the closed-loop stability. More recently, robust dynamic positioning using robust MPC has been studied for the ASV with parametric uncertainties and external disturbances in [16, 181].

Path following: Much effort has been devoted to the path following problem of AMVs [133, 134]. However, the control performance may degrade due to various constraints on states and inputs. In [75], the path following problem of ASVs with roll constraints has been solved by using MPC. Further, a multi-objective MPC method is proposed for the AUV considering the flexibility of adjusting the vehicle's velocity. On the other hand, MPC has been adopted for the fully-actuated marine vehicles [75, 131]

and underactuated marine vehicles [48,72,107,112,176]. The robust MPC is employed to solve the path following problem of the AMV with disturbances in [176].

1.3.2.2 Trajectory tracking and cooperative control

Trajectory tracking: Another classic control problem of AMVs is trajectory tracking [91, 133]. The unpredictable sea environment, highly nonlinear system dynamics, and various constraints lead to technical difficulties in developing the trajectory tracking controller. In [167], a neurodynamic optimization-based MPC method is proposed for the tracking control of underactuated vessels, in which a single-layer recurrent neural network is used to solve the formulated quadratic programming problem. A nonlinear MPC method is presented to address the trajectory tracking problem of ASVs in the presence of ocean currents in [33]. For the real-time implementation of AUVs, a modified Ohtsuka's continuation/generalized minimal residual algorithm has been developed to solve the nonlinear MPC optimization problem [127]. The authors in [128] further decompose the original MPC optimization problem into several smaller size subproblems and then solve them in a distributed manner. This method significantly alleviates the heavy computational burden. A unified MPC scheme to jointly handle the path planning and trajectory tracking control problem for the AUV is proposed in [129]. The conventional MPC employs the terminal cost and terminal set to ensure the closed-loop stability, which is hard to design for the AUV with nonlinear dynamics. A Lyapunov-based stability constraint is designed and imposed into the MPC optimization problem. The robust MPC method is developed for the trajectory tracking problem of the AMV with external disturbances in [35,36,178]. Since the challenges with the practical implementation, such as accurate system dynamics, algorithm deployment, and code debugging, make the experiment hard to verify. The researchers generally verify the theoretical results with simulation studies instead of experiments. Recently, the experiment tests on the trajectory tracking task of the underactuated ASV under the nonlinear MPC algorithm are provided [77].

Cooperative control: DMPC algorithm that applies to cooperative AMVs has become an important research topic. In [180], a distributed predictive path following controller is proposed for multiple waterborne automated guided vessels. The alternating direction method of multiplier is employed to accelerate the convergence rate of the DMPC optimization problem. Moreover, this method is extended as robust DMPC to deal with external disturbances. The authors apply the DMPC method to

solve the formation tracking control problem of multiple underactuated AUVs [69]. A Lyapunov-based DMPC method is designed to achieve the formation tracking of cooperative AUVs with environmental disturbances while ensuring collision avoidance during the operational period [160]. Due to the limited communication bandwidth among AUVs, an offline quantization design and an online DMPC algorithm with quantization are proposed to solve these issues. The communication burden is alleviated by using the event-triggered based DMPC method in [40]. Especially, the authors apply DMPC algorithms for the heterogeneous ASV platoon to improve the efficiency of waterborne transport in [5, 161].

1.4 Organization and Contributions

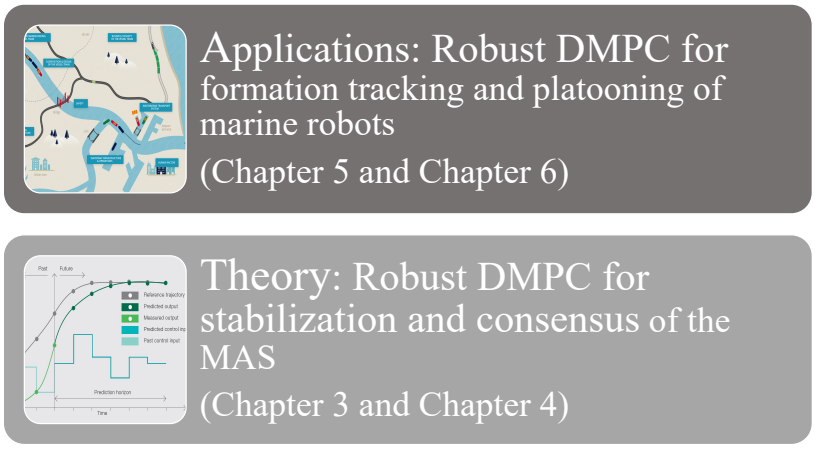

Figure 1.2: Organization of this dissertation.

As illustrated in Figure 1.2, **Chapters 3** and **4** present two theoretical results, including robust DMPC for the formation stabilization problem and the consensus problem of the constrained MAS with uncertainties; **Chapters 5** and **6** develop DMPC algorithms for cooperative marine vehicles under uncertainties. The dissertation outline and main contributions are summarized as follows.

- In **Chapter 2**, we review some preliminaries and introduce notations that are useful throughout this dissertation.
- In **Chapter 3**, we study the formation stabilization problem of the asynchronous nonlinear MAS subject to parametric uncertainties, external disturbances, and bounded time-varying communication delays. A self-triggered min-

max DMPC approach is proposed to handle these practical issues. At triggering instants, each agent solves a local min-max optimization problem based on local system states and predicted system states of neighbors, determines its next triggering instant, and broadcasts its predicted state trajectory to its neighbors. As a result, the communication load is greatly alleviated while retaining robustness and comparable control performance compared to periodic DMPC algorithms. In order to handle time-varying delays, a novel consistency constraint is incorporated into each local optimization problem to restrict the deviation between the newest predicted states and previously broadcast predicted states. Consequently, each agent can utilize previously predicted states of its neighbors to achieve cooperation in the presence of time-varying delays and asynchronous communication induced by the distributed triggered scheduler. The proposed algorithm's recursive feasibility and MAS's closed-loop stability at triggering time instants are proven. Finally, numerical simulations are conducted to verify the efficiency of the proposed control method.

- In **Chapter 4**, we consider the consensus problem of the general linear discrete-time MAS with input constraints and time-varying communication delays. We propose a robust DMPC consensus protocol that integrates the offline consensus design with online DMPC optimization to exploit their respective advantages. One feature of this approach is that each agent is equipped with an offline consensus protocol, which is *a priori* designed, depending only on the estimated states of its immediate neighbors. Under mild technical assumptions, the estimation errors propagated over time due to inaccurate neighboring information is proved bounded, based on which a robust DMPC strategy is deliberately designed to achieve robust consensus while guaranteeing the satisfaction of constraint on control inputs. Moreover, it is shown that, with the suitably designed cost function and constraints, the feasibility of the associated optimization problem can be recursively ensured. We further provide the consensus convergence result of constrained MAS in the presence of bounded varying delays. Finally, two numerical examples are given to verify the effectiveness of the proposed distributed consensus algorithm.

- In **Chapter 5**, we investigate the formation tracking problem of a group of AUVs with the ocean current disturbances. A distributed Lyapunov-based model predictive controller (DLMPC) is designed such that AUVs can keep

the desired formation while tracking the reference trajectory, despite the presence of external disturbances. The DLMPC inherits the stability and robustness of the extended state observer (ESO) based auxiliary control law and invokes online optimization to improve the formation tracking performance of the multi-AUV system. The closed-loop stability of the multi-AUV system is guaranteed by the stability constraint that utilizes the ESO-based auxiliary controller and the associated Lyapunov function. Furthermore, the inter-AUV collision avoidance is achieved by incorporating well-designed artificial potential field-based cost term in the formation tracking cost function. Extensive simulations on AUVs are carried out, demonstrating the proposed method's superior control performance and robustness.

- In **Chapter 6**, we propose to apply a robust distributed model predictive platooning control approach for a group of heterogeneous ASVs with the input constraint and bounded external disturbances. The control input for each ASV is composed of two parts: the optimal nominal control input and the ancillary control input. The optimal nominal control input is generated by solving a DMPC problem based on the state information of itself and its neighbors. The offline ancillary control law ensures that the actual system state trajectory evolves in a hyper-tube centered along the optimal nominal state trajectory. A coupled inter-vehicle safety constraint is designed in the DMPC optimization problem to guarantee inter-ASV collision avoidance. Theoretical results on the feasibility of the proposed robust DMPC algorithm are provided, and the closed-loop systems are proved to be input-to-state stable (ISS). Numerical simulations are performed to illustrate the theoretical results.

- In **Chapter 7**, we summarize the work in this dissertation and present several potential future research directions.

Chapter 2

Preliminaries

This chapter presents main notations used in the dissertation, the communication model for the MAS, and some definitions and properties from control theory.

2.1 Notations

The symbols $\mathbb{R}_{\geq 0}$, $\mathbb{N}_{\geq m}$ and $\mathbb{N}_{[m,n]}$ denote the sets of nonnegative real numbers, the integers greater than or equal to m and integers in the interval $[m, n]$, respectively. $\mathbb{R}^n$ and $\mathbb{R}^{m\times n}$ represent the n-dimensional Euclidean space and the set of all $m \times n$ real matrices, respectively. For $x \in \mathbb{R}^n$, $\|\cdot\|$ denotes the Euclidean norm, $\|\cdot\|_\infty$ denotes the infinity norm, $\|x\|_P := \sqrt{x^{\mathrm{T}} P x}$ denotes the weighted Euclidean norm, where P is positive definite. $[x_1^{\mathrm{T}}, \ldots, x_n^{\mathrm{T}}]^{\mathrm{T}}$ is written as $\mathrm{col}(x_1, \ldots, x_n)$. The superscript 'T' represents the transposition. Given two sets $\mathcal{X}, \mathcal{Y} \subseteq \mathbb{R}^n$, the set operation $\mathcal{X}\backslash\mathcal{Y}$ is defined as $\mathcal{X}\backslash\mathcal{Y} := \{x \mid x \in \mathcal{X}, x \notin \mathcal{Y}\}$. The set addition is defined by $\mathcal{X} \oplus \mathcal{Y} := \{x + y \mid x \in \mathcal{X}, y \in \mathcal{Y}\}$, the set subtraction is $\mathcal{X} \ominus \mathcal{Y} := \{x \in \mathbb{R}^n \mid x \oplus \mathcal{Y} \subseteq \mathcal{X}\}$, and the set multiplication is $K\mathcal{X} := \{Kx \mid x \in \mathcal{X}\}$, with $K \in \mathbb{R}^{m\times n}$. The Minkowski sum of multiple sets is given by $\mathcal{X}_1 \oplus \mathcal{X}_2 \oplus \cdots \oplus \mathcal{X}_M := \bigoplus_{i=1}^{M} \mathcal{X}_i$. The distance between the state x and the set $\mathcal{Y}$ is defined as $|x|_{\mathcal{Y}} := \inf_{y\in\mathcal{Y}} \|x - y\|$. $I_M \in \mathbb{R}^{M\times M}$ denotes the identity matrix. $\mathrm{diag}(C_1, C_2, \ldots, C_M)$ represents a block diagonal matrix with main diagonal block matrix C_i, $i = 1, 2, \ldots, M$. $\bar{\lambda}(P)$ and $\underline{\lambda}(P)$ denote the largest and smallest eigenvalues of the matrix P, respectively. For matrices $C \in \mathbb{R}^{m\times n}$,

$D \in \mathbb{R}^{p\times q}$, the Kronecker product is denoted by

$$C \otimes D = \begin{bmatrix} c_{11}D & \cdots & c_{1n}D \\ \vdots & \ddots & \vdots \\ c_{m1}D & \cdots & c_{mn}D \end{bmatrix}.$$

$x(t)$ denotes the state x at time t, and $x(k|t)$ denotes the predicted state at future time $t+k$ determined at time t.

2.2 Communication Model

In this dissertation, a weighted graph $\mathcal{G} = \{\mathcal{V}, \mathcal{E}\}$ is used to describe the communication network of the MAS, where $\mathcal{V} := \{1, 2, \ldots, M\}$ denotes the vertex set and $\mathcal{E} := \{(i,j) \mid i,j \in \mathcal{V}, i \neq j\}$ denotes the edge set. The neighbor set of agent i is denoted by $\mathcal{N}_i := \{j \in \mathcal{V} \mid (i,j) \in \mathcal{E}, i \neq j\}$ and the number of agents in $\mathcal{N}_i$ is denoted as $|\mathcal{N}_i|$. Let $\mathcal{A} = [a_{ij}] \in \mathbb{R}^{M\times M}$ be the adjacency matrix of $\mathcal{G}$ with $j \in \mathcal{N}_i$, $a_{ij} = 1/|\mathcal{N}_i|$ and $a_{ij} = 0$ otherwise; $a_{ii} = \sum_{j=1}^{M} a_{ij} = 1$ for all $i \neq j$. The Laplacian matrix of the weighted graph $\mathcal{G}$ is $\mathcal{L} = I_M - \mathcal{A}$.

2.3 Stability Theory

Here we review some stability definitions and properties of the discrete-time system [44, 119]. The stability properties of the continuous-time system can be found in [50].

Consider a discrete-time perturbed nonlinear system

$$x^+ = f(x, w), \tag{2.1}$$

in which the state x lies in $\mathbb{X} \subset \mathbb{R}^n$, the disturbance w lies in $\mathbb{W} \subset \mathbb{R}^w$, and x^+ is the successor state. The function $f : \mathbb{R}^n \times \mathbb{R}^w \to \mathbb{R}^n$ is assumed to be continuous. Let $\phi(t, x(0), w(t))$ denote the solution of the difference function in (2.1) at time t, $t \in \mathbb{N}_{\geq 0}$.

Definition 2.1 ($\mathcal{K}$ function)**.** *A function $\alpha : \mathbb{R}_{\geq 0} \to \mathbb{R}_{\geq 0}$ belongs class $\mathcal{K}$ if it is continuous and strictly increasing, with $\alpha(0) = 0$; $\beta : \mathbb{R}_{\geq 0} \to \mathbb{R}_{\geq 0}$ belongs to class $\mathcal{K}_\infty$ if it is a class $\mathcal{K}$ function and unbounded (i.e., $\beta(x) \to \infty$ as $x \to \infty$). A function $\gamma : \mathbb{R}_{\geq 0} \times \mathbb{N}_{\geq 0} \to \mathbb{R}_{\geq 0}$ belongs class $\mathcal{KL}$ if it is continuous and if, for $t \in \mathbb{N}_{\geq 0}$,*

$\gamma(\cdot, t)$ is a class $\mathcal{K}$ function and for $x \in \mathbb{R}_{\geq 0}$, $\gamma(x, \cdot)$ is nonincreasing and satisfies $\lim_{t\to\infty} \gamma(x, t) = 0$. A function $\sigma : \mathbb{R} \to \mathbb{R}_{\geq 0}$ belongs to class $\mathcal{PD}$ (i.e., positive definite) if it is continuous, zero at zero, and positive everywhere else.

Set invariance plays an important role in control, and several forms of sets are introduced below.

Definition 2.2 (Positive invariant set)**.** *A set Ω is positive invariant for the system $x^+ = f(x)$, if $x \in \Omega$ implies $x^+ \in \Omega$.*

Definition 2.3 (Robust positive invariant set)**.** *A set Ω is robust positive invariant for the perturbed system in* (2.1)*, if $x \in \Omega$ implies $x^+ \in \Omega$ for all $w \in \mathbb{W}$.*

Definition 2.4 (Robust control invariant set)**.** *A set Ω is robust control invariant for the system $x^+ = f(x, u, w)$, if $x \in \Omega$, there exists an admissible control input u such that $x^+ \in \Omega$ for all $w \in \mathbb{W}$.*

Definition 2.5 (ℓ-step robust stabilizable set)**.** *A set $\mathbb{X}^\ell(\Omega)$ is ℓ-step robust stabilizable for the system $x^+ = f(x, u, w)$, if $\forall x \in \mathbb{X}^\ell(\Omega)$, there exists an admissible control input u such that the system can be steered into Ω in ℓ steps for all $w \in \mathbb{W}$, with $\ell \in \mathbb{N}_{\geq 0}$.*

Note that the above definition implies that $\mathbb{X}^\ell(\Omega) = \{x \in \mathbb{X} \mid \exists\, u \in \mathbb{U}$ such that $f(x, u, \mathbb{W}) \subseteq \mathbb{X}^{\ell-1}(\Omega)\}$, with $f(x, u, \mathbb{W}) := \{f(x, u, w) \mid \forall w \in \mathbb{W}\}$. In addition, $\mathbb{X}^0(\Omega) = \Omega$.

In what follows, some properties from the Lyapunov theory are provided to establish the stability or robust stability of the constrained system under uncertainty.

Definition 2.6 (Lyapunov function)**.** *A function $V : \mathbb{R}^n \to \mathbb{R}_{\geq 0}$ is a Lyapunov function for the system $x^+ = f(x)$ with $x \in \mathbb{X}$ and a positive invariant set $\Omega \subset \mathbb{X}$, if there exist functions $\alpha_1(\cdot), \alpha_2(\cdot) \in \mathcal{K}_\infty$ and $\alpha_3(\cdot) \in \mathcal{PD}$ such that for all $x \in \mathbb{R}^n$,*

$$\begin{aligned} &\alpha_1(|x|_\Omega) \leq V(x) \leq \alpha_2(|x|_\Omega), \\ &V(f(x)) - V(x) \leq -\alpha_3(|x|_\Omega). \end{aligned}$$

Theorem 2.1 (Asymptotic stability)**.** *If the system $x^+ = f(x)$ admits a Lyapunov function $V(\cdot)$ with $\alpha_3(\cdot) \in \mathcal{K}_\infty$, then it is asymptotically stable.*

Definition 2.7 (ISS)**.** *The system in* (2.1) *is said to be ISS if there exist a* $\mathcal{KL}$ *function* $\beta(\cdot,\cdot)$ *and a* $\mathcal{K}$ *function* $\gamma(\cdot)$ *such that, for each* $x \in \mathbb{X}$*, and each disturbance sequence* $\mathbf{w}_t = \{w(0), w(1), \ldots, w(t-1)\}$*,*

$$|\phi(t, x(0), \mathbf{w}_t)| \leq \beta(|x(0)|, t) + \gamma(|\mathbf{w}_t|_\infty),$$

where $|\mathbf{w}_t|_\infty := \sup_{0 \leq s \leq t} |w(t)|$ *and* $\phi(t, x(0), \mathbf{w}_t)$ *is the solution at time* t*.*

Definition 2.8 (ISS-Lyapunov function)**.** *A function* $V : \mathbb{R}^n \to \mathbb{R}_{\geq 0}$ *is an ISS-Lyapunov function for the system in* (2.1) *if there exist* $\mathcal{K}_\infty$ *functions* $\alpha_1(\cdot), \alpha_2(\cdot), \alpha_3(\cdot)$ *and a* $\mathcal{K}$ *function* $\sigma(\cdot)$ *such that for all* $x \in \mathbb{X}$ *and* $w \in \mathbb{W}$

$$\begin{aligned} &\alpha_1(|x|) \leq V(x) \leq \alpha_2(|x|), \\ &V(x^+) - V(x) \leq -\alpha_3(|x|) + \sigma(|w|). \end{aligned}$$

Lemma 2.1 (ISS-Lyapunov function implies ISS)**.** *Suppose that there exists a continuous ISS-Lyapunov function* $V(\cdot)$ *for the system in* (2.1)*. Then the system is ISS.*

Definition 2.9 (ISpS)**.** *The system in* (2.1) *is said to be ISpS, if there exists a* $\mathcal{KL}$ *function* $\beta(\cdot,\cdot)$*, a* $\mathcal{K}$ *function* $\gamma(\cdot)$ *and a nonnegative constant* c_0*, such that for any initial state* $x(0) \in \mathbb{X}$ *and any disturbance sequence* $\mathbf{w}_t$*, the solution* $\phi(t, x(0), \mathbf{w}_t)$ *exists and satisfies*

$$|\phi(t, x(0), \mathbf{w}_t)| \leq \beta(|x(0)|, t) + \gamma(|\mathbf{w}_t|_\infty) + c_0.$$

Definition 2.10 (ISpS-Lyapunov function)**.** *A function* $V : \mathbb{R}^n \to \mathbb{R}_{\geq 0}$ *is an ISpS-Lyapunov function for the system in* (2.1) *if there exist* $\mathcal{K}_\infty$ *functions* $\alpha_1(\cdot), \alpha_2(\cdot), \alpha_3(\cdot)$*, a* $\mathcal{K}$ *function* $\sigma(\cdot)$ *and constants* $c_1, c_2 \in \mathbb{R}_{\geq 0}$ *such that for all* $x \in \mathbb{X}$ *and* $w \in \mathbb{W}$

$$\begin{aligned} &\alpha_1(|x|) \leq V(x) \leq \alpha_2(|x|) + c_1, \\ &V(x^+) - V(x) \leq -\alpha_3(|x|) + \sigma(|w|) + c_2. \end{aligned}$$

Lemma 2.2 (ISpS-Lyapunov function implies ISpS)**.** *Suppose that there exists a continuous ISpS-Lyapunov function* $V(\cdot)$ *for the system in* (2.1)*. Then the system is ISpS.*

Chapter 3

Self-Triggered Min-Max DMPC for Multi-Agent Systems with Uncertainties and Time-Varying Communication Delays

3.1 Introduction

In this chapter, we study the formation stabilization control problem of the MAS with the heavy communication burden, the time-varying communication delays, and uncertainties. For solving this problem, we propose a self-triggered min-max DMPC method that is distributed among agents.

Generally speaking, the periodically distributed control algorithms for the MAS require all agents to synchronously communicate with their neighbors at each sampling instant, which may lead to an undesirable communication burden and nontrivial energy consumption. Alternatively, the aperiodically distributed control method is an attractive solution to alleviate the communication burden among the MAS while guaranteeing the comparable control performance, in which the system states are only updated and transmitted to neighbors at triggering instants [15]. Based on different triggering mechanisms, the aperiodic DMPC methods in existing literature can be mainly classified into two categories: event-triggered [32, 53, 73, 85, 183], and self-triggered DMPC [100, 156, 174]. Compared with the event-triggered algorithms, the requirement of the continuous check of the controlled system and predesigned trigger-

ing conditions at each sampling instant are removed in the self-triggered DMPC algorithms. However, these communication-efficient DMPC algorithms may result in the asynchronous information transmission among agents, which may degrade the control performance or even destroy the closed-loop stability [58]. The authors in [100] propose a co-design self-triggered DMPC method for the linear MAS with asynchronous communication. To be specific, the previously broadcast predicted sequence is used to estimate current optimal states; however, the estimation errors induced by the asynchronous communication are ignored. Other promising DMPC methods for the distributed coordination problem of the asynchronous MAS can be found in [41,87,183]. On the other hand, the delay-free communication networks of the MAS, assumed in the literature mentioned above, are impractical. Understandably, the time-varying communication delays may prevent the MAS from reaching the control objective due to neighbors' inaccurate information. Some efforts have been devoted to overcoming this drawback, e.g., [20,61,62,140]. Notably, most of the abovementioned works only concentrate on one of these communication issues while ignoring others. Simultaneously addressing these issues of the constrained MAS remains a challenging and open problem, especially for the uncertain constrained MAS with nonlinear dynamics. Considering this, in this chapter, we propose a self-triggered min-max DMPC method for the distributed formation stabilization problem of the asynchronous MAS with uncertainties, the heavy communication burden, and varying delays. The main contributions of this work are summarized in the following:

- A self-triggered min-max DMPC method is proposed for the dynamically decoupled asynchronous nonlinear MAS subject to parametric uncertainties, external disturbances, and bounded time-varying delays. In this scheme, the distributed self-triggered scheduler significantly reduces the communication burden and the frequency of solving the DMPC optimization problem.

- A new consistency constraint that restricts the deviation between the currently optimal predicted states and the previously broadcast predicted states is incorporated into the local optimization problem. Consequently, agents can achieve cooperation in the presence of time-varying communication delays. Furthermore, the proposed algorithm for the asynchronous MAS is proved to be recursively feasible, and the closed-loop systems with time-varying delays are proved to be ISpS at triggering instants.

3.2 Problem Formulation

3.2.1 Basic setup

Consider an MAS consisting of M dynamically decoupled nonlinear systems. The discrete-time dynamics of agent i takes the following form

$$x_i(t+1) = f(x_i(t), u_i(t), d_i(t)),\ t \in \mathbb{N}_{\geq 0}, \tag{3.1}$$

in which $x_i(t)$, $u_i(t)$ and $d_i(t)$ denote, respectively, the system state, the control input and the uncertainty. Agent i is subject to the state and control input constraints

$$x_i(t) \in \mathbb{X}_i,\ u_i(t) \in \mathbb{U}_i,$$

where the state constraint set $\mathbb{X}_i \subset \mathbb{R}^n$ is closed and the control input set $\mathbb{U}_i \subset \mathbb{R}^m$ is compact. The disturbance $d_i = [w_i, v_i]^{\mathrm{T}}$ is bounded, i.e., $d_i \in \mathbb{D}_i \subset \mathbb{R}^d$; $\mathbb{D}_i := \mathbb{W}_i \times \mathbb{V}_i$, with the external disturbance $w_i \in \mathbb{W}_i \subset \mathbb{R}^w$ and the parametric uncertainty $v_i \in \mathbb{V}_i \subset \mathbb{R}^v$; its upper bound is given by $\bar{d} := \max_{d_i \in \mathbb{D}_i} \|d_i\|$. $\mathbb{W}_i$ and $\mathbb{V}_i$ are compact and contain the origin in their interiors. The function $f : \mathbb{R}^n \times \mathbb{R}^m \times \mathbb{R}^d \to \mathbb{R}^n$ is assumed to be differentiable and satisfies $f(0,0,0) = 0$. In the following, an assumption is made on the system in (3.1).

Assumption 3.1. *There exist constants ν, $\xi \in \mathbb{R}_{\geq 0}$ such that the conditions*

$$\|f(x,u,d) - f(y,u,d)\| \leq \nu \|x - y\|,$$

and

$$\|f(x,u,d) - f(x,u,d')\| \leq \xi \|d - d'\|,$$

hold for all $x, y \in \mathbb{X}_i$, $u \in \mathbb{U}_i$, $d, d' \in \mathbb{D}_i$, $i \in \mathcal{V}$.

Assumption 3.1 implies that the system dynamics in (3.1) is Lipschitz continuous; it helps to quantify a bound on the deviation between the currently optimal predicted states and the assumed predicted states, which will be specified in **Lemma 3.1**.

Let t_k^i, $k \in \mathbb{N}_{\geq 0}$ be the triggering instant of agent i, $i \in \mathcal{V}$. The sampling instant sequence is denoted as $\{t_k^i\}$. At the triggering instant t_k^i, agent i measures the local system states, receives its neighbors' predicted state sequences, and applies the calculated control inputs to update the system states.

Definition 3.1. *The MAS in* (3.1) *is said to be synchronous if for* $i, j \in \mathcal{V}$, $\{t_k^i\} = \{t_k^j\}$, *i.e.,* $t_k^i = t_k^j$, $\forall k \in \mathbb{N}_{\geq 0}$. *The MAS in* (3.1) *is said to be asynchronous if for* $i, j \in \mathcal{V}, i \neq j$, $\{t_k^i\}$ *is independent of* $\{t_k^j\}$, *i.e, agents may not update their system states at the same time.*

Note that it is hard to synchronize the sampling and control instants for the spatially separated MAS. Thus, the asynchronous MAS will be discussed in this chapter. If sampling periods are arbitrarily large, it is hard to guarantee the MAS's stability property without new measurements. Hence, an upper bound of the sampling period is assumed to exist. For the MAS, the local sampling time t_k^i, $i \in \mathcal{V}$ and the communication delay τ_k^{ij} satisfy the following assumption.

Assumption 3.2. *For agent* i, $i \in \mathcal{V}$, *the local sampling instant* t_k^i *and the communication delay* τ_k^{ij}, $k \in \mathbb{N}_{\geq 0}$, *satisfy: 1)* $1 \leq t_{k+1}^i - t_k^i \leq \bar{H}$; *2)* $0 < \tau_k^{ij} \leq \bar{\tau}$; *3) There is no disordering transmission among agents, where* $\bar{H} \in \mathbb{N}_{\geq 0}$ *and* $\bar{\tau} \in \mathbb{N}_{\geq 0}$ *denote the maximum admissible sampling interval and the maximum communication delay, respectively.*

3.2.2 Asynchronous communication with varying delays

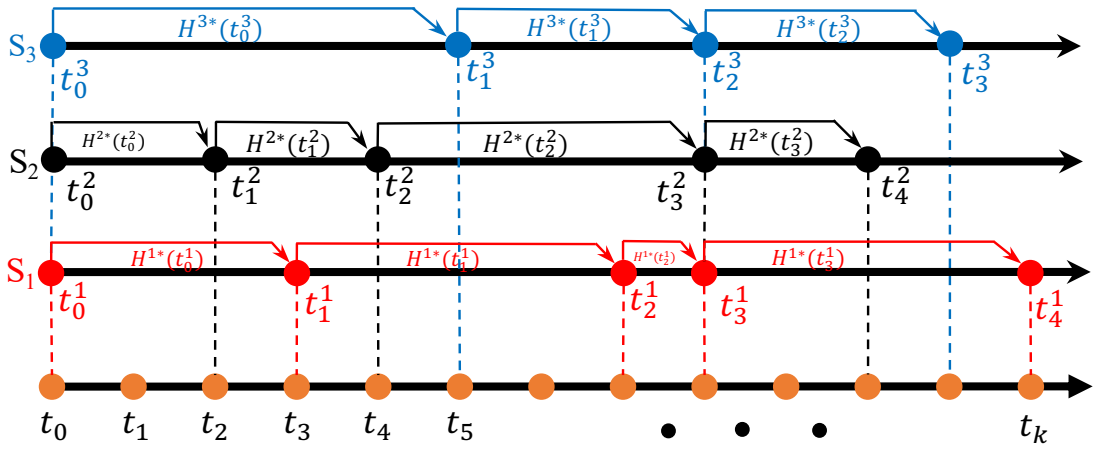

Figure 3.1: An asynchronous MAS with three agents (S_1, S_2 and S_3).

As illustrated in Figure 3.1, each agent is allowed to asynchronously receive and broadcast the predicted system state sequence with a global time stamp t_k. The distributed self-triggered scheduler determines local triggering instants (denoted by the dots in the top three lines). The bottom line represents the global time instants.

At time t_k^i, agent i, $i \in \mathcal{V}$ receives its neighbors' predicted state sequence $\boldsymbol{x}_j^b(t_k^j), j \in \mathcal{N}_i$, and then broadcasts the newest predicted state sequence $x_i^b(\cdot|t_k^i)$ to its neighbors. The newest broadcast states of agent i at t_k^i is constructed as

$$x_i^b(s|t_k^i) = \begin{cases} x_i^*(s|t_k^i), & s \in \mathbb{N}_{[0,N)}, \\ 0, & s \in \mathbb{N}_{[N,H^{i*}(t_k^i)+\bar{\tau}+N]}, \end{cases} \tag{3.2}$$

where $x_i^*(s|t_k^i)$ denotes the optimal predicted system state and $H^{i*}(t_k^i) \in \mathbb{N}_{[1,\bar{H}]}$ denotes the optimal triggering interval at t_k^i. The calculation of $x_i^*(s|t_k^i)$ and $H^{i*}(t_k^i)$ will be introduced in Section 3.3.

Remark 3.1. *Note that all agents are cooperatively stabilized towards their separate terminal sets, which share the same setpoint. Hence, the tail of the broadcast predicted states of agent i, $i \in \mathcal{V}$ can be supplemented with zero as in* (3.2)*. By choosing reasonable weighting matrices of the cost function and the terminal control law, the third inequality in* **Assumption 3.2** *holds for the MAS.*

Now we describe the bounded time-varying communication delays for the asynchronous MAS. Let $\boldsymbol{x}_j^b(t_k^{ij})$ represent the newest message broadcast by agent j, $j \in \mathcal{N}_i$ at t_k^{ij}, where $t_k^{ij} := \max\{t_k^j \in \mathbb{N}_{\geq 0} \mid \ t_k^j < t_k^i\}$. The communication delays are categorized into the following two cases:
Case 1: $0 \leq \tau_k^{ij} \leq t_k^i - t_k^{ij}$, i.e., the newest message $\boldsymbol{x}_j^b(t_k^{ij})$ of agent j is received by agent i at t_k^i;
Case 2: $t_k^i - t_k^{ij} < \tau_k^{ij} \leq \bar{\tau}$, i.e., the newest message $\boldsymbol{x}_j^b(t_k^{ij})$ cannot be received by agent i at t_k^i, therefore, agent i can only utilize the message $\boldsymbol{x}_j^b(t_{k-1}^{ij})$ broadcast at previous triggering instants, which includes the neighbor j's state sequence $x_j^b(s|t_{k-1}^{ij}), s \in \mathbb{N}_{[0,H^{i*}(t_{k-1}^{ij})+\bar{\tau}+N]}$.

Based on the above cases, the predicted state sequence $\boldsymbol{x}_j(t_k^i)$ of the neighbor $j \in \mathcal{N}_i$ used in the local distributed optimization problem $\mathcal{P}_i$ of agent i in the next section can be constructed as

$$\boldsymbol{x}_j(t_k^i) := \{x_j^b(0|t_k^i), x_j^b(1|t_k^i), \cdots, x_j^b(N-1|t_k^i)\}. \tag{3.3}$$

3.2.3 Problem formulation

Our objective is to design a robust DMPC method for the nonlinear constrained MAS with uncertainties and bounded time-varying communication delays, such that all

agents are cooperatively stabilized. Furthermore, we aim to develop a distributed self-triggered scheduler under this control framework to reduce the communication burden and the frequency of solving the corresponding distributed optimization problem.

3.3 Self-Triggered Min-Max DMPC

This section presents the min-max DMPC optimization problem. Furthermore, a distributed self-triggered scheduler for the nonlinear asynchronous MAS with bounded varying communication delays is designed.

3.3.1 Min-max DMPC optimization problem

3.3.1.1 The objective function design

At time t_k^i, each agent receives its neighbors' newest predicted state sequence $x_j^b(\cdot|t_k^j)$, $j \in \mathcal{N}_i$ defined in (3.2) and (3.3). Then, the following objective function is formulated for the DMPC optimization problem

$$\begin{aligned}
&J_{i,N}^{H^i(t_k^i)}(x_i(t_k^i), \boldsymbol{x}_{-i}(t_k^i), \boldsymbol{u}_i(t_k^i), \boldsymbol{d}_i(t_k^i)) \\
=&\sum_{s=0}^{H^i(t_k^i)-1} \frac{1}{\hbar_i} L_i(x_i(s|t_k^i), x_{-i}(s|t_k^i), u_i(s|t_k^i), d_i(s|t_k^i)) \\
&+ \sum_{s=H^i(t_k^i)}^{N-1} L_i(x_i(s|t_k^i), x_{-i}(s|t_k^i), u_i(s|t_k^i), d_i(s|t_k^i)) + F_i(x_i(N|t_k^i)),
\end{aligned}$$

in which N is the prediction horizon, $H^i(t_k^i)$ denotes the triggering interval, $\boldsymbol{u}_i(t_k^i) = \{u_i(0|t_k^i), \ldots, u_i(N-1|t_k^i)\}$ and $\boldsymbol{d}_i(t_k^i) = \{d_i(0|t_k^i), \ldots, d_i(N-1|t_k^i)\}$. The parameter $\hbar_i > 1$ makes a trade-off between the control performance (with respect to the optimal value of the objective function) and the communication load (in terms of the average sampling rate). $\boldsymbol{x}_{-i}(t_k^i) = \{\boldsymbol{x}_{i_1}(t_k^i), \ldots, \boldsymbol{x}_{i_{n_i}}(t_k^i)\}$ denotes the collection of the predicted state sequence of agent i's neighbors, with $i_q \in \mathcal{N}_i$, $q \in \mathbb{N}_{[1,n_i]}$, $x_{-i}(s|t_k^i) := \{x_{i_1}^b(s|t_k^i), \ldots, x_{i_{n_i}}^b(s|t_k^i)\}$, $s \in \mathbb{N}_{[0,N]}$.

The local stage cost function of agent i, $i \in \mathcal{V}$ is designed as

$$\begin{aligned}
&L_i(x_i(s|t_k^i), x_{-i}(s|t_k^i), u_i(s|t_k^i), d_i(s|t_k^i)) \\
=&\|x_i(s|t_k^i)\|_{Q_i}^2 + \|u_i(s|t_k^i)\|_{R_i}^2 + \sum_{j\in\mathcal{N}_i} \|x_i(s|t_k^i) - x_j(s|t_k^i)\|_{Q_{ij}}^2,
\end{aligned}$$

in which the weighting matrices Q_i and Q_{ij} are symmetric and positive definite; R_i is symmetric and positive definite. Intuitively, the coupling cost term $\|x_i(s|t_k^i) - x_j(s|t_k^i)\|_{Q_{ij}}^2$, $j \in \mathcal{N}_i$ makes agents to achieve cooperation. The local terminal cost function is designed as

$$F_i(x_i(N|t_k^i)) = \|x_i(N|t_k^i)\|_{P_i}^2,$$

where the weighting matrix P_i is symmetric and positive definite.

Assumption 3.3. *For agent i, $i \in \mathcal{V}$, the local decoupled terminal set $\Omega_i \subseteq \mathbb{X}_i$ is an RPI set with a local feedback controller $\kappa_i(x_i(t)) \in \mathbb{U}_i$, $t \in \mathbb{N}_{\geq 0}$. There exist a $\mathcal{K}$ function $\sigma_i(\cdot)$ and a constant $c_4 \in \mathbb{R}_{\geq 0}$ such that*

$$F_i(x_i(t+1)) - F_i(x_i(t)) \leq -L_i(x_i(t), x_{-i}(t), \kappa_i(x_i(t)), d_i(t)) + \epsilon_i,$$

where $\epsilon_i = \sigma_i(\|w_i(t)\|) + c_4$, $x_{-i}(t) = 0$, for all $x_i(t) \in \Omega_i$ and $d_i(t) \in \mathbb{D}_i$.

When $x_i(N|t_k^i) \in \Omega_i$, from the definition of $x_j^b(\cdot|t_k^j)$ in (3.2), we know that the states of its neighbors $x_j(N|t_k^i) = x_j(N + t_k^i - t_k^j|t_k^j) = 0$, $j \in \mathcal{N}_i$. **Assumption** 3.3 is valid, and a similar assumption for the single system can be found in [116].

3.3.1.2 The distributed min-max MPC optimization problem

At time t_k^i, agent i solves the following min-max DMPC optimization problem $\mathcal{P}_i$

$$\begin{aligned}
&\min_{u_i(s|t_k^i)} \Big\{ \max_{d_i(s|t_k^i) \in \mathbb{D}_i} \{\bar{J}_{i,N}^{H^i}(x_i(t_k^i), \boldsymbol{x}_{-i}(t_k^i), u_i(s|t_k^i), d_i(s|t_k^i))\}, \\
&\text{such that } x_i(H^i|t_k^i) \in \mathbb{X}_i^{N-H^i}(\Omega_i), \forall d_i(s|t_k^i) \in \mathbb{D}_i \Big\} \\
&\quad \text{s.t. } x_i(s+1|t_k^i) = f(x_i(s|t_k^i), u_i(s|t_k^i), d_i(s|t_k^i)), \\
&\qquad x_i(0|t_k^i) = x_i(t_k^i), && \text{(3.4a)} \\
&\qquad u_i(s|t_k^i) \in \mathbb{U}_i, && \text{(3.4b)} \\
&\qquad x_i(s|t_k^i) \in \mathbb{X}_i, && \text{(3.4c)} \\
&\qquad \|x_i(s|t_k^i) - x_i^b(s + t_k^i - t_{k-1}^i|t_{k-1}^i)\| \leq \Delta_i, && \text{(3.4d)}
\end{aligned}$$

where the triggering interval $H^i(t_k^i)$ is abbreviated as H^i in the following, $s \in \mathbb{N}_{[0,H^i)}$, $\Omega_i := \{x_i \in \mathbb{X}_i \mid \|x_i\|_{P_i} \leq \rho_i, \rho_i \in \mathbb{R}_{\geq 0}\}$ is the terminal set, $\Delta_i \in \mathbb{R}_{\geq 0}$ is a design parameter and $V_{i,N}^{H^i}(x_i(t_k^i), \boldsymbol{x}_{-i}(t_k^i))$ denotes the optimal value of the objective function

of the DMPC optimization $\mathcal{P}_i$.

$$\begin{aligned}
&\bar{J}_{i,N}^{H^i}(x_i(t_k^i), \boldsymbol{x}_{-i}(t_k^i), u_i(s|t_k^i), d_i(s|t_k^i)) \\
&= \sum_{s=0}^{H^i-1} \frac{1}{\hbar_i} L_i(x_i(t_k^i), x_{-i}(s|t_k^i), u_i(s|t_k^i), d_i(s|t_k^i)) \\
&\quad + V_{i,N-H^i}(x_i(H^i|t_k^i), x_{-i}(H^i|t_k^i)),
\end{aligned}$$

with

$$\begin{aligned}
&V_{i,\ell}(x_i(s|t_k^i), x_{-i}(s|t_k^i)) \\
&= \min_{\mu_{i,\ell}(s|t_k^i)\in\mathbb{U}_i} \Big\{ \max_{d_i(s|t_k^i)\in\mathbb{D}_i} \{L_i(x_i(s|t_k^i), x_{-i}(s|t_k^i), \mu_{i,\ell}(s|t_k^i), d_i(s|t_k^i)) \\
&\quad + V_{i,\ell-1}(f(x_i(s|t_k^i), \mu_{i,\ell}(s|t_k^i), d_i(s|t_k^i)), x_{-i}(s+1|t_k^i))\}, \\
&\quad \text{such that } x_i(s|t_k^i) \in \mathbb{X}_i^{\ell}(\Omega_i), \\
&\quad f(x_i(s|t_k^i), \mu_{i,\ell}(s|t_k^i), d_i(s|t_k^i)) \subseteq \mathbb{X}_i^{\ell-1}(\Omega_i), \\
&\quad \|x_i(s|t_k^i) - x_i^b(s + t_k^i - t_{k-1}^i|t_{k-1}^i)\| \le \Delta_i \Big\},
\end{aligned} \tag{3.5}$$

where $V_{i,0}(x_i(N|t_k^i)) = F_i(x_i(N|t_k^i))$ and $\mathbb{X}_i^{\ell}(\Omega_i)$ denotes the ℓ-step robustly stabilizable set of agent i, $\ell = N - s$. Solving the optimization problem $\mathcal{P}_i$ yields the optimal control sequence $\boldsymbol{u}_i^*(t_k^i) := \{u_i^*(0|t_k^i), \ldots, u_i^*(H^i-1|t_k^i), \mu_{i,\ell}^*(s|t_k^i), \ldots, \mu_{i,1}^*(N-1|t_k^i)\}$ and the optimal disturbance sequence $\boldsymbol{d}_i^*(t_k^i) = \{d_i^*(0|t_k^i), d_i^*(1|t_k^i), \ldots, d_i^*(N-1|t_k^i)\}$, where $u_i^*(s|t_k^i), s \in \mathbb{N}_{[0,H^i)}$ denotes the optimal open-loop control input and $\mu_{i,\ell}^*(s|t_k^i), s \in \mathbb{N}_{[H^i,N)}$ denotes the optimal feedback control law generated by solving (3.5) via dynamic programming.

Remark 3.2. *For the asynchronous MAS with uncertainties and bounded time-varying communication delays, agent i, $i \in \mathcal{N}_j$ may sample its local system states and broadcast its predicted states multiple times during the period $[t_k^j, t_{k+1}^j]$. In this case, the constraint* (3.4d)*, which restricts the deviation between the current predicted states and previously predicted states at the same future time instant, is used to ensure the closed-loop stability. A similar constraint is exploited for the synchronous MAS over the delay-free communication networks [19].*

3.3.2 Distributed self-triggered scheduler

A distributed self-triggered scheduler is designed to generate a local triggering instant sequence $\{t_k^i\}$. The triggering condition is constructed based on the local system states and the newest neighbors' predicted state sequences. Motivated by [83], the

distributed self-triggered scheduler for agent i is designed as

$$\begin{aligned} t_{k+1}^i &= t_k^i + H^{i*}(t_k^i), \\ H^{i*}(t_k^i) &= \max\{H^i \in \mathbb{N}_{[1,\bar{H}]} \mid V_{i,N}^{H^i}(x_i(t_k^i), \boldsymbol{x}_{-i}(t_k^i)) \\ &\qquad \leq V_{i,N}^{1}(x_i(t_k^i), \boldsymbol{x}_{-i}(t_k^i))\}, \end{aligned} \tag{3.6}$$

where $t_0^i = 0$, $H^{i*}(t_k^i)$ denotes the maximum triggering interval of agent i at time t_k^i. $H^{i*}(t_k^i)$ will be abbreviated as H^{i*} hereafter. Applying the first H^{i*} open-loop control inputs $\boldsymbol{u}_i^{\mathrm{mpc}}(t_k^i) := u_i^*(s|t_k^i)$, $s \in \mathbb{N}_{[0,H^{i*})}$ to the system (3.1) yields the following closed-loop system

$$x_i(t_k^i + s + 1) = f(x_i(t_k^i + s), u_i^*(s|t_k^i), d_i(t_k^i + s)). \tag{3.7}$$

and $\boldsymbol{d}_i^a(t_k^i) = \{(d_i(t_k^i), d_i(t_k^i + 1), \ldots, d_i(t_k^i + H^{i*} - 1)\}$ is the actual disturbance sequence.

Remark 3.3. *Note that the self-triggered scheduler* (3.6) *for the decoupled MAS is distributed, which is consistent with the min-max DMPC optimization problem* $\mathcal{P}_i$*. In other words, based on the local measurements and the neighboring latest broadcasting predicted state sequences, the self-triggered scheduler determines the next triggering instant, and solving the DMPC optimization problem generates the optimal control inputs.*

3.3.3 Self-triggered asynchronous min-max DMPC algorithm

The overall self-triggered asynchronous min-max DMPC algorithm for the MAS is summarized in **Algorithm 1**.

Algorithm 1 Self-triggered asynchronous min-max DMPC

Require: For agent i, $i \in \mathcal{V}$, the weighting matrices Q_i, Q_{ij}, R_i and P_i; the prediction horizon N, the terminal set Ω_i, the design parameter Δ_i, the initial state $x_i(t_k^i)$ and other related parameters. Set $k = 0$, $t_k^i = 0$, $H^i(t_k^i) = 1$, $x_i^b(\cdot|t_k^i) = 0$.

1: **while** The control action is not stopped **do**
2: Sample the system state $x_i(t_k^i)$;
3: Receive the newest predicted state sequence of neighbors $\boldsymbol{x}_j^b(t_k^{ij})$, $j \in \mathcal{N}_i$;
4: Construct the state sequence $\boldsymbol{x}_j(t_k^i)$ as in (3.3);
5: Let $H^i(t_k^i) = 1$, solve $\mathcal{P}_i$ to generate $u_i^*(t_k^i)$ and $V_{i,N}^1$, then set $H^i(t_k^i) = \bar{H}$;
6: Solve $\mathcal{P}_i$ in (3.4) to generate $u_i^*(t_k^i)$ and $V_{i,N}^{H^i}$;
7: **if** the inequality $V_{i,N}^{H^i} > V_{i,N}^1$ is satisfied **then**
8: $H^i(t_k^i) = H^i(t_k^i) - 1$; Go to Step 6;
9: **else**
10: Generate the optimal triggering interval $H^{i*} = H^i(t_k^i)$ and $V_{i,N}^{H^{i*}}$;
11: **end if**
12: Broadcast the predicted state sequence $\boldsymbol{x}_i^b(t_k^i)$ as in (3.2) to its neighbors;
13: Apply control input $\boldsymbol{u}_i^{\mathrm{mpc}}(t_k^i)$ to agent i;
14: $t_{k+1}^i = t_k^i + H^{i*}$, $k = k + 1$;
15: **end while**

Note that the distributed optimization problem $\mathcal{P}_i$ is solved without considering the constraint (3.4d) in the initialization step. Besides, for agent i, the predicted states of neighbors are assumed to be zeros over the period $[t_0^i, t_0^i + N]$, and the communication delay at t_0^i is zero, i.e., $\tau_0^{ij} = 0$.

3.4 Theoretical Analysis

This section shows that the proposed self-triggered min-max DMPC algorithm is recursively feasible, and the closed-loop MAS under the proposed algorithm is ISpS at triggering instants.

A technical lemma is presented before proceeding to the feasibility analysis.

Lemma 3.1. *Suppose that **Assumptions 3.1** and **3.2** are satisfied. If the optimization problem $\mathcal{P}_i$ is feasible at t_k^i, and the condition*

$$\Delta_i \geq \max\{\nu^{N-1-\bar{H}}\bar{\phi}, \rho_i/\underline{\lambda}(P_i^{1/2})\} \tag{3.8}$$

holds, with $\bar{\phi} = 2\sum_{s=0}^{\bar{H}+t_k^i-t_\tau^i} \nu^s \xi \bar{d}$ *and* $t_\tau^i \in [t_k^i - \bar{H}, t_k^i]$. *Then, it holds that*

$$\|\tilde{x}_i(s|t_{k+1}^i) - x_i^b(t_{k+1}^i + s - t_k^i|t_k^i)\| \leq \Delta_i, \tag{3.9}$$

with $s \in \mathbb{N}_{[0,N]}, t_{k+1}^i = t_k^i + H^{i*}$.

Proof. For $s \in \mathbb{N}_{[N-H^{i*},N]}$, it follows from (3.2) that $x_i^b(t_{k+1}^i + s - t_\tau^i|t_\tau^i) = 0$, and we have

$$\|\tilde{x}_i(s|t_{k+1}^i) - x_i^b(t_{k+1}^i + s - t_\tau^i|t_\tau^i)\| = \|\tilde{x}_i(s|t_{k+1}^i)\|.$$

Using the condition in (3.8), one obtains $\|\tilde{x}_i(s|t_{k+1}^i)\| \leq \rho_i/\underline{\lambda}(P_i^{1/2}) \leq \Delta_i$.

When $s = 0$, by **Assumption 3.1**, we get

$$\begin{aligned}
&\|\tilde{x}_i(0|t_{k+1}^i) - x_i^b(t_{k+1}^i - t_\tau^i|t_\tau^i)\| \\
=&\|f(x_i(t_{k+1}^i - 1), u_i^*(t_{k+1}^i - 1 - t_\tau^i|t_\tau^i), d_i(t_{k+1}^i - 1)) \\
&- f(x_i^*(t_{k+1}^i - 1 - t_\tau^i|t_\tau^i), u_i^*(t_{k+1}^i - 1 - t_\tau^i|t_\tau^i), d_i^*(t_{k+1}^i - 1 - t_\tau^i|t_\tau^i))\| \\
\leq&\nu\|x_i(t_{k+1}^i - 1) - x_i^*(t_{k+1}^i - 1 - t_\tau^i|t_\tau^i)\| + \xi\|d_i(t_{k+1}^i - 1) - d_i^*(t_{k+1}^i - 1 - t_\tau^i|t_\tau^i)\| \\
\leq&\nu\|x_i(t_{k+1}^i - 1) - x_i^*(t_{k+1}^i - 1 - t_\tau^i|t_\tau^i)\| + 2\xi\bar{d}.
\end{aligned}$$

Then, using $x_i(t_\tau^i) = x_i^b(0|t_\tau^i)$, we have

$$\|\tilde{x}_i(0|t_{k+1}^i) - x_i^b(t_{k+1}^i - t_\tau^i|t_\tau^i)\| \leq 2\sum_{s=0}^{t_{k+1}^i - t_\tau^i} \nu^s \xi \bar{d} = \phi.$$

Next, we establish the upper bound of $\|\tilde{x}_i(s|t_{k+1}^i) - x_i^b(t_{k+1}^i + s - t_k^i|t_k^i)\|$ for $s \in \mathbb{N}_{(0,N-H^{i*})}$

$$\begin{aligned}
&\|\tilde{x}_i(s|t_{k+1}^i) - x_i^b(t_{k+1}^i + s - t_\tau^i|t_\tau^i)\| \\
=&\|f(\tilde{x}_i(s-1|t_{k+1}^i), u_i^*(t_{k+1}^i + s - 1 - t_\tau^i|t_\tau^i), d_i^*(t_{k+1}^i + s - 1 - t_\tau^i|t_\tau^i)) \\
&- f(x_i^*(t_{k+1}^i - 1 - t_\tau^i|t_\tau^i), u_i^*(t_{k+1}^i - 1 - t_\tau^i|t_\tau^i), d_i^*(t_{k+1}^i - 1 - t_\tau^i|t_\tau^i))\| \\
\leq&\nu\|\tilde{x}_i(s-1|t_{k+1}^i) - x_i^*(t_{k+1}^i + s - 1 - t_\tau^i|t_\tau^i)\|,
\end{aligned}$$

which implies

$$\begin{aligned}
&\|\tilde{x}_i(N-H^{i*}-1|t^i_{k+1})-x^b_i(t^i_{k+1}+N-H^{i*}-1-t^i_\tau|t^i_\tau)\|\\
\leq&\nu^{N-1-H^{i*}}\|\tilde{x}_i(0|t^i_{k+1})-x^b_i(t^i_{k+1}-t^i_\tau|t^i_\tau)\|\\
\leq&\nu^{N-1-H^{i*}}\phi\\
\leq&\nu^{N-1-\bar{H}}\bar{\phi}.
\end{aligned}$$

Based on the condition $\Delta_i \geq \max\{\nu^{N-1-\bar{H}}\bar{\phi},\, \rho_i/\underline{\lambda}(P_i^{1/2})\}$, we have

$$\|\tilde{x}_i(s|t^i_{k+1})-x^b_i(t^i_{k+1}+s-t^i_\tau|t^i_\tau)\| \leq \Delta_i.$$

Then the inequality (3.9) holds, thereby concluding the proof. □

Following the idea in [78], we provide the following lemma to show the monotonicity property of the value function for the optimization problem $\mathcal{P}_i$, which serves as a sufficient condition for the closed-loop stability.

Lemma 3.2. *Suppose that* ***Assumption 3.3*** *holds. Then,*

$$\begin{aligned}
&V_{i,\ell+1}(x_i(t),x_{-i}(t))-V_{i,\ell}(x_i(t),x_{-i}(t))\\
\leq&\max_{d_i}\{V_{i,\ell}(x_i(t+1),x_{-i}(t+1))-V_{i,\ell-1}(x_i(t+1),x_{-i}(t+1))\},
\end{aligned}\tag{3.10}$$

where $t\in\mathbb{N}_{\geq 0}$, $\forall x_i(t)\in\mathbb{X}_i^\ell(\Omega_i)$, $\forall x_j(t)\in\mathbb{X}_j^\ell(\Omega_j), j\in\mathcal{N}_i$, $\forall d_i\in\mathbb{D}_i$. *In addition, we have that*

$$V_{i,\ell}(x_i(t),x_{-i}(t))-V_{i,\ell-1}(x_i(t),x_{-i}(t))\leq\epsilon_i$$

and

$$V_{i,\ell}(x_i(t),x_{-i}(t))\leq V_{i,0}(x_i(t))+\ell\epsilon_i.$$

Proof. For simplicity, let x_i denote $x_i(t)$ and x_i^+ denote $x_i(t+1)$ in the following. Since $x_i\in\Omega_i$, $x_j\in\Omega_j, j\in\mathcal{N}_i$, $V_{i,0}(x_i)=F_i(x_i)$, by **Assumption 3.3**, it follows

$$\begin{aligned}
&V_{i,1}(x_i,x_{-i})-V_{i,0}(x_i)\\
\leq&\max_{d_i}\{L_i(x_i,x_{-i},\kappa_i(x_i),d_i)+V_{i,0}(x_i^+)-V_{i,0}(x_i)\}\\
=&\max_{d_i}\{L_i(x_i,x_{-i},\kappa_i(x_i),d_i)+F_i(x_i^+)-F_i(x_i)\}\\
\leq&\epsilon_i.
\end{aligned}\tag{3.11}$$

When $x_i \in \mathbb{X}_i^{\ell}(\Omega_i)$, agent i satisfies $x_i^+ = f(x_i, \mu_{i,\ell}^*, d_i)$. For the agent j, $j \in \mathcal{N}_i$, it can be observed that the transmitted state sequence in (3.2) satisfies $x_j \in \mathbb{X}_j^{\ell}(\Omega_j)$, and $x_j^+ = f(x_j, \mu_{j,\ell}^*, d_j)$. Moreover,

$$\begin{aligned}
&V_{i,\ell+1}(x_i, x_{-i}) - V_{i,\ell}(x_i, x_{-i}) \\
=&\max_{d_i} \Big\{ L_i(x_i, x_{-i}, \mu_{i,\ell+1}^*, d_i) + V_{i,\ell}(f(x_i, \mu_{i,\ell+1}^*, d_i), x_{-i}^+) \Big\} \\
&- \max_{d_i} \Big\{ L_i(x_i, x_{-i}, \mu_{i,\ell}^*, d_i) + V_{i,\ell-1}(f(x_i, \mu_{i,\ell}^*, d_i), x_{-i}^+) \Big\} \\
\leq&\max_{d_i} \Big\{ L_i(x_i, x_{-i}, \mu_{i,\ell}^*, d_i) + V_{i,\ell}(f(x_i, \mu_{i,\ell}^*, d_i), x_{-i}^+) \Big\} \\
&- \max_{d_i} \Big\{ L_i(x_i, x_{-i}, \mu_{i,\ell}^*, d_i) + V_{i,\ell-1}(f(x_i, \mu_{i,\ell}^*, d_i), x_{-i}^+) \Big\} \\
\leq&\max_{d_i} \Big\{ V_{i,\ell}(x_i^+, x_{-i}^+) - V_{i,\ell-1}(x_i^+, x_{-i}^+) \Big\}.
\end{aligned} \tag{3.12}$$

By induction, one gets $V_{i,\ell}(x_i, x_{-i}) - V_{i,\ell-1}(x_i, x_{-i}) \leq \epsilon_i$. By summing up inequalities (3.11) and (3.12), one that the inequality $V_{i,\ell}(x_i, x_{-i}) \leq V_{i,0}(x_i) + \ell\epsilon_i$ holds. □

Lemma 3.3. *For the min-max DMPC optimization problem $\mathcal{P}_i$ in* (3.4)*, it holds that*

$$V_{i,N}^1(x_i(t_k^i), \boldsymbol{x}_{-i}(t_k^i)) \leq V_{i,N}(x_i(t_k^i), \boldsymbol{x}_{-i}(t_k^i)),$$

in which

$$\begin{aligned}
&V_{i,N}(x_i(t_k^i), \boldsymbol{x}_{-i}(t_k^i)) \\
=&J_{i,N}(x_i(t_k^i), \boldsymbol{x}_{-i}(t_k^i), \boldsymbol{u}_i^*(t_k^i), \boldsymbol{d}_i^*(t_k^i)) \\
=&\sum_{s=0}^{N-1} L_i(x_i^*(s|t_k^i), x_{-i}(s|t_k^i), u_i^*(s|t_k^i), d_i^*(s|t_k^i)) + F_i(x_i^*(N|t_k^i)).
\end{aligned}$$

The proof of **Lemma 3.3** can follow the idea in [83], so it is omitted here. The recursive feasibility and the closed-loop stability of the perturbed MAS with the proposed algorithm are presented in what follows.

Theorem 3.1. *Suppose that **Assumptions 3.1**, **3.2** and **3.3** hold, and the optimization problem $\mathcal{P}_i$ is feasible at the initial time t_0^i. 1) Then, by application of **Algorithm 1**, the optimization problem $\mathcal{P}_i$ is recursively feasible at time $t_k^i, k \in \mathbb{N}_{\geq 1}$, if the condition in **Lemma 3.1** holds. 2) Furthermore, the closed-loop uncertain MAS with the self-triggered min-max DMPC strategy is ISpS at triggering instants.*

Proof. 1) **Feasibility**: For agent i, $i \in \mathcal{V}$, by assumption, there is a feasible solution

for the optimization problem $\mathcal{P}_i$ at t_k^i and the recursive feasibility for all subsequent triggering instants is proven by induction. The optimal control input sequence obtained at t_k^i is $\boldsymbol{u}_i^*(t_k^i) := \{u_i^*(0|t_k^i), \ldots, u_i^*(H^{i*}-1|t_k^i), \mu_{i,\ell}^*(H^{i*}|t_k^i), \ldots, \mu_{i,1}^*(N-1|t_k^i)\}$. The first H^{i*} open-loop control inputs are implemented to the system in (3.1). At time t_{k+1}^i, a candidate control input sequence $\tilde{\boldsymbol{u}}_i(t_{k+1}^i) := \{\tilde{u}_i(0|t_{k+1}^i), \tilde{u}_i(1|t_{k+1}^i), \ldots, \tilde{u}_i(N-1|t_{k+1}^i)\}$ is constructed as

$$\tilde{u}_i(s|t_{k+1}^i) = \begin{cases} \mu_{i,\ell}^*(H^{i*}+s|t_k^i), & s \in \mathbb{N}_{[0,N-H^{i*})}, \\ \kappa_i(\tilde{x}_i(s|t_{k+1}^i)), & s \in \mathbb{N}_{[N-H^{i*},N)}. \end{cases} \tag{3.13}$$

Then the corresponding system states become

$$\tilde{x}_i(s+1|t_{k+1}^i) = f_i(\tilde{x}_i(s|t_{k+1}^i), \tilde{u}_i(s|t_{k+1}^i), d_i^*(s+H^{i*}|t_k^i)), \tag{3.14}$$

where $\tilde{x}_i(0|t_{k+1}^i) = x_i(t_{k+1}^i)$. From **Assumption 3.3** and the optimal feedback control inputs calculated at the previous time instant t_k^i, we have $\tilde{u}_i(s|t_{k+1}^i) \in \mathbb{U}_i, s \in \mathbb{N}_{[0,N)}$, the control input constraint (3.4b) is satisfied. The remainder of recursive feasibility is to prove that the state constraint is satisfied. For $s \in \mathbb{N}_{[0,N-H^{i*}]}$, we have the candidate state $\tilde{x}_i(s|t_{k+1}^i) \in \mathbb{X}_i^{N-H^{i*}-s}(\Omega_i) \subset \mathbb{X}_i$; then, for $s \in \mathbb{N}_{(N-H^{i*},N]}$, under the terminal controller $\kappa_i(\tilde{x}_i(s|t_{k+1}^i))$ given in **Assumption 3.3**, the system state always belongs to the robust invariant set Ω_i. Thus, the system state constraint (3.4c) is fulfilled. From **Lemma 3.1**, the feasibility of the constraint (3.4d) is guaranteed. The recursive feasibility of the proposed algorithm is established.

2) **Stability**: To prove the closed-loop stability, we need to show that the optimal value function $V_{i,N}^{H^{i*}}$ is an ISpS Lyapunov function at triggering instants. Since the stage cost function L_i for agent i, $i \in \mathcal{V}$ is quadratic and matrices Q_i, Q_{ij} are positive definite, it can be derived that $L_i \geq \alpha_L(\|x_i(t_k^i)\|)$, where $\alpha_L(\|x_i(t_k^i)\|) = \underline{\lambda}(Q_i)\|x_i(t_k^i)\|^2$ is a $\mathcal{K}_\infty$ function. Then we obtain $V_{i,N}^{H^{i*}} \geq \alpha_L(\|x_i(t_k^i)\|)$. The similar way to establish the upper bound of $V_{i,N}^{H^{i*}}$ is adopted here [78, 83]. Define a set $B_{i,r} = \{x_i \in \mathbb{R}^n \mid \|x_i\| \leq r_i\} \subseteq \Omega_i$. Due to the compactness of $\mathbb{X}_i$ and $\mathbb{U}_i$, the optimal value of the min-max DMPC cost function is upper bounded, i.e., $V_{i,N}^{H^{i*}}(x_i(t_k^i), \boldsymbol{x}_{-i}(t_k^i)) \leq \bar{V}_{i,N}$. If $x_i(t_k^i) \in \Omega_i$, by **Assumption 3.3** and **Lemma 3.2**, one has

$$\begin{aligned} &F_i(x_i(s+1|t_k^i)) - F_i(x_i(s|t_k^i)) \\ \leq &- L_i(x_i(s|t_k^i), x_{-i}(s|t_k^i), \kappa_i(x_i(s|t_k^i)), d_i(s|t_k^i)) + \epsilon_i. \end{aligned} \tag{3.15}$$

By summing up (3.15) from $s=0$ to N, we get

$$\sum_{s=0}^{N-1} L_i(x_i(s|t_k^i), x_{-i}(s|t_k^i), \kappa_i(x_i(s|t_k^i)), d_i(s|t_k^i)) + F_i(x_i(N|t_k^i)) \leq F_i(x_i(t_k^i)) + N\epsilon_i,$$

where $F_i(x_i(t_k^i)) = F_i(x_i(0|t_k^i))$.

If the distributed triggering condition (3.6) is satisfied, i.e., $V_{i,N}^{H^{i*}}(x_i(t_k^i), \boldsymbol{x}_{-i}(t_k^i)) \leq V_{i,N}^{1}(x_i(t_k^i), \boldsymbol{x}_{-i}(t_k^i))$. In the view of the definition of the terminal cost function, we have $F_i(x_i(t_k^i)) \leq \bar{\alpha}_F(\|x_i(t_k^i)\|)$, where $\bar{\alpha}_F(\|x_i(t_k^i)\|) = \overline{\lambda}(P_i)\|x_i(t_k^i)\|^2$ is a $\mathcal{K}_\infty$ function. Then,

$$\begin{aligned} &V_{i,N}^{H^{i*}}(x_i(t_k^i), \boldsymbol{x}_{-i}(t_k^i)) \\ \leq &V_{i,N}^{1}(x_i(t_k^i), \boldsymbol{x}_{-i}(t_k^i)) \\ \leq &V_{i,N}(x_i(t_k^i), \boldsymbol{x}_{-i}(t_k^i)) \\ \leq &\bar{\alpha}_F(\|x_i(t_k^i)\|) + N\epsilon_i. \end{aligned} \tag{3.16}$$

The second inequality follows from the fact in **Lemma 3.3**. If $x_i(t_k^i) \in \mathbb{X}_i^N(\Omega_i)\backslash\Omega_i$, it implies that $\bar{\alpha}_F(\|x_i(t_k^i)\|) \geq \bar{\alpha}_F(r_i)$, where $\mathbb{X}_i^N(\Omega_i)$ is the N-step robustly stabilizable set of agent i. And thus

$$V_{i,N}^{H^{i*}}(x_i(t_k^i), \boldsymbol{x}_{-i}(t_k^i)) \leq \bar{V}_{i,N}\frac{\bar{\alpha}_F(\|x_i(t_k^i)\|)}{\bar{\alpha}_F(r_i)} \leq \theta_i\bar{\alpha}_F(\|x_i(t_k^i)\|) + N\epsilon_i, \tag{3.17}$$

where $\theta_i = \max\{1, \frac{\bar{V}_{i,N}}{\bar{\alpha}_F(r_i)}\}$.

At time t_k^i, the sequence of optimal control policies $\boldsymbol{u}_i^*(t_k^i)$ for the problem $\mathcal{P}_i$ can steer $x_i(t_k^i)$ of agent i, $i \in \mathcal{V}$ to the terminal set Ω_i in N steps under the disturbance sequence $\boldsymbol{d}_i^*(t_k^i) = \{d_i^*(0|t_k^i), \ldots, d_i^*(N-1|t_k^i)\}$. If the control inputs $\boldsymbol{u}_i^{\text{mpc}}(t_k^i)$ and the actual disturbance $\boldsymbol{d}_i^a(t_k^i)$ are applied, then agent i evolves to $x_i(t_{k+1}^i)$, where $\boldsymbol{d}_i^a(t_k^i) = \{d_i(t_k^i), d_i(t_k^i+1), \ldots, d_i(t_k^i+H^{i*}-1)\}$. For agent j, $j \in \mathcal{N}_i$, the broadcast state evolves to $x_j^*(H^{i*}|t_k^i)$ with the control inputs $u_j^*(s|t_k^i)$ and the disturbance input $d_j^*(s|t_k^i)$, $s \in \mathbb{N}_{[0,H^{i*})}$. Then, it is easy to obtain

$$\begin{aligned} &J_{i,N-H^{i*}}(x_i(t_{k+1}^i), \boldsymbol{x}_{-i}(t_{k+1}^i), \boldsymbol{\mu}_i^*(t_k^i), \boldsymbol{d}_i'(t_k^i)) \\ =&J_{i,N}^{H^{i*}}(x_i(t_k^i), \boldsymbol{x}_{-i}(t_k^i), \boldsymbol{u}_i^*(t_k^i), \boldsymbol{d}_i''(t_k^i)) - \frac{1}{\hbar_i}\sum_{s=0}^{H^{i*}-1} L_i(x_i(s|t_k^i), x_{-i}(s|t_k^i), u_i^*(s|t_k^i), \boldsymbol{d}_i^a(t_k^i)), \end{aligned} \tag{3.18}$$

where $\boldsymbol{\mu}_i^*(t_k^i) = \{\mu_{i,N-H^{i*}}^*(H^{i*}|t_k^i), \ldots, \mu_{i,1}^*(N-1|t_k^i)\}$, $\boldsymbol{d}_i'(t_k^i) = \{d_i^*(0|t_{k+1}^i), \ldots, d_i^*(N-H^{i*}-1|t_{k+1}^i)\}$ and $\boldsymbol{d}_i''(t_k) = \{d_i(t_k^i), \ldots, d_i(t_k^i+H^{i*}-1), d_i^*(0|t_{k+1}^i), \ldots, d_i^*(N-H^{i*}-$

$1|t_{k+1}^i)\}$. From (3.18), we have

$$\begin{aligned} &J_{i,N-H^{i*}}(x_i(t_{k+1}^i), \boldsymbol{x}_{-i}(t_{k+1}^i), \boldsymbol{\mu}_i^*(t_k^i), \boldsymbol{d}_i'(t_k^i)) \\ \leq &J_{i,N}^{H^{i*}}(x_i(t_k^i), \boldsymbol{x}_{-i}(t_k^i), \boldsymbol{u}_i^*(t_k^i), \boldsymbol{d}_i''(t_k^i)) - H^{i*}/\hbar_i \alpha_L(\|x_i(t_k^i)\|), \end{aligned} \tag{3.19}$$

Further, the system state $x_i(t_{k+1}^i)$ can be steered into the terminal set Ω_i in $N - H^{i*}$ steps by the candidate control input $\tilde{\boldsymbol{u}}_i(t_{k+1}^i)$. Then, it follows from the inequality (3.19) and **Assumption 3.3** that

$$\begin{aligned} &J_{i,N}(x_i(t_{k+1}^i), \boldsymbol{x}_{-i}(t_{k+1}^i), \tilde{\boldsymbol{u}}_i(t_{k+1}^i), \boldsymbol{d}_i^*(t_{k+1}^i)) \\ \leq &J_{i,N}^{H^{i*}}(x_i(t_k^i), \boldsymbol{x}_{-i}(t_k^i), \boldsymbol{u}_i^*(t_k^i), \boldsymbol{d}_i''(t_k^i)) - H^{i*}/\hbar_i \alpha_L(\|x_i(t_k^i)\|) + H^{i*}\epsilon_i, \end{aligned} \tag{3.20}$$

where $\boldsymbol{d}_i^*(t_{k+1}^i) = \{d_i^*(0|t_{k+1}^i), \ldots, d_i^*(N-1|t_{k+1}^i)\}$.

Consider the time-varying communication delays in **Case 2**, i.e., $t_{k+1}^i - t_{k+1}^{ij} < \tau_{k+1}^{ij} \leq \bar{\tau}$, the predicted states of neighbors transmitted at the previous triggering instant $\boldsymbol{x}_{-i}(t_{k+1}^i) = \{x_{-i}(H^{i*}|t_k^i), \ldots, x_{-i}(H^{i*}+N-1|t_k^i)\}$ will be used. Based on the triggering condition and **Lemma 3.3**, we obtain

$$\begin{aligned} &V_{i,N}^{H^{i*}(t_{k+1}^i)}(x_i(t_{k+1}^i), \boldsymbol{x}_{-i}(t_{k+1}^i)) \\ \overset{(3.6)}{\leq} &V_{i,N}^1(x_i(t_{k+1}^i), \boldsymbol{x}_{-i}(t_{k+1}^i)) \\ \leq &V_{i,N}(x_i(t_{k+1}^i), \boldsymbol{x}_{-i}(t_{k+1}^i)) \\ = &J_{i,N}(x_i(t_{k+1}^i), \boldsymbol{x}_{-i}(t_{k+1}^i), \boldsymbol{u}_i^*(t_{k+1}^i), \boldsymbol{d}_i^*(t_{k+1}^i)) \\ \leq &J_{i,N}(x_i(t_{k+1}^i), \boldsymbol{x}_{-i}(t_{k+1}^i), \tilde{\boldsymbol{u}}_i(t_{k+1}^i), \boldsymbol{d}_i^*(t_{k+1}^i)) \\ \overset{(3.20)}{\leq} &J_{i,N}^{H^{i*}}(x_i(t_k^i), \boldsymbol{x}_{-i}(t_k^i), \boldsymbol{u}_i^*(t_k^i), \boldsymbol{d}_i''(t_k^i)) - H^{i*}/\hbar_i \alpha_L(\|x_i(t_k^i)\|) + H^{i*}\epsilon_i \\ \leq &V_{i,N}^{H^{i*}}(x_i(t_k^i), \boldsymbol{x}_{-i}(t_k^i)) - H^{i*}/\hbar_i \alpha_L(\|x_i(t_k^i)\|) + H^{i*}\epsilon_i. \end{aligned} \tag{3.21}$$

The last inequality is derived from the fact that $\boldsymbol{d}_i''(t_k^i)$ is not the optimal solution of the min-max DMPC optimization problem $\mathcal{P}_i$.

Consider the time-varying communication delays in **Case 1**, i.e., $\tau_{k+1}^{ij} \leq t_{k+1}^i - t_{k+1}^{ij}$, the newest predicted states of neighbors $\boldsymbol{x}'_{-i}(t_{k+1}^i) = \{x_{-i}(0|t_{k+1}^i), \ldots, x_{-i}(N-1|t_{k+1}^i)\}$ will be received and used by agent i. Because of the triangle inequality and

the consistency constraint (3.4d), we have

$$\begin{aligned}
&\|x_i(s|t_{k+1}^i) - x_j(s|t_{k+1}^i)\| \\
\leq &\|x_i(s|t_{k+1}^i) - x_j^b(H^{i*}+s|t_k^i)\| + \|x_j(s|t_{k+1}^i) - x_j^b(H^{i*}+s|t_k^i)\| \\
\overset{(3.4d)}{\leq} &\|x_i(s|t_{k+1}^i) - x_j^b(H^{i*}+s|t_k^i)\| + \Delta_j.
\end{aligned} \tag{3.22}$$

Since $x_i(\cdot|t_k^i) \in \mathbb{X}_i$, there exists a constant $\Lambda_i > 0$ such that $\|x_i(s|t_k^i)\| \leq \Lambda_i$, $k \in \mathbb{N}_{\geq 0}$. Then it can be obtained that

$$\begin{aligned}
&\|x_i(s|t_{k+1}^i) - x_j(s|t_{k+1}^i)\|_{Q_{ij}}^2 \\
\leq &\|x_i(s|t_{k+1}^i) - x_j^b(H^{i*}+s|t_k^i)\|_{Q_{ij}}^2 + \|x_j(s|t_{k+1}^i) - x_j^b(H^{i*}+s|t_k^i)\|_{Q_{ij}}^2 \\
&+ 2\bar{\lambda}(Q_{ij})\|x_i(s|t_{k+1}^i) - x_j^b(H^{i*}+s|t_k^i)\| \cdot \|x_j(s|t_{k+1}^i) - x_j^b(H^{i*}+s|t_k^i)\| \\
\overset{(3.4d)}{\leq} &\|x_i(s|t_{k+1}^i) - x_j^b(H^{i*}+s|t_k^i)\|_{Q_{ij}}^2 + 4\bar{\lambda}(Q_{ij})\Lambda_i\Delta_j + \bar{\lambda}(Q_{ij})\Delta_j^2.
\end{aligned} \tag{3.23}$$

Based on the triggering condition and **Lemma 3.2**, we obtain that

$$\begin{aligned}
&V_{i,N}^{H^{i*}(t_{k+1}^i)}(x_i(t_{k+1}^i), \boldsymbol{x}'_{-i}(t_{k+1}^i)) \\
\overset{(3.6)}{\leq} &V_{i,N}^1(x_i(t_{k+1}^i), \boldsymbol{x}'_{-i}(t_{k+1}^i)) \\
\leq &V_{i,N}(x_i(t_{k+1}^i), \boldsymbol{x}'_{-i}(t_{k+1}^i)) \\
= &J_{i,N}(x_i(t_{k+1}^i), \boldsymbol{x}'_{-i}(t_{k+1}^i), \boldsymbol{u}_i^*(t_{k+1}^i), \boldsymbol{d}_i^*(t_{k+1}^i)) \\
\leq &J_{i,N}(x_i(t_{k+1}^i), \boldsymbol{x}'_{-i}(t_{k+1}^i), \tilde{\boldsymbol{u}}_i(t_{k+1}^i), \boldsymbol{d}_i^*(t_{k+1}^i)) \\
\overset{(3.23)}{\leq} &J_{i,N}(x_i(t_{k+1}^i), \boldsymbol{x}_{-i}(t_{k+1}^i), \tilde{\boldsymbol{u}}_i(t_{k+1}^i), \boldsymbol{d}_i^*(t_{k+1}^i)) + (N - H^{i*})\bar{\lambda}(Q_{ij}) \sum_{j\in\mathcal{N}_i}(4\Lambda_i\Delta_j + \Delta_j^2) \\
\overset{(3.20)}{\leq} &J_{i,N}^{H^{i*}}(x_i(t_k^i), \boldsymbol{x}_{-i}(t_k^i), \boldsymbol{u}_i^*(t_k^i), \boldsymbol{d}_i''(t_k^i)) - H^{i*}/\hbar_i\alpha_L(\|x_i(t_k^i)\|) + \Xi_i \\
\leq &V_{i,N}^{H^{i*}}(x_i(t_k^i), \boldsymbol{x}_{-i}(t_k^i)) - H^{i*}/\hbar_i\alpha_L(\|x_i(t_k^i)\|) + \Xi_i,
\end{aligned}$$

where $\Xi_i = (N - H^{i*})\bar{\lambda}(Q_{ij})\sum_{j\in\mathcal{N}_i}(4\Lambda_i\Delta_j + \Delta_j^2) + H^{i*}\epsilon_i$. By now, we have shown that the function $V_{i,N}^{H^{i*}}(x_i(t_k^i), \boldsymbol{x}_{-i}(t_k^i))$ is an ISpS Lyapunov function. Based on **Lemma 2.2**, it can be concluded that the closed-loop system in (3.7) is ISpS with respect to Ω_i at triggering instants [55, Theorem 2.5]. This concludes the proof. □

3.5 Numerical Example

In this section, five simulation tests are conducted to compare the control performance and communication load, i.e., periodic min-max DMPC (P-DMPC), self-triggered min-max DMPC without communication delays (ST-DMPC), self-triggered min-max DMPC with communication delays (ST-DMPC-D), periodic min-max decentralized MPC (P-DeMPC), and self-triggered min-max decentralized MPC without communication delays (ST-DeMPC). We follow the similar simulation setup from [83]. Agent i, $i \in \mathcal{V}$ is characterized by

$$\begin{cases} x_{i,1}^{+} = x_{i,1} + T(x_{i,2}), \\ x_{i,2}^{+} = x_{i,2} - \dfrac{T}{m_i}(k_i' e^{-x_{i,1}} x_{i,1} + h_i' x_{i,2} - u_i + v_i x_{i,2} - w_i), \end{cases}$$

where $m_i = 1\text{kg}$, $k_i' = 0.33\text{N/m}$, $h_i' = 1.1\text{Ns/m}$ and the sampling period $T = 0.3\text{s}$. The uncertainties are bounded by $-0.1 \leq w_i \leq 0.1$, $-0.15 \leq v_i \leq 0.15$. The control input and state constraints are given by $-4\text{N} \leq u_i \leq 4\text{N}$, $-1.95\text{m} \leq x_{i,1} \leq 1.95\text{m}$. According to [50, Lemma 3.2 and Lemma 3.3], the local Lipschitz constants can be calculated as $\nu = 1.23$ and $\xi = 0.42$.

The prediction horizon $N = 5$ and the largest triggering interval $\bar{H} = 4$. The communication delay is an integer, which is randomly generated on the interval $[1, \bar{\tau}]$, with $\bar{\tau}$=3. The weighting matrices are chosen as $Q_i = \text{diag}(0.6, 0.6)$, $Q_{ij} = \text{diag}(0.5, 0.5)$ and $R_i = 1$. The parameters $\hbar_i$ and Δ_i are chosen as $\hbar_i = 1.1$ and $\Delta_i = 3.58$. According to [83, 94], the terminal conditions are designed as $\Omega_i = \{x_i \mid \|x_i\|_{P_i} \leq \sqrt{6.0}\}$ with $P_i = [8.05, 2.90; 2.90, 3.48]$ and the terminal control law is chosen as $\kappa_i(x_i) = [-0.87, -1.04]x_i$. The feedback control policy is $\mu_i(x_i) = a\kappa_i(x_i) + b\|x_i\|^2 + c$, where $a, b, c \in \mathbb{R}$ are the decision variables for the optimization problem. The actual parametric uncertainty and external disturbance are $0.1\sin(t/4\pi)$ and $0.15\cos(t/3\pi)$, respectively. A digraph $\mathcal{G}$ is used described the communication network of the MAS, with $\mathcal{N}_1 = \{2\}$, $\mathcal{N}_2 = \{1, 5\}$, $\mathcal{N}_3 = \{2, 4\}$, $\mathcal{N}_4 = \{3\}$, $\mathcal{N}_5 = \{2\}$.

The initial states of five agents are given as $x_1 = [1.5, 0.7]^{\text{T}}$; $x_2 = [-0.5, -1.1]^{\text{T}}$; $x_3 = [-2.0, 0.5]^{\text{T}}$; $x_4 = [0.7, -1.0]^{\text{T}}$; $x_5 = [1.95, 0]^{\text{T}}$. Figure 3.2 depicts five agents' states and triggering instants without communication delays under the periodic min-max DMPC method and the proposed self-triggered min-max DMPC method. The control inputs obtained using the periodic min-max DMPC method and the proposed method for the asynchronous MAS are shown in Figure 3.3. The states and control

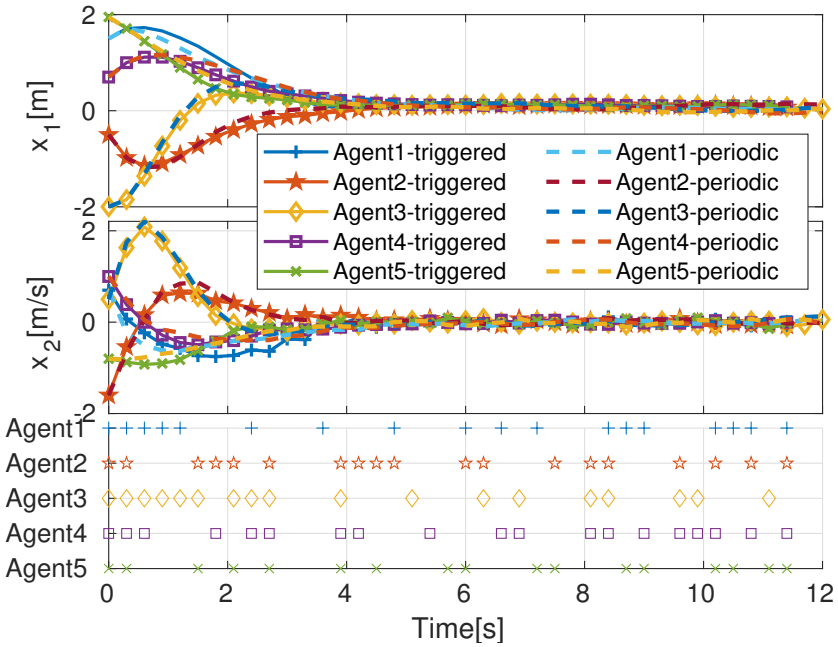

Figure 3.2: States and triggering instants of self-triggered and periodic DMPC without communication delays. Top: The displacements. Middle: The velocities. Bottom: The triggering instants.

inputs of five agents with time-varying communication delays are shown in Figures 3.4 and 3.5, respectively. Furthermore, the comparisons using the P-DeMPC and ST-DeMPC without communication are conducted. The corresponding results can be seen in Figures 3.6 and 3.7. It can be seen that the DMPC methods achieve better control performance than the decentralized MPC method.

Let $\mu(t) = \sum_{i\in\mathcal{V}} \|x_i(t)\|^2_{Q_i}/M$ denote the average stabilization error. Also, we denote $\psi(t) = \sum_{i\in\mathcal{V}} \sum_{j\in\mathcal{N}_i} \|x_i(t) - x_j(t)\|^2_{Q_{ij}}/M$ as the difference among agents. For the distributed MPC case, the coupling term $\|x_i - x_j\|_{Q_{ij}}, i \in \mathcal{V}, j \in \mathcal{N}_i$ is involved in the objective function. As shown in Figure 3.8 (bottom), agents with the DMPC approaches have a better cooperation performance before reaching stabilization than the decentralized MPC approaches. It is also shown that DMPC performs better than the DeMPC with respect to the stabilization control performance. Additionally, the average stabilization error and the cooperation difference of triggered DMPC/DeMPC decrease faster than periodic DMPC/DeMPC.

To further compare the control performance and communication load, the average sampling time and the control performance index are summarized in Table 3.1. Let $\bar{T} := \sum_{i\in\mathcal{V}} T_{\text{sim}}/Ms_i$ denote the average sampling time, where s_i is the total triggering

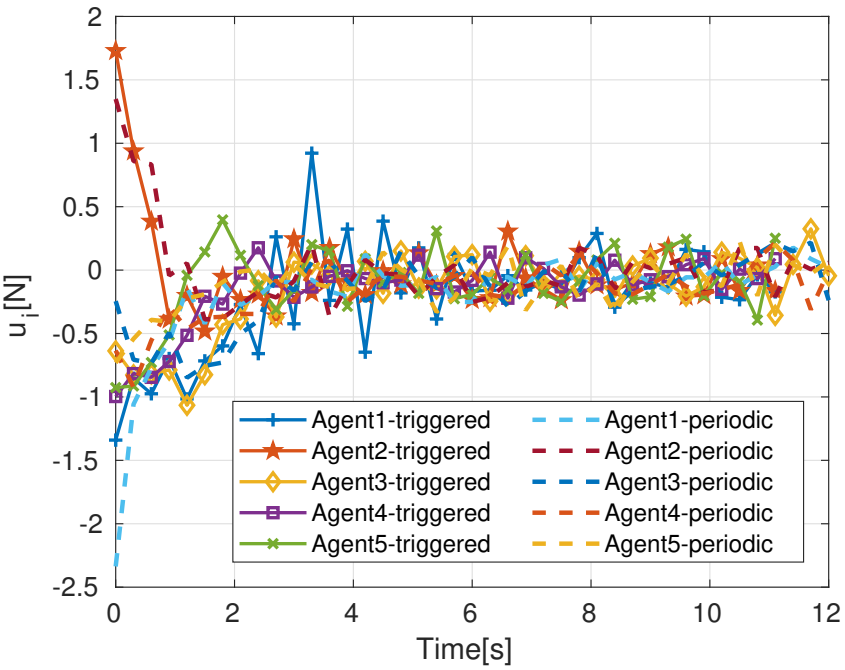

Figure 3.3: Control inputs u_i of self-triggered and periodic DMPC without delays.

times of agent i during the simulation time T_{sim}. The control performance index is defined by $\bar{J} = \sum_{i\in\mathcal{V}} J_i/M$, $J_i = \sum_{t=0}^{T_{\text{sim}}} \|x_i(t)\|^2_{Q_i} + \sum_{j\in\mathcal{N}_i} \|x_i(t) - x_j(t)\|^2_{Q_{ij}} + \|u_i(t)\|^2_{R_i}$. From Table 3.1, it can be seen that the total communication load of the MAS with delays and without delays are significantly reduced by using the proposed self-triggered min-max DMPC algorithm while achieving comparable control performance compared with periodic min-max DMPC.

Table 3.1: Performance comparison.

Method	Average sampling time	Control performance index
P-DMPC	0.3000	51.3016
ST-DMPC	0.6303	52.2235
ST-DMPC-D	0.6105	51.4515
P-DeMPC	0.3000	58.3909
ST-DeMPC	0.5878	59.1528

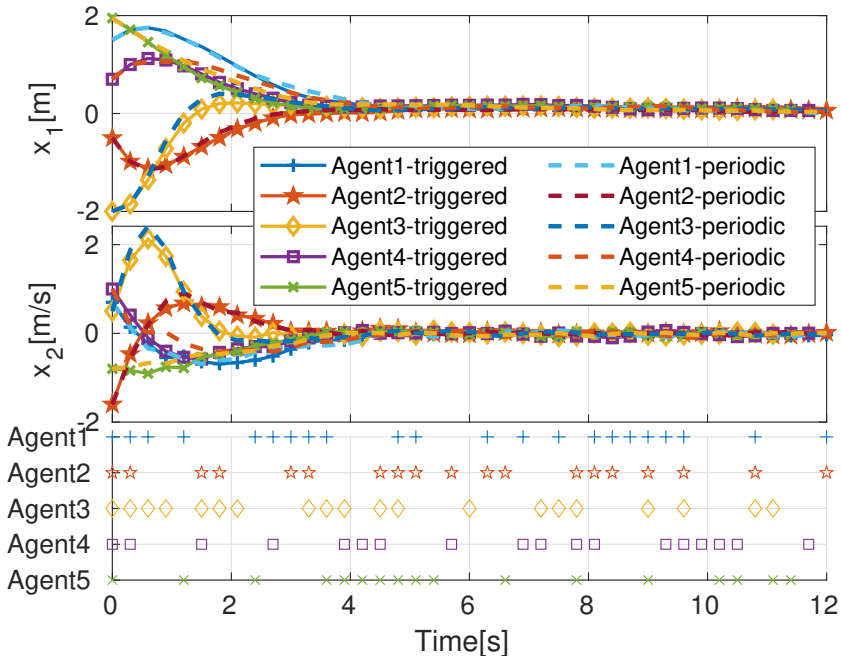

Figure 3.4: States and triggering instants of self-triggered and periodic DMPC with communication delays. Top: The displacements. Middle: The velocities. Bottom: The triggering instants.

3.6 Conclusion

This chapter proposed a self-triggered min-max DMPC algorithm for the nonlinear perturbed MAS with bounded time-varying communication delays. In this scheme, agents aperiodically sampled their system states and asynchronously broadcast the newest predicted states to neighbors based on the local triggering instants determined by the distributed self-triggered scheduler. Hence, the overall communication load was significantly reduced. A new consistency constraint, which forced the deviation between the newest predicted states and the previously predicted states to lie in a prescribed region, was incorporated into the local optimization problem. As a result, the cooperation among agents could be achieved despite the time-varying delays and asynchronous communication.

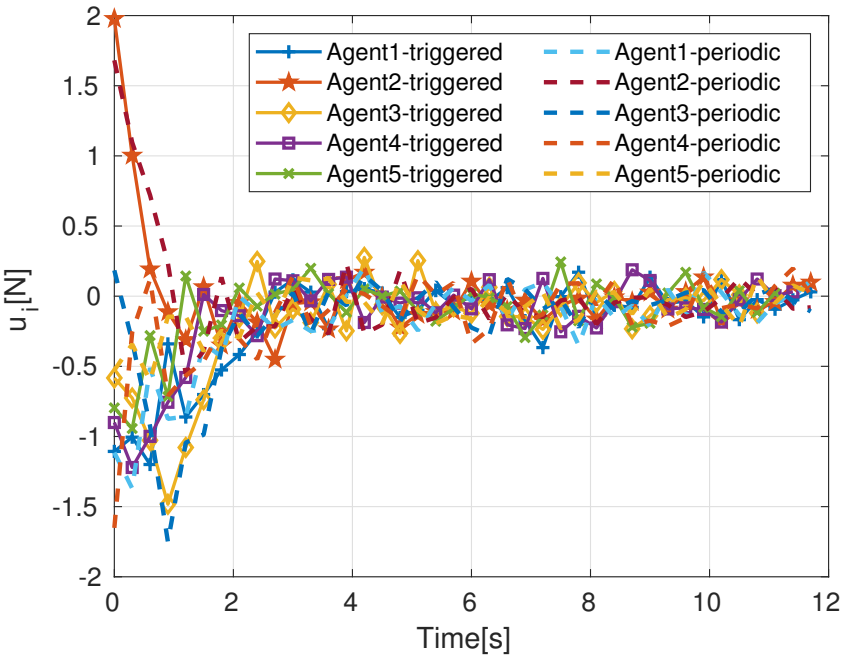

Figure 3.5: Control inputs of self-triggered and periodic DMPC with delays.

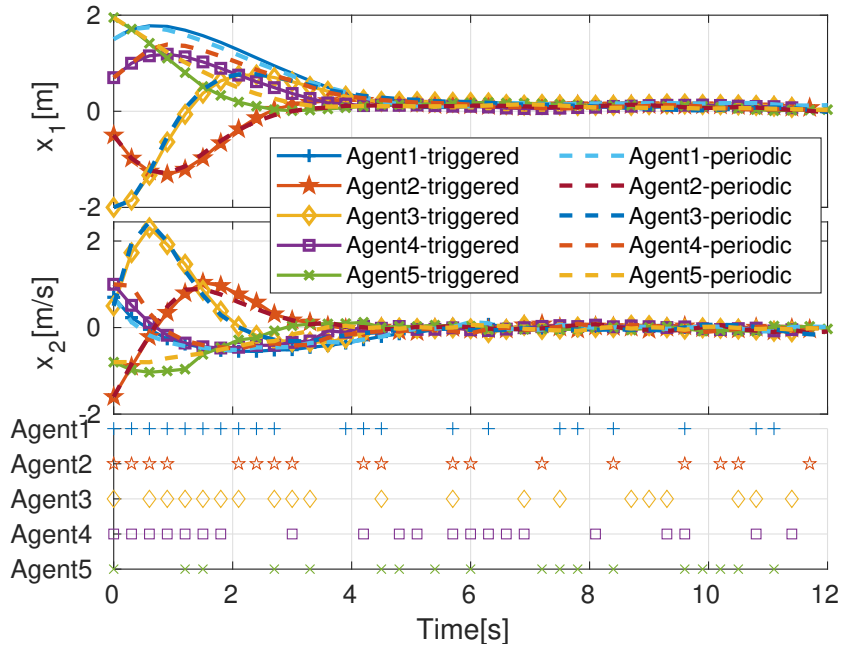

Figure 3.6: States and triggering instants of self-triggered and periodic Decentralized MPC without communication delays. Top: The displacements. Middle: The velocities. Bottom: The triggering instants.

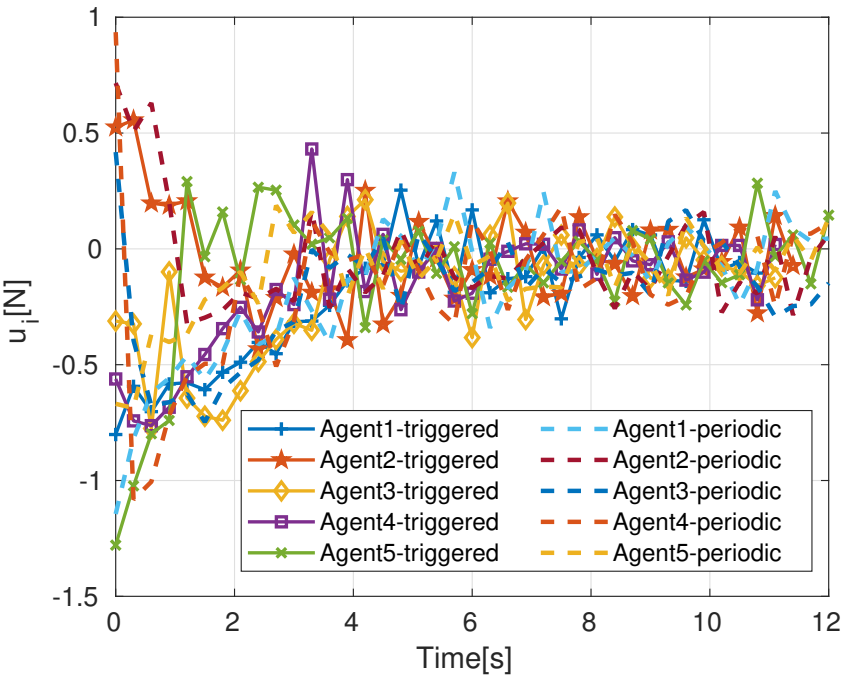

Figure 3.7: Control inputs of self-triggered and periodic Decentralized MPC without delays.

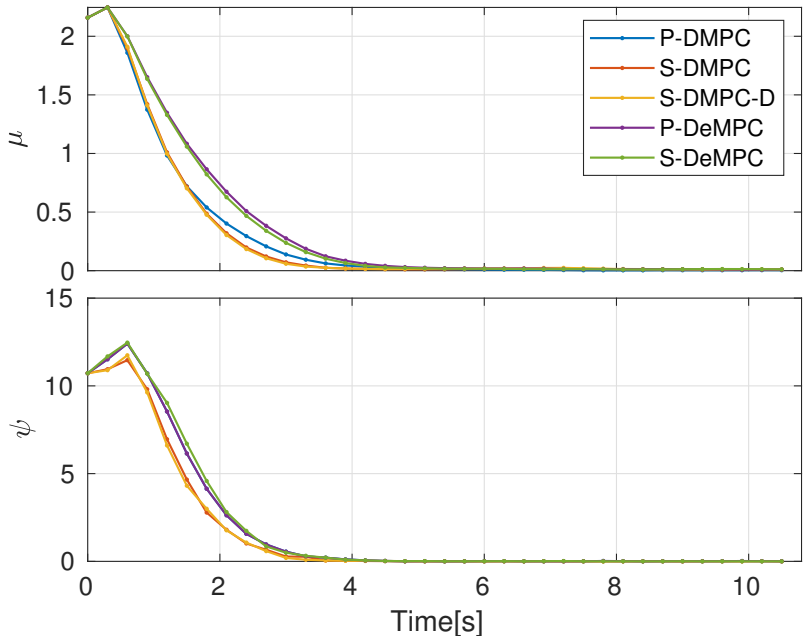

Figure 3.8: Top: The average stabilization error μ and Bottom: the difference ψ.

Chapter 4

A Robust Distributed Model Predictive Control Framework for Consensus of Multi-Agent Systems with Input Constraints and Varying Delays

4.1 Introduction

Consensus for the MAS requires all agents to achieve an agreement of common interest based on the local and neighboring information. To date, many decent consensus algorithms have exhibited impressive results; see [108, 109, 121] and the references therein. Nonetheless, reaching consensus becomes more challenging when the MAS is subject to constraints and varying communication delays in real-world applications. The aim of this chapter is to address the constrained consensus problem of the MAS with bounded time-varying communication delays.

Related work. The research on the constrained consensus can be found in [80, 81, 110, 120, 166, 169, 179]. Several works study the MAS with input saturation; see, e.g., [120, 166, 169, 179]. These solutions use hyperbolic tangent functions or the low gain feedback technique to construct bounded consensus protocols. More recently, the work [110] presents an output consensus scheme based on the reference governor and the maximal constraint admissible invariable set for heterogeneous linear the MAS

with input constraints and switching networks. For the case of the MAS subject to state constraints, the authors of [80] design the projection algorithms based on the projection operator theory, which attains consensus convergence while meeting state constraints. However, most of these aforementioned algorithms cannot explicitly optimize the consensus performance, which motivates the new consensus protocol design for the constrained MAS.

Another powerful class of methods for solving the constrained consensus problem is DMPC since it has remarkable advantages in handling practical constraints and providing optimal control performance for the MAS [9]. Most of the existing results focus on the cooperative stabilization problems of the MAS [19, 158]. Recent advances in DMPC algorithms lead to a profound interest in consensus problems, and previous works along this line include [23, 37, 66, 71, 154, 155, 175]. In [23], an MPC-based consensus protocol is proposed for multiple integrators over the time-varying networks, where the geometric properties of the optimal path are used to prove the consensus convergence. These two papers [66, 71] investigate the consensus problem of the first-order and general linear MAS and develop explicit consensus protocols via solving unconstrained DMPC problems. In [154], the optimal consensus problem of the asynchronous MAS with single- and double integrator dynamics is addressed via a DMPC-based algorithm. The authors further extend this method for the general linear MAS in [155], in which a consensus manifold is introduced such that the final consensus state and inputs are regarded as the augmented decision variables of the DMPC optimization problem. It is worth emphasizing that the aforementioned studies either focus on simple integrator dynamics [7, 23, 154] or consider unconstrained consensus problems [66, 71, 175]. However, the above algorithms typically require the simultaneous computation and communication at each time instant and neglect the transmission delays, rendering them not feasible in many practical scenarios.

Contribution. In this chapter, a robust DMPC-based consensus protocol is proposed to ensure that the general linear constrained MAS reach consensus despite bounded time-varying delays. The main contribution of this chapter is threefold.

- *Distributed consensus protocol for the constrained MAS with delays*: We propose a distributed consensus protocol for the general linear MAS with input constraints and varying delays. Based on the inverse optimal control [39], a consensus protocol is firstly designed offline for the unconstrained MAS with the goal of achieving global optimality and set stability. By minimizing the gap between the online DMPC input and the predesigned consensus input, the

consensus performance of the MAS is guaranteed, while satisfying control input constraints. In contrast to existing DMPC-based consensus methods [28, 174], the topology of communication graph is explicitly utilized in the offline consensus protocol design, which facilitates the analysis of the consensus convergence.

- *Robust DMPC handles delay-induced estimation errors*: Most of existing DMPC-based consensus algorithms typically require that all agents simultaneously compute control inputs and exchange optimal predicted states via delay-free wireless networks at each instant (see, e.g., [67, 174]). In this work, we relax these strict communication requirements and consider the non-simultaneous communication and computation, and delay-involved communication networks, in which the optimal predicted states (i.e., the assumed predicted states) of each agent broadcast at some previous time instant are used to estimate the current optimal predicted states. The estimated states would inevitably induce estimation errors that might prevent the MAS from achieving consensus. In this context, we leverage tube-based MPC techniques [8, 99] to account for the estimation errors. By bounding the deviation between the assumed and actual predicted states using a properly designed estimation error set, the MAS converges to a neighborhood of the consensus set.

- *Guaranteed feasibility and consensus convergence regardless of delays*: Given the robust DMPC-based consensus protocol, conditions for preserving the recursive feasibility are developed. Furthermore, we provide rigorous theoretical analysis of the consensus convergence for the general linear constrained MAS with bounded time-varying communication delays. Finally, two numerical examples are provided to verify the theoretical results.

4.2 Problem Formulation

Consider M agents that are inter-connected via an undirected graph $\mathcal{G}$. The system model of agent i, $i \in \mathcal{V}$ is characterized by

$$x_i(t+1) = Ax_i(t) + Bu_i(t),\ t \in \mathbb{N}_{\geq 0}, \tag{4.1}$$

where $x_i(t) \in \mathbb{R}^n$ and $u_i(t) \in \mathbb{R}^m$ are the system state and control input, respectively. Agent i, $i \in \mathcal{V}$ is subject to control input constraints, i.e.,

$$u_i(t) \in \mathcal{U}_i,\ t \in \mathbb{N}_{\geq 0}, \tag{4.2}$$

in which the set $\mathcal{U}_i \subset \mathbb{R}^m$ contains the origin.

The following definition describes the consensus of the discrete-time MAS [171].

Definition 4.1 (Consensus of the discrete-time MAS)**.** *The discrete-time MAS in* (4.1) *over the fixed graph $\mathcal{G}$ is said to achieve consensus, if for any $x_i(0)$, $i \in \mathcal{V}$, there exists a consensus protocol $u_i(t) = \kappa_i(x_i(t), x_{-i}(t))$ such that $\lim_{t\to+\infty} \|x_i(t) - x_j(t)\| = 0$, $j \in \mathcal{N}_i$, where $x_{-i}(t)$ represents the collection of agent i's neighboring states and $\kappa_i : \underbrace{\mathbb{R}^n \times \cdots \times \mathbb{R}^n}_{|\mathcal{N}_i|+1} \to \mathbb{R}^m$.*

In this work, we make the standard assumption on the system dynamics and the communication graph as follows.

Assumption 4.1. *The pair (A, B) of the MAS in* (4.1) *is stabilizable, and the associated communication graph $\mathcal{G}$ is connected.*

The connectivity of the graph $\mathcal{G}$ implies that the eigenvalues of $\mathcal{L}$ satisfy $\lambda_i \geq 0$, $i = 1, 2, \ldots, M$ [109]. In this work, the broadcast communication model is adopted for the MAS, i.e., each agent broadcasts the information to its neighbors via the broadcaster and receives the information from its neighbors via the receiver at each time instant.

Let $\mathbf{x}(t) := \mathrm{col}(x_1(t), x_2(t), \ldots, x_M(t))$ and $\mathbf{u}(t) := \mathrm{col}(u_1(t), u_2(t), \ldots, u_M(t))$. Then the system in (4.1) can be written in a compact form

$$\mathbf{x}(t+1) = (I_M \otimes A)\mathbf{x}(t) + (I_M \otimes B)\mathbf{u}(t), \tag{4.3}$$

in which $\mathbf{x}(0) = \mathrm{col}(x_1(0), x_2(0), \ldots, x_M(0))$ is the initial state of the MAS, the augmented input constraint defined by the Cartesian product of multiple control input constraint sets is $\mathcal{U} := \mathcal{U}_1 \times \mathcal{U}_2 \times \cdots \times \mathcal{U}_M$. The consensus problem under consideration can be equivalently transformed a set stabilization problem subject to the control input constraints. A consensus set is introduced for the MAS in (4.3) as

$$\mathcal{C} := \{\mathbf{x}(t) \in \mathbb{R}^{Mn} \mid x_1(t) = x_2(t) = \cdots = x_M(t)\}, \tag{4.4}$$

where $t \in \mathbb{N}_{\geq 0}$. The MAS in (4.1) achieving consensus implies that the system state $\mathbf{x}(t)$ reaches the consensus set $\mathcal{C}$. It follows that the distance between the state $\mathbf{x}(t)$ and the consensus set $\mathcal{C}$ becomes zero, i.e., $|\mathbf{x}(t)|_{\mathcal{C}} = 0$.

The following lemma ([76, Theorem 1]) provides a sufficient and necessary condition for the MAS to reach consensus.

Lemma 4.1. *For agent i, $i \in \mathcal{V}$ in (4.1) over a fixed communication graph $\mathcal{G}$, the consensus of the MAS can be achieved if and only if there exists a predesigned consensus gain $K \in \mathbb{R}^{m\times n}$ such that $\rho(A + \lambda_i BK) < 1$, where λ_i, $i = 2, 3, \ldots, M$, are the nonzero eigenvalues of the Laplacian matrix $\mathcal{L}$.*

In what follows, the assumption on the predesigned consensus gain K in **Lemma 4.1** is required to hold.

Assumption 4.2. *There exist a feedback control matrix K and a forward invariant set Ω such that: 1) $\rho(A + BK) < 1$; 2) $K\sum_{j\in\mathcal{N}_i} a_{ij}(x_i - x_j) \in \mathcal{U}_i$, when the states $x_i \in \Omega$, $i \in \mathcal{V}$ and $x_j \in \Omega$, $j \in \mathcal{N}_i$.*

The forward invariant set (i.e., the terminal set) will be given in Section 4.4.3. The control objective is to design a distributed consensus protocol for the MAS in (4.1) such that agents over wireless networks $\mathcal{G}$ attain:

1) *Agreement*: For agents i, $j \in \mathcal{V}$, the following condition

$$\lim_{t\to\infty} \|x_i(t) - x_j(t)\| = 0,\ j \in \mathcal{N}_i, \tag{4.5}$$

holds, which is equivalent to $\lim_{t\to\infty} |\mathbf{x}(t)|_{\mathcal{C}} = 0$.

2) *Constraint satisfaction*: The system i, $i \in \mathcal{V}$

$$x_i(t+1) = Ax_i(t) + Bu_i(t), \tag{4.6}$$

satisfies control input constraints in (4.2) for all $t \in \mathbb{N}_{\geq 0}$.

4.3 Delayed Communication among the MAS

In this section, we introduce the assumed information broadcast among the MAS over delay-involved wireless networks.

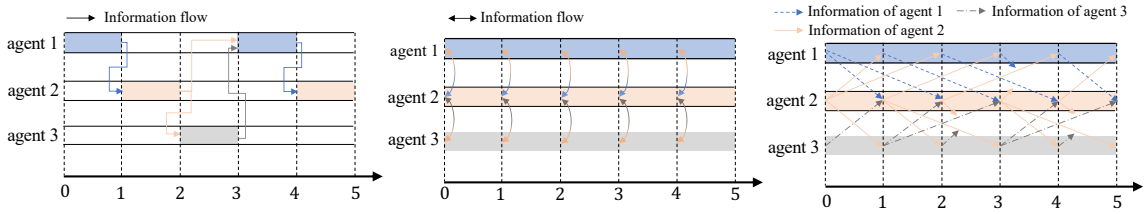

(a) Sequential execution [102, 123].

(b) Simultaneous parallel execution [158].

(c) Non-simultaneous parallel execution.

Figure 4.1: Three types of implementations of DMPC algorithms for the MAS with $\mathcal{N}_1 = \{2\}$, $\mathcal{N}_2 = \{1, 3\}$, $\mathcal{N}_3 = \{2\}$.

Most existing DMPC algorithms for MAS only consider delay-free networks, and some of them even require stricter communication settings (e.g., simultaneous communication and computation). Here, three types of DMPC schemes are presented in Figure 4.1, including

1) *Sequential execution:* As shown in Figure 4.1a, agents solve local optimization problems and communicate with their neighbors sequentially. That is, at each time instant, only one agent calculates the optimal control inputs and broadcasts the optimal predicted state sequence.

2) *Parallel execution with simultaneous computation and communication:* As presented in Figure 4.1b, at each time instant, all agents simultaneously receive neighbors' information, solve the optimization problems and broadcast information to their neighbors.

3) *Parallel execution with non-simultaneous computation and communication:* As depicted in Figure 4.1c, at each time instant, agents broadcast the predicted states. But these broadcast predicted states may be used by their neighbors a few time instants later due to the time-varying communication delays.

In contrast to sequential algorithms [102, 123], parallel DMPC algorithms [65] provide a more efficient coordination solution for the constrained MAS in terms of both computation and communication. Most of the existing results assume that the communication among agents is perfect, and the information can be synchronously exchanged as shown in Figure 4.1b (e.g., see [158]). However, it is unrealistic for agents to calculate the optimal predicted states while exchanging them simultaneously and instantaneously. Especially, the communication delays are unavoidable during the

information exchange for the MAS in many practical scenarios, which may result in the non-simultaneous parallel algorithm execution as shown in Figure 4.1c. That is, the optimal predicted state sequence broadcast at the previous time instant t', $t' \in \mathbb{N}_{[t-\bar{\tau},t-1]}$, $\bar{\tau} \in \mathbb{N}_{\geq 1}$ (the assumed predicted state sequence) is used to estimate the current optimal predicted state sequence at t, $t \in \mathbb{N}_{\geq 0}$. For the case with bounded varying delays, the resulting estimation errors can be treated as external disturbances.

The assumed states of agent i at time t are constructed based on the previous optimal predicted states at time t', i.e.,

$$\hat{x}_i(k|t) = \begin{cases} x_i^*(t-t'+k|t'), & k \in \mathbb{N}_{[0,N']}, \\ A\hat{x}_i(k-1|t) + B\hat{u}(k-1|t), & k \in \mathbb{N}_{(N',N]}, \end{cases} \tag{4.7}$$

in which $t' \in \mathbb{N}_{[t-\bar{\tau},t-1]}$, $N' = t'+N-t$, N is the prediction horizon, $x_i^*(\cdot|t')$ represents the optimal state and $\hat{u}_i(k|t) = K\sum_{j\in\mathcal{N}_i} a_{ij}(x_i(k|t) - \hat{x}_j(k|t))$ with $k \in \mathbb{N}_{(N',N]}$. Note that states $x_j^*(\cdot|t')$, $j \in \mathcal{N}_i$, $t' \in \mathbb{N}_{[t-\bar{\tau},t-1]}$ are available for agent i at time t. Let $\hat{\boldsymbol{x}}_i(t) := \{\hat{x}_i(k|t)\}$, $t \in \mathbb{N}_{\geq 0}$, $k \in \mathbb{N}_{[0,N]}$ be the assumed predicted state sequence of agent i, $i \in \mathcal{V}$ at time t hereafter.

We make the following assumption on the communication delays among the MAS.

Assumption 4.3. *For agent i, $i \in \mathcal{V}$, the time-varying communication delays $\tau(t) \in \mathbb{N}_{\geq 0}$ between agent i and j, $j \in \mathcal{N}_i$, satisfy $1 \leq \tau(t) \leq \bar{\tau} < N$, with $\tau(0) = 0$, with $\tau(0) = 0$ and $\bar{\tau}$ being the largest communication delay.*

The upper bound of the communication delays ensures that the previously broadcast assumed predicted states can be used to estimate the actually optimal predicted states. For example, at time t, agent i can receive the assumed predicted state sequence $x_i^*(\cdot|t')$ from its neighbor j, $j \in \mathcal{N}_i$ broadcast at time $t' \in \mathbb{N}_{[t-\bar{\tau},t-1]}$. Then, the received information will be adopted as in (4.7) to construct the current assumed predicted state sequence at time t. On the other hand, the case of unbounded delays can be modeled as the packet dropouts in networked control systems [63] and also the denial-of-service attacks in cyber-physical systems [141], which is beyond the scope of current work.

Remark 4.1. *Many consensus algorithms have been proposed for the MAS with delays. For example, the conditions based on special stochastic matrix properties and extended state space are derived for discrete-time the MAS, e.g., [165], and linear matrix inequality conditions for the continuous-time MAS, e.g., [142]. In contrast,*

the previously broadcast predicted states can be used to design the distributed consensus protocol owing to the predictive mechanism of MPC. Particularly, in existing DMPC results (e.g., [67, 174]), the assumed predicted state sequence (one-step ahead predicted state sequence) are generally used to estimate the current optimal state sequence, which can be regarded as a special case of the assumed predicted state sequence of the MAS with varying delays in (4.7)*, with* $\tau(t) = 1$.

Note that restricting the deviation between the current and the assumed predicted states is necessary for the MAS to reach consensus. In particular, the current optimal predicted state of agent i, $i \in \mathcal{V}$ is supposed to lie in a bounded neighborhood (i.e., the estimation error set Δ) of the assumed predicted state,

$$x_i^*(k|t) \in \hat{x}_i(k|t) \oplus \Delta,\ k \in \mathbb{N}_{[0,N]}, \tag{4.8}$$

where $\Delta := \{\delta \in \mathbb{R}^n \mid \|\delta\| < \eta\}$ is symmetric and contains the origin with $\eta > 0$.

We consider a scenario where agents are subject to bounded varying communication delays. In this context, the control objective presented in Section 4.2 can be restated as follows.

1) *Robust agreement*: For agents $i,\ j \in \mathcal{V}$, applying the proposed distributed consensus protocol, then

$$\lim_{t\to\infty} \|x_i(t) - x_j(t)\| \leq \gamma,\ j \in \mathcal{N}_i, \tag{4.9}$$

holds, where the invariant set $\mathcal{R}_i^\infty := \{x \in \mathbb{R}^n \mid \|x\| \leq \gamma\}$ and $\gamma > 0$.

2) *Constraint satisfaction*: The system i, $i \in \mathcal{V}$

$$x_i(t+1) = Ax_i(t) + Bu_i(t), \tag{4.10}$$

satisfies control input constraints in (4.2) for all $t \in \mathbb{N}_{\geq 0}$.

Note that using **Assumption 4.2** allows us to get a minimal robust invariant set $\mathcal{R}_i^k$ as $k \to \infty$ [99].

4.4 Robust DMPC-based Consensus Protocol

The robust DMPC-based consensus scheme for the MAS is illustrated in Figure 4.2, which mainly consists of five parts: the controlled system, the robust DMPC con-

troller, the broadcaster, the receiver and wireless communication networks. At each time instant, the Broadcaster of agent i, $i \in \mathcal{V}$ broadcasts the assumed predicted state sequence $\hat{\boldsymbol{x}}_i$ and the Receiver receives the assumed predicted state sequence $\hat{\boldsymbol{x}}_j$ from agent j, $j \in \mathcal{N}_i$ via wireless communication networks.

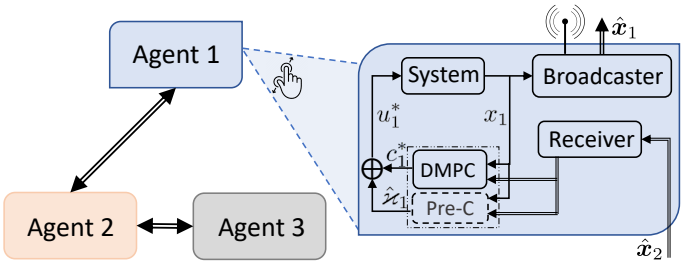

Figure 4.2: Illustration of the robust DMPC-based consensus scheme for the MAS with $\mathcal{N}_1 = \{2\}$, $\mathcal{N}_2 = \{1, 3\}$, $\mathcal{N}_3 = \{2\}$.

4.4.1 Predesigned consensus protocol for the MAS without delays

At time t, agent i calculates control inputs, broadcasts predicted states $\hat{\boldsymbol{x}}_i(t)$ to its neighbor j, $j \in \mathcal{N}_i$ via the network $\mathcal{G}$ and updates system states $x_i(t)$. The predesigned consensus is determined based on the relative states between local agent and its neighbors under the assumption that the wireless network is delay-free, i.e.,

$$u_i(t) = \kappa_i(x_i(t), x_{-i}(t)) = K \sum_{j \in \mathcal{N}_i} a_{ij}(x_i(t) - x_j(t)) + c_i(t), \tag{4.11}$$

where $K \in \mathbb{R}^{m \times n}$, $\varkappa_i(t) := -K \sum_{j \in \mathcal{N}_i} a_{ij}(x_i(t) - x_j(t))$ is the predesigned consensus input and $c_i(t)$ is the control decision variable of the robust DMPC optimization problem in Section 4.4.3.

Remark 4.2. *Note that the proposed consensus protocol* (4.11) *is motivated by the well-known "pre-stabilizing" control method for the stabilization problem of the single system in [8, 30], in which the MPC control input is given by* $u(t) = Kx(t) + c(t)$. *The feedback gain* K *is chosen offline for the unconstrained system to achieve some desired properties such as LQR optimality and stability, and* $c(t)$ *is calculated online. In this work, an inverse optimal consensus protocol* $\varkappa_i(t)$ *is designed offline for the unconstrained MAS in* (4.1) *and* $c_i(t)$ *is determined via solving the online optimization problem. The resulting consensus protocol achieves the suboptimal performance*

while guaranteeing the satisfaction of control input constraints. In contrast to the existing DMPC methods in [28, 67, 174], the topology of the communication graph is explicitly exploited to construct the predesigned consensus protocol, which facilitates the consensus convergence analysis of the constrained MAS.

4.4.2 Predesigned consensus protocol for the MAS with delays

We now present the predesigned consensus protocol for the MAS with the time-varying communication delays. Based on the assumed predicted states of neighbors, the consensus protocol in (4.11) then becomes

$$u_i(t) = K \sum_{j\in\mathcal{N}_i} a_{ij}(x_i(t) - \hat{x}_j(t)) + c_i(t), \tag{4.12}$$

and the MAS in (4.1) under the consensus protocol in (4.12) can be written as

$$x_i(t+1) = Ax_i(t) + BK \sum_{j\in\mathcal{N}_i} a_{ij}(x_i(t) - \hat{x}_j(t)) + Bc_i(t). \tag{4.13}$$

The overall estimation error of agent i, $i \in \mathcal{V}$ is defined as $w_i(t) = \sum_{j\in\mathcal{N}_i} a_{ij}(\hat{x}_j(t) - x_j(t))$, and it satisfies $w_i(t) \in \mathcal{W} := \{w \in \mathbb{R}^n | w \in \bigoplus_{j\in\mathcal{N}_i} a_{ij}\Delta\}$. In particular, the estimation error will be treated as the disturbance in the following. Thanks to $\sum_{j\in\mathcal{N}_i} a_{ij} = 1$, it holds that $\mathcal{W} = \Delta$.

Under the consensus protocol (4.12), the closed-loop system in (4.13) becomes

$$x_i(t+1) = Ax_i(t) + B(K \sum_{j\in\mathcal{N}_i} a_{ij}(x_i(t) - x_j(t)) + c_i(t)) - BKw_i(t).$$

Remark 4.3. *Existing DMPC-based consensus methods (e.g., [67, 174]) do not consider the estimation errors explicitly, which may not be applicable for the practical MAS. Because the estimation errors may prevent the MAS from achieving consensus. Inspired by the tube-based MPC for the uncertain linear system in [99], one may choose to impose the estimation error set to bound the estimation errors that are regarded as external disturbances in this work.*

4.4.3 Design of robust DMPC for consensus

In this work, the terminal set for the MAS in (4.3) is defined as $\mathbf{X}^f := \{\mathbf{x} \in \mathbb{R}^{Mn} \mid \|\mathbf{x}\|_{\mathbb{S}} \leq \epsilon^2\}$, in which $\mathbb{S} = \sigma\mathcal{L}\otimes S$, with the positive definite weighting matrix $S \in \mathbb{R}^{n\times n}$ and the positive constants ϵ and σ. The matrix S can be chosen following the method provided in Lemmas 6 and 7 in [68]. The terminal set $\mathcal{X}_i^f$ for agent i, $i \in \mathcal{V}$ is given by

$$\mathcal{X}_i^f := \{x_i \in \mathbb{R}^n \mid \sum_{j\in\mathcal{N}_i} a_{ij} x_i^{\mathrm{T}} S(x_i - x_j) \leq \epsilon^2/M\}. \tag{4.14}$$

The cost function $J_i(\cdot)$ for agent i, $i \in \mathcal{V}$ is defined by

$$J_i(\boldsymbol{c}_i(t)) := \sum_{k=0}^{N-1} \|c_i(k|t)\|_{P_i}^2, \tag{4.15}$$

where $\boldsymbol{c}_i(t) := \{c_i(0|t), c_i(1|t), \ldots, c_i(N-1|t)\}$ denotes the control sequence generated at time instant t and the matrix P_i is positive definite. Note that the suboptimal performance can be guaranteed by minimizing the cost function in (4.15) while ensuring the satisfaction of control input constraints.

At time t, given the current state $x_i(t)$ of agent i, $i \in \mathcal{V}$ and neighbors' assumed predicted state sequence $\hat{\boldsymbol{x}}_j(t)$, $j \in \mathcal{N}_i$, the robust DMPC optimization problem $\mathcal{P}_i$ is formulated as

$$\begin{aligned}
&\min_{\boldsymbol{c}_i(t)} \ J_i(\boldsymbol{c}_i(t)) \\
&\text{s.t. } x_i(0|t) = x_i(t), && \text{(4.16a)}\\
&\quad x_i(k+1|t) = Ax_i(k|t) + Bu_i(k|t), && \text{(4.16b)}\\
&\quad u_i(k|t) = \hat{\varkappa}_i(k|t) + c_i(k|t), && \text{(4.16c)}\\
&\quad u_i(k|t) \in \mathcal{U}_i, && \text{(4.16d)}\\
&\quad x_i(k|t) \in \hat{x}_i(k|t) \oplus \Delta, && \text{(4.16e)}\\
&\quad x_i(N|t) \in \mathcal{X}_i^f, && \text{(4.16f)}
\end{aligned}$$

in which $k \in \mathbb{N}_{[0,N-1]}$ and $\hat{\varkappa}_i(k|t) := K\sum_{j\in\mathcal{N}_i} a_{ij}(x_i(k|t) - \hat{x}_j(k|t))$. Note that the constraint (4.16e) bounds the optimal predicted state sequence $x_i^*(k|t)$ within a predesigned tube centered along the assumed state $\hat{x}_i(k|t)$, $k \in \mathbb{N}_{[0,N-1]}$. Let $\boldsymbol{c}_i^*(t) := \{c_i^*(0|t), \ldots, c_i^*(N-1|t)\}$ be the optimal solution to the robust DMPC prob-

lem $\mathcal{P}_i$ at time t. We then have the corresponding optimal control input

$$u_i^*(k|t) = K \sum_{j \in \mathcal{N}_i} a_{ij}(x_i^*(k|t) - \hat{x}_j(k|t)) + c_i^*(k|t), \tag{4.17}$$

where $k \in \mathbb{N}_{[0,N-1]}$, and the optimal control sequence at time t is $\boldsymbol{u}_i^*(t) := \{u_i^*(0|t), u_i^*(1|t), \ldots, u_i(N-1|t)\}$. The resulting optimal predicted state satisfies

$$x_i^*(1|t) = Ax_i^*(0|t) + Bu_i^*(0|t), \tag{4.18}$$

where $k \in \mathbb{N}_{[0,N-1]}$, $x_i^*(0|t) = x_i(t)$, and the optimal predicted state sequence is denoted by $\boldsymbol{x}_i^*(t) := \{x_i^*(0|t), x_i^*(1|t), \ldots, x_i^*(N|t)\}$.

At time t, applying $u_i^*(0|t)$ to the system in (4.1) yields the closed-loop system

$$\begin{aligned} x_i(t+1) =& Ax_i(t) + Bu_i^*(0|t) \\ =& Ax_i(t) + B(K \sum_{j \in \mathcal{N}_i} a_{ij}(x_i^*(0|t) - \hat{x}_j(0|t)) + c_i^*(0|t)). \end{aligned}$$

And according to (4.18), one has $x_i(t+1) = x_i^*(1|t)$.

The proposed robust DMPC-based consensus algorithm is presented as follows.

Algorithm 2 Robust DMPC-based consensus algorithm

Require: The prediction horizon N, the predesigned consensus gain K, the terminal set $\mathcal{X}_i^f$, the estimation error set Δ, the weighting matrix P_i, the initial state $x_i(0)$, the assumed state sequence $\hat{\boldsymbol{x}}_i(0) := \{x_i(0), \ldots, A^{N-1}x_i(0)\}$, and other parameters.

1: Broadcast the assumed predicted state sequence $\hat{\boldsymbol{x}}_i(0)$ to its neighbors $j, j \in \mathcal{N}_i$;
2: **while** for agent i, the control is not stopped **do**
3: Measure the current system state $x_i(t)$;
4: Receive the information $\hat{\boldsymbol{x}}_j(t)$, $j \in \mathcal{N}_i$ defined in (4.7);
5: Solve the problem $\mathcal{P}_i$ to generate $\boldsymbol{u}_i^*(t)$ and $\boldsymbol{x}_i^*(t)$;
6: Broadcast $\hat{\boldsymbol{x}}_i(t)$ to agent j, $j \in \mathcal{N}_i$;
7: Apply the control $u_i^*(0|t)$ to agent i;
8: $t = t + 1$;
9: **end while**

Note that in Step 4 of **Algorithm 2**, agent i collects the assumed predicted state sequence from its neighbors j, $j \in \mathcal{N}_i$. The predicted state sequences of neighbors

broadcast at the synchronous instant t', $t' \in \mathbb{N}_{[t-\bar{\tau},t-1]}$ as in (4.7), instead of the most recently received predicted state sequences, will be used in Step 5 to generate the consensus input $\boldsymbol{u}_i^*(t)$.

Remark 4.4. *Note that many DMPC algorithms have been developed for the formation stabilization control problem of the MAS, e.g., [19]. However, they cannot be easily extended to consensus problems since the optimal cost function may not be directly used as Lyapunov function [23, 102]. In this case, the major difficulty when analyzing the consensus convergence of the MAS is designing some specific conditions such that the Lyapunov theorem holds [67, 174]. Alternatively, this work exploits the knowledge of the communication topology to design an offline optimal consensus protocol $\sum_{j\in\mathcal{N}_i} a_{ij}K(x_i - x_j)$ for the unconstrained MAS. Then the difference c_i between the unconstrained control input $\hat{\boldsymbol{\varkappa}}_i$ and the control input u_i is minimized, which will be proved to be a vanishing input in* ***Lemma 4.3****.*

4.5 Theoretical Analysis

In this section, we provide the theoretical analysis of the recursive feasibility and the consensus convergence of the MAS. Before presenting the main results, the relationship between the theoretical results is illustrated in Figure 4.3.

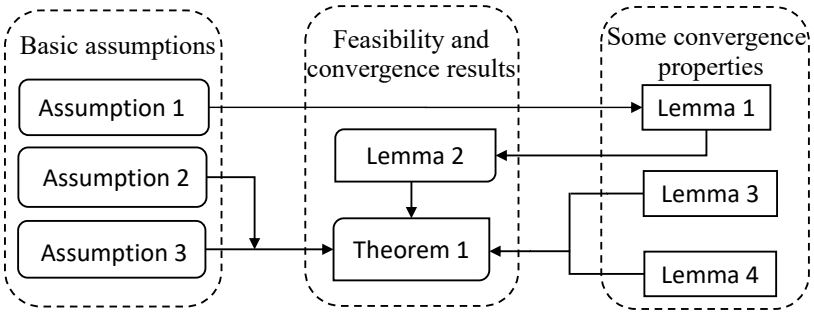

Figure 4.3: The roadmap of the theoretical results.

4.5.1 Recursive feasibility result

In this subsection, the recursive feasibility of the robust DMPC optimization problem will be analyzed. It is assumed that an initial feasible solution to the optimization problem $\mathcal{P}_i$ exists for the given initial state $x_i(t)$, $t \in \mathbb{N}_{\geq 0}$.

Based on the optimal predicted control sequence at time t'', $t'' \in \mathbb{N}_{[t+1-\bar{\tau},t]}$, a candidate input sequence $\tilde{\boldsymbol{c}}_i(t+1)$ at time $t+1$ is created by dropping the first $t-t''$ input element and appending final $t-t''$ terminal zero element of the optimal control sequence at t'', i.e.,

$$\tilde{c}_i(k|t+1) = \begin{cases} c_i^*(k|t''), & k \in \mathbb{N}_{[1,t''+N-t)}, \\ 0, & k \in \mathbb{N}_{[t''+N-t,N]}, \end{cases} \tag{4.19}$$

and the corresponding control input sequence $\tilde{\boldsymbol{u}}_i(t+1) := \{\tilde{u}_i(0|t+1), \tilde{u}_i(1|t+1), \ldots, \tilde{u}_i(N-1|t+1)\}$ for agent i is then constructed as

$$\tilde{u}_i(k-1|t+1) = K \sum_{j \in \mathcal{N}_i} a_{ij}(\tilde{x}_i(k-1|t+1) - \hat{x}_j(k-1|t+1)) + \tilde{c}_i(k-1|t+1), \tag{4.20}$$

where $k \in \mathbb{N}_{[1,N]}$ and the corresponding system state $\tilde{x}_i(k|t+1)$ satisfies the following difference equation

$$\tilde{x}_i(k+1|t+1) = A\tilde{x}_i(k|t+1) + B\tilde{u}_i(k|t+1), \tag{4.21}$$

with the initial condition $\tilde{x}_i(0|t+1) = x_i(t+1)$.

In the following lemma, we provide the conditions under which the control input sequence defined in (4.19) and (4.20) will be a feasible solution to the robust DMPC optimization problem $\mathcal{P}_i$ at time $t+1$.

Lemma 4.2. *For the MAS in* (4.1)*, suppose* ***Assumptions 4.1, 4.2, 4.3*** *and the condition in* ***Lemma 4.1*** *hold. If there exist the predesigned consensus gain K, the maximum delay $\bar{\tau}$ and the prediction horizon N, such that the conditions*

$$\max_{k \in \mathbb{N}_{[1,N'-1]}} \left\{ \rho\Big(\sum_{s=0}^{k-1} A_K^{k-1-s} BK + A_K^k\Big) \right\} \leq 1, \text{ and } \max_{k \in \mathbb{N}_{[N',N-1]}} \left\{ \rho\Big(\sum_{s=0}^{N'-1} A_K^{k-1-s} BK + A_K^k\Big) \right\} \leq 1, \tag{4.22}$$

hold, with $\rho(\cdot)$ denotes the spectral radius, $A_K := A + BK$ and $N' := N - \tau(t'')$. If, in addition, the robust DMPC optimization problem $\mathcal{P}_i$ has a feasible solution at time t, then it admits a feasible solution at time $t+1$, $t \in \mathbb{N}_{\geq 0}$.

Proof. An initial feasible solution to the optimization problem $\mathcal{P}_i$, $i \in \mathcal{V}$ is assumed to exist at time t, $t \in \mathbb{N}_{\geq 0}$ implying that the constraint $x_i^*(k|t) \in \hat{x}_i(k|t) \oplus \Delta$ in (4.16e) holds, i.e., $x_i^*(k|t) \in x_i^*(k|t') \oplus \Delta$, with $x_i^*(t-t'+k+1|t') = Ax_i^*(t-t'+k|t') + Bu_i^*(t-t'+k|t')$ and $t' \in \mathbb{N}_{[t-\bar{\tau},t-1]}$.

Note that the previous optimal predicted states $x_j^*(\cdot|t'')$ of agent j, $j \in \mathcal{N}_i$ are available for agent i, $i \in \mathcal{V}$ at time $t+1$, with $t'' \in \mathbb{N}_{[t+1-\bar{\tau},t]}$. By (4.7), one gets $\hat{x}_j(0|t+1) = x_j^*(t-t''+1|t'')$. Thus, from $\tilde{x}_i(0|t+1) = x_i^*(1|t)$ and (4.19), it is easy to have that

$$\begin{aligned}
&\tilde{u}_i(0|t+1)\\
=&K\sum_{j\in\mathcal{N}_i} a_{ij}(\tilde{x}_i(0|t+1) - \hat{x}_j(0|t+1)) + \tilde{c}_i(0|t+1)\\
=&K\sum_{j\in\mathcal{N}_i} a_{ij}(\tilde{x}_i(0|t+1) - \hat{x}_j(t-t''+1|t'') + \hat{x}_j(t-t''+1|t'') - \hat{x}_j(0|t+1))\\
&+\tilde{c}_i(0|t+1)\\
=&K\sum_{j\in\mathcal{N}_i} a_{ij}(x_i^*(1|t) - \hat{x}_j(t-t''+1|t'')) + c_i^*(t-t''+1|t'')\\
&+K\sum_{j\in\mathcal{N}_i} a_{ij}(\hat{x}_j(t-t''+1|t'') - \hat{x}_j(0|t+1))\\
=&K\sum_{j\in\mathcal{N}_i} a_{ij}(x_i^*(t-t''+1|t'') - x_i^*(t-t''+1|t'') + x_i^*(1|t) - \hat{x}_j(t-t''+1|t''))\\
&+c_i^*(t-t''+1|t'') + K\sum_{j\in\mathcal{N}_i} a_{ij}(\hat{x}_j(t-t''+1|t'') - \hat{x}_j(0|t+1))\\
=&u_i^*(t-t''+1|t'') + K\sum_{j\in\mathcal{N}_i} a_{ij}(\hat{x}_j(t-t''+1|t'') - x_j^*(t-t''+1|t'')))\\
&+K\sum_{j\in\mathcal{N}_i} a_{ij}(x_i^*(1|t) - x_i^*(t-t''+1|t'')).
\end{aligned}$$

Since the constraint $x_i^*(k|t) \in x_i^*(t-t'+k|t') \oplus \Delta$ holds, one then has $x_i^*(k|t) \in x_i^*(t-t''+k|t'') \oplus \Delta$. Let $w_i'(1|t) := x_i^*(1|t) - \hat{x}_i(1|t) = x_i^*(1|t) - x_i^*(t-t''+1|t'')$. From the definition of $w_i(k|t) = \sum_{j\in\mathcal{N}_i} a_{ij}(\hat{x}_j(k|t) - x_j^*(k|t))$, we obtain

$$\tilde{u}_i(0|t+1) = u_i^*(t-t''+1|t'') + Kw_i'(1|t) + Kw_i(t-t''+1|t'').$$

Applying the above control input, we have the predicted system state $\tilde{x}_i(1|t+1)$ as follows

$$\begin{aligned}
\tilde{x}_i(1|t+1) =&A\tilde{x}_i(0|t+1) + B\tilde{u}_i(0|t+1)\\
=&x_i^*(t-t''+2|t'') + A_K w_i'(1|t) + BKw_i(t-t''+1|t'').
\end{aligned} \tag{4.23}$$

Analogously, we have

$$\begin{aligned}
&\tilde{u}_i(1|t+1)\\
=&K\sum_{j\in\mathcal{N}_i} a_{ij}(\tilde{x}_i(1|t+1)-\hat{x}_j(1|t+1))+\tilde{c}_i(1|t+1)\\
=&u_i^*(t-t''+2|t'')+KBKw_i(t-t''+1|t'')+Kw_i(t-t''+2|t'')+KA_Kw_i'(1|t),
\end{aligned}$$

and

$$\begin{aligned}
&\tilde{x}_i(2|t+1)\\
=&A\tilde{x}_i(1|t+1)+B\tilde{u}_i(1|t+1)\\
=&x_i^*(t-t''+3|t'')+A_KBKw_i(t-t''+1|t'')+BKw_i(t-t''+2|t'')+A_K^2w_i'(1|t).
\end{aligned}$$

Then, the state sequence candidate $\tilde{x}_i(k-1|t+1)$ evolves in an iterative way according to

$$\tilde{x}_i(k|t+1)=x_i^*(t+1-t''+k|t'')+A_K^kw_i'(1|t)+\sum_{s=0}^{k-1}A_K^{k-1-s}BKw_i(t+1-t''+s|t''), \tag{4.24}$$

with $k\in\mathbb{N}_{[1,N')}$. Define the variable $r_i^k(t+1)\in\mathbb{R}^n$ for agent i, $i\in\mathcal{V}$ by

$$r_i^k(t+1):=\begin{cases} w_i'(1|t), & k=0,\\ \sum_{s=0}^{k-1}A_K^{k-1-s}BKw_i(s)+A_K^kw_i'(1|t), & k\in\mathbb{N}_{[1,N')},\\ \sum_{s=0}^{N'-1}A_K^{k-1-s}BKw_i(s)+A_K^kw_i'(1|t), & k\in\mathbb{N}_{[N',N)},\end{cases}$$

in which $w_i(s):=w_i(t+1-t''+s|t'')$.

Considering $w_i(t-t''+k|t'')\in\mathcal{W}$, $k\in\mathbb{N}_{[1,N']}$ and $w_i'(1|t)\in\mathcal{W}$, one gets the corresponding set $\mathcal{R}_i^k$

$$\mathcal{R}_i^k:=\begin{cases} \mathcal{W}, & k=0,\\ \bigoplus_{s=0}^{k-1}A_K^{k-1-s}BK\mathcal{W}+A_K^k\mathcal{W}, & k\in\mathbb{N}_{[1,N')},\\ \bigoplus_{s=0}^{N'-1}A_K^{k-1-s}BK\mathcal{W}+A_K^k\mathcal{W}, & k\in\mathbb{N}_{[N',N)},\end{cases} \tag{4.25}$$

with $r_i^k(t+1) \in \mathcal{R}_i^k$.

Since the condition $\max_{k\in\mathbb{N}_{[1,N-1]}}\{\rho(\sum_{s=0}^{N'-1} A_K^{k-1-s}BK + A_K^k), \rho(\sum_{s=0}^{k-1} A_K^{k-1-s}BK + A_K^k)\} \leq 1$ holds, and by (4.24) and (4.25), we get $\mathcal{R}_i^k \subseteq \Delta$, $k \in \mathbb{N}_{[1,N)}$. Hence, the constraint (4.16e) at $t+1$ is satisfied.

Let $\bar{u}_i^*(t-t''+k|t'') := K\sum_{j\in\mathcal{N}_i} a_{ij}(x_i^*(t-t''+k|t'')-x_j^*(t-t''+k|t''))+c_i^*(t-t''+k|t'')$ be the nominal optimal control input with $k \in \mathbb{N}_{[1,N'-1]}$. Due to all admissible disturbances $w_i(t-t''+k|t'') \in \Delta$, the nominal optimal control input satisfies $\bar{u}_i^*(t-t''+k|t'') \in \overline{\mathcal{U}}_i$, where $\overline{\mathcal{U}}_i := \mathcal{U}_i \ominus K\Delta$. It should be mentioned that the nominal control input $\bar{u}_i^*(\cdot|t'')$ might not be implemented to the actual system, since $x_j^*(t-t''+k|t'')$, $j \in \mathcal{N}_i$ is not available for agent i, $i \in \mathcal{V}$ at time t''. But the nominal control input is used in the feasibility analysis here. Next, substituting (4.24) into (4.20) yields

$$\tilde{u}_i(k|t+1) = \bar{u}_i^*(t-t''+k|t'') + Kr_i^{k-1}(t+1), \tag{4.26}$$

where $k \in \mathbb{N}_{[1,N']}$. Since the optimal control input sequence $\boldsymbol{u}_i^*(t'')$ is assumed to be feasible at time t'', we have $\bar{u}_i^*(t-t''+k|t'') \in \overline{\mathcal{U}}_i$, $k \in \mathbb{N}_{[1,N']}$. Additionally, $r_i^{k-1}(t+1) \in \Delta$. When $k \in \mathbb{N}_{(N',N]}$, it follows from **Assumption 4.2** that $\tilde{u}_i(k-1|t+1) \in \mathcal{U}_i$. Hence, at time $t+1$, from (4.19) and (4.20), we further obtain that

$$\tilde{u}_i(k-1|t+1) \in \mathcal{U}_i, \tag{4.27}$$

where $k \in \mathbb{N}_{[1,N]}$. This implies that the control input constraint in (4.16d) holds.

Given the initial state $\tilde{x}_i(0|t+1) = x_i(t+1)$ and the control inputs defined in (4.20), one gets

$$\begin{aligned}
&\tilde{x}_i(N|t+1)\\
=&A\tilde{x}_i(N-1|t+1) + B\tilde{u}_i(N-1|t+1)\\
=&A\tilde{x}_i(N-1|t+1) + BK\sum_{j\in\mathcal{N}_i} a_{ij}(\tilde{x}_i(N-1|t+1) - \hat{x}_j(N-1|t+1))\\
=&A(x_i^*(t-t''+N|t'') + r_i^{N-1}(t+1))\\
&+ BK\sum_{j\in\mathcal{N}_i} a_{ij}(x_i^*(t-t''+N|t'') + r_i^{N-1}(t+1) - x_j^*(t-t''+N|t''))\\
=&Ax_i^*(t-t''+N|t'') + A_K r_i^{N-1}(t+1)\\
&+ BK\sum_{j\in\mathcal{N}_i} a_{ij}(x_i^*(t-t''+N|t'') - x_j^*(t-t''+N|t'')),
\end{aligned} \tag{4.28}$$

in which $x_i^*(t+1-t''+k|t'') := Ax_i^*(t-t''+k|t'') + Bu_i^*(t-t''+k|t'')$, with $u_i^*(t-t''+k|t'') := K\sum_{j\in\mathcal{N}_i} a_{ij}(x_i^*(t-t''+k|t'') - x_j^*(t-t''+k|t''))$, $k \in \mathbb{N}_{[N',N]}$.

Let $\tilde{\mathbf{x}}(N-1|t+1) := \mathrm{col}(\tilde{x}_1(N-1|t+1), \ldots, \tilde{x}_M(N-1|t+1))$ and $\mathbf{x}^*(t-t''+N|t'') := \mathrm{col}(x_1^*(t-t''+N|t''), \ldots, x_M^*(t-t''+N|t''))$. Then, (4.28) can be written as

$$\begin{aligned}&\tilde{\mathbf{x}}(N|t+1)\\ =&(I_M\otimes A + \mathcal{L}\otimes BK)\mathbf{x}^*(t-t''+N|t'') + (I_M\otimes(A+BK))\mathbf{r}^{N-1}(t+1),\end{aligned} \tag{4.29}$$

where $\mathbf{r}^{N-1}(t+1) = \mathrm{col}(r_1^{N-1}(t+1), r_2^{N-1}(t+1), \ldots, r_M^{N-1}(t+1)) \in \mathbf{\Delta}$, with $\mathbf{\Delta} = \{\mathbf{r}^{N-1} \in \mathbb{R}^{Mn} \mid \|\mathbf{r}^{N-1}\|^2 \le M\eta^2\}$. Let the tightened terminal set be $\overline{\mathbf{X}}^f := \mathbf{X}^f \ominus \mathbf{\Delta}$. When $\mathbf{x}^*(t-t''+N|t'') \in \overline{\mathbf{X}}^f$, **Assumption 4.1** implies that $(I_M\otimes A+\mathcal{L}\otimes BK)\mathbf{x}^*(t-t''+N|t'') \in \overline{\mathbf{X}}^f$. The corresponding tightened terminal set for agent i, $i \in \mathcal{V}$ becomes

$$\overline{\mathcal{X}}_i^f := \mathcal{X}_i^f \ominus \Delta, \tag{4.30}$$

with the constant $\eta > 0$ and $\overline{\mathcal{X}}_i^f \neq \emptyset$.

As a result, combining the above with (4.28) and (4.29), one obtains

$$\tilde{x}_i(N|t+1) \in \overline{\mathcal{X}}_i^f + A_K\Delta \subseteq \mathcal{X}_i^f, \tag{4.31}$$

which implies that the terminal set (4.16f) is satisfied. By now, we have shown that $\tilde{\boldsymbol{c}}_i(t+1)$ is a feasible solution to the robust DMPC problem $\mathcal{P}_i$ at time $t+1$. □

Remark 4.5. *When the delay bound $\bar{\tau}$ increases, a larger prediction horizon N is needed to construct the assumed predicted state sequence. The resulting DMPC optimization problem becomes more computationally challenging. Additionally, it is hard to ensure the satisfaction of the condition* (4.22)*, which may lead to an infeasible solution. Therefore, one would choose suitable parameters to make a trade-off between the delay tolerant capability and computational complexity.*

Remark 4.6. *Note that the state constraints must be satisfied by every optimized sequence $x_i^*(k|t)$ in the tube $\hat{x}_i(k|t) \oplus \Delta$, $t \in \mathbb{N}_{\ge 0}$. That is, the estimation errors take values in the specified set Δ. From* (4.25)*, a minimal robust invariant set $\mathcal{R}_i^\infty$ can be obtained following the method in [99]. Also notice that $\Delta \subset \mathcal{R}_i^\infty$. Here we direct our attention to the prediction horizon $\mathbb{N}_{[0,N]}$, then replacing $\mathcal{R}_i^\infty$ with $\mathcal{R}_i^k$, $k \in \mathbb{N}_{[0,N]}$ yields a less conservative set. Here, the predesigned consensus gain matrix K, the communication delay bound $\bar{\tau}$ and the prediction horizon N should be suitably chosen*

such that the set R_i^k satisfies $R_i^k \subseteq \Delta$. It is natural to ask if the estimation error set $\Delta(t)$ can be time-varying. The answer is yes, and this set can be useful in more complex situation, such as the MAS with time-varying communication graph and the time-varying bounds on the estimation errors.

4.5.2 Consensus analysis

In this subsection, we first provide two technical lemmas, and then present the convergence analysis in **Theorem 4.1**.

The following result on $c_i(t)$ is fundamental to the convergence analysis.

Lemma 4.3. *Provided that the initial state $x_i(0)$ is feasible, the MAS in (4.1) under the distributed consensus protocol $u_i^*(0|t) = K\sum_{j\in\mathcal{N}_i} a_{ij}(x_i^*(0|t) - \hat{x}_j(0|t)) + c_i^*(0|t)$, with $c_i(t) = c_i^*(0|t)$, satisfies the following property:*

$$\lim_{t\to\infty} c_i(t) = 0.$$

Proof. To prove the convergence of $c_i(t)$ as $t \to \infty$, we introduce the following function

$$V_i(t) := J_i(\boldsymbol{c}_i^*(t)) = \sum_{k=0}^{N-1} \|c_i^*(k|t)\|_{P_i}^2.$$

For the control candidate sequence $\tilde{\boldsymbol{c}}_i(t+1)$, we have

$$\tilde{V}_i(t+1) = \sum_{k=0}^{N-1} \|\tilde{c}_i(k|t+1)\|_{P_i}^2 = V_i(t) - \|c_i^*(0|t)\|_{P_i}^2.$$

The control candidate sequence $\tilde{\boldsymbol{c}}_i(t+1)$ is a feasible, but not necessarily optimal solution of the robust DMPC optimization problem $\mathcal{P}_i$ at $t+1$. Hence, it follows

$$V_i(t+1) \le \tilde{V}_i(t+1) = V_i(t) - \|c_i^*(0|t)\|_{P_i}^2.$$

Furthermore, one gets

$$V_i(t+1) - V_i(t) \le -\|c_i^*(0|t)\|_{P_i}^2, \tag{4.32}$$

which implies the Lyapunov function $V_i(t)$ is monotonically non-increasing as $t \to \infty$.

Summing $V_i(t+1) - V_i(t)$ in (4.32), we then have

$$\lim_{k\to\infty}\sum_{t=0}^{k}(V_i(t+1) - V_i(t)) = \lim_{k\to\infty} V_i(k+1) - V_i(0) \leq -\lim_{k\to\infty}\sum_{t=0}^{k}\|c_i^*(0|t)\|_{P_i}^2, \quad (4.33)$$

and $V_i(t)$ as $t \to \infty$, satisfies

$$0 \leq V_i(\infty) \leq V_i(0) - \lim_{k\to\infty}\sum_{t=0}^{k}\|c_i^*(0|t)\|_{P_i}^2 < \infty,$$

where $V_i(\infty) := \lim_{t\to\infty} V_i(t)$. Hence, it holds that

$$\lim_{t\to\infty}\|c_i^*(0|t)\|_{P_i}^2 = 0.$$

Thus, $\lim_{t\to\infty}\|c_i(t)\| = 0$ holds. By now, we have proved that the control variable $c_i(t)$ vanishes to zero as $t \to \infty$. □

The next lemma ([103, Lemma 7]) discussing the convergence property of the summable convolution sequence will be used in the proof of **Theorem 4.1**.

Lemma 4.4. *For any given scalar $\beta \in (0,1)$, and the summable sequence $\{\alpha(t)\}$ satisfying $\lim_{t\to\infty}\alpha(t) = 0$, it holds that $\lim_{k\to\infty}\sum_{t=0}^{k}\beta^{k-1-t}\alpha(t) = 0$.*

Now, based on **Lemmas 4.3** and **4.4**, the consensus convergence analysis of the MAS is reported as follows.

Theorem 4.1. *For the system in* (4.1)*, suppose* ***Assumptions 4.1****,* ***4.2****,* ***4.3*** *and the condition in* ***Lemma 4.1*** *hold. Then, the robust consensus of the MAS can be achieved under the robust DMPC consensus protocol.*

Proof. Applying the optimal control input $u_i^*(0|t)$ to the MAS in (4.1) yields $x_i(t+1) = Ax_i(t) + Bu_i^*(0|t)$, with $x_i(0|t) = x_i(t)$. Then, we know that $x_i(t+1) = x_i^*(1|t)$. The closed-loop MAS in (4.4.3) can be rewritten as

$$\mathbf{x}(t+1) = (I_M \otimes A + \mathcal{L} \otimes BK)\mathbf{x}(t) + (I_M \otimes B)\mathbf{c}(t) + (I_M \otimes BK)\mathbf{w}(t),$$

where $\mathbf{c}(t) := \mathrm{col}(c_1(t), c_2(t), \ldots, c_M(t))$. The average state of the MAS is defined by $\bar{x}(t) := 1/M(\mathbf{1}^{\mathrm{T}} \otimes I_n)\mathbf{x}(t) \in \mathbb{R}^n$, with $\mathbf{1}$ being an all-one vector of proper dimensions.

Then,

$$\begin{aligned}
&\bar{x}(t+1)\\
=&\frac{1}{M}(\mathbf{1}^{\mathrm{T}}\otimes A)\mathbf{x}(t)+\frac{1}{M}(\mathbf{1}^{\mathrm{T}}\mathcal{L}\otimes BK)\mathbf{x}(t)+\frac{1}{M}(\mathbf{1}^{\mathrm{T}}\otimes B)\mathbf{c}(t)+\frac{1}{M}(\mathbf{1}^{\mathrm{T}}\otimes BK)\mathbf{w}(t)\\
=&\frac{1}{M}(\mathbf{1}^{\mathrm{T}}\otimes A)\mathbf{x}(t)+B\bar{c}(t)+BK\bar{w}(t)\\
=&A\bar{x}(t)+B\bar{c}(t)+BK\bar{w}(t),
\end{aligned}$$

with $\bar{c}(t) := 1/M(\mathbf{1}^{\mathrm{T}}\otimes I_n)\mathbf{c}(t)$ and $\bar{w}(t) := 1/M(\mathbf{1}^{\mathrm{T}}\otimes I_n)\mathbf{w}(t)$. Define further $\bar{\mathbf{c}}(t) = 1/M((\mathbf{1}^{\mathrm{T}}\mathbf{1})\otimes I_m)\mathbf{c}(t)$ and $\bar{\mathbf{w}}(t) = 1/M((\mathbf{1}^{\mathrm{T}}\mathbf{1})\otimes I_n)\mathbf{w}(t)$. Using notation $\xi_i(t) := x_i(t)-\bar{x}(t)$ and $\boldsymbol{\xi} := \mathrm{col}(\xi_1,\xi_2,\ldots,\xi_M)$, we have that

$$\begin{aligned}
&\boldsymbol{\xi}(t+1)\\
=&(I_M\otimes A+\mathcal{L}\otimes BK)\boldsymbol{\xi}(t)+(I_M\otimes B)I'_{Mm}\mathbf{c}(t)+(I_M\otimes BK)I'_{Mn}\mathbf{w}(t).
\end{aligned}\tag{4.34}$$

with $I'_{Mm} = I_{Mm}-1/M((\mathbf{1}^{\mathrm{T}}\mathbf{1})\otimes I_m)$ and $I'_{Mn} = I_{Mn}-1/M((\mathbf{1}^{\mathrm{T}}\mathbf{1})\otimes I_n)$.

Let $U := [1/M, U_2,\ldots,U_M]\in\mathbb{R}^{M\times M}$ be an orthogonal matrix with which $U_i^{\mathrm{T}}\mathcal{L} = \lambda_i U_i^{\mathrm{T}}$ and the Laplacian matrix can be diagonalized, that is

$$U^{\mathrm{T}}\mathcal{L}U = \mathrm{diag}(0,\lambda_2,\ldots,\lambda_M).$$

Using the property of Kronecker product, we obtain that

$$(U^{\mathrm{T}}\otimes I_n)(I_M\otimes A+\mathcal{L}\otimes BK)(U\otimes I_n) = \mathrm{diag}(A, A+\lambda_2 BK,\ldots,A+\lambda_M BK).$$

Define $\tilde{\boldsymbol{\xi}}(t) = \mathrm{col}(\tilde{\xi}_1(t),\tilde{\xi}_2(t),\ldots,\tilde{\xi}_M(t)) := (U^{\mathrm{T}}\otimes I_n)\boldsymbol{\xi}(t)$. Then (4.34) can be expressed as

$$\begin{aligned}
&\tilde{\boldsymbol{\xi}}(t+1)\\
=&\mathrm{diag}(A, A+\lambda_2 BK,\ldots,A+\lambda_M BK)\tilde{\boldsymbol{\xi}}(t)+(U^{\mathrm{T}}\otimes I_n)(I_M\otimes B)I'_{Mm}\mathbf{c}(t)\\
&+(U^{\mathrm{T}}\otimes I_n)(I_M\otimes BK)I'_{Mn}\mathbf{w}(t).
\end{aligned}\tag{4.35}$$

Next, we define the transition matrix $\Phi := \mathrm{diag}(A, A+\lambda_2 BK,\ldots,A+\lambda_M BK)$, $\mathcal{B} := (U^{\mathrm{T}}\otimes I_n)(I_M\otimes B)I'_{Mm}$, and $\mathcal{B}_k := (U^{\mathrm{T}}\otimes I_n)(I_M\otimes BK)I'_{Mn}$, then (4.34) becomes

$$\tilde{\boldsymbol{\xi}}(t+1) = \Phi\tilde{\boldsymbol{\xi}}(t)+\mathcal{B}\mathbf{c}(t)+\mathcal{B}_k\mathbf{w}(t),\tag{4.36}$$

and thus

$$\tilde{\boldsymbol{\xi}}(t) = \Phi^t \tilde{\boldsymbol{\xi}}(0) + \sum_{k=0}^{t-1} \Phi^k \mathcal{B}\mathbf{c}(t-1-k) + \sum_{k=0}^{t-1} \Phi^k \mathcal{B}_k \mathbf{w}(t-1-k),$$

with $t \in \mathbb{N}_{\geq 1}$. From the definition of $\tilde{\boldsymbol{\xi}}(t) = (U^{\mathrm{T}} \otimes I_n)\boldsymbol{\xi}(t)$, it is easy to know that $\tilde{\xi}_1(t) = 1/M(\sum_{i=1}^{M} \xi_i(t)) = 0$. Also, By invoking **Lemma 4.1** (i.e., $\rho(A + \lambda_i BK) < 1$, $i = 2, 3, \ldots, M$), we get

$$\lim_{t\to\infty} \Phi^t \tilde{\boldsymbol{\xi}}(0) = 0. \tag{4.37}$$

From $I'_{Mm} = I_{Mm} - 1/M((\mathbf{1}^{\mathrm{T}}\mathbf{1}) \otimes I_m) = (I_M - 1/M(\mathbf{1}^{\mathrm{T}}\mathbf{1})) \otimes I_m$, one gets the matrix I'_{Mm} has eigenvalue 0 with multiplicity m and eigenvalue 1 with multiplicity $Mm - m$. Here, it is obtained that $\rho(I'_{Mm}) \leq 1$. In addition, $\rho(A + \lambda_i BK) \leq 1$, one gets $I'_{Mm}(\rho(A+\lambda_i BK))^k < 1$, $k \in \mathbb{N}_{\geq 1}$. In light of this, there always exists a constant $\beta \in (0, 1)$ such that

$$\|I'_{Mm}\Phi^k\| \leq \beta^k < 1. \tag{4.38}$$

Let $E(t-1-k) = \|(U^{\mathrm{T}} \otimes I_n)\|\|I_M \otimes B\|\|\mathbf{c}(t-1-k)\|$. By application of the Cauchy-Schwarz inequality and the inequality in (4.38), we have

$$\begin{aligned}
&\lim_{t\to\infty} \sum_{k=0}^{t-1} \Phi^k \mathcal{B}\mathbf{c}(t-1-k) \\
\leq &\lim_{t\to\infty} \sum_{k=0}^{t-1} \|\Phi^k \mathcal{B}\mathbf{c}(t-1-k)\| \\
\leq &\lim_{t\to\infty} \sum_{k=0}^{t-1} \|I'_{Mm}\Phi^k\| \cdot \|(U^{\mathrm{T}} \otimes I_n)\| \cdot \|I_M \otimes B\| \cdot \|\mathbf{c}(t-1-k)\| \\
\leq &\lim_{t\to\infty} \sum_{k=0}^{t-1} \beta^k E(t-1-k).
\end{aligned} \tag{4.39}$$

Further, according to **Lemmas 4.3** and **4.4**, we obtain

$$\lim_{t\to\infty} \sum_{k=0}^{t-1} \Phi^k \mathcal{B}\mathbf{c}(t-1-k) = 0. \tag{4.40}$$

From the definition of set $\mathcal{R}_i^{\infty}$, we know that

$$\lim_{t\to\infty} \sum_{k=0}^{t-1} \Phi^k \mathcal{B}_k \mathbf{w}(t-1-k) = \boldsymbol{R}^{\infty}, \tag{4.41}$$

where $\boldsymbol{R}^{\infty} = \text{col}(\mathcal{R}_1^{\infty}, \mathcal{R}_2^{\infty}, \ldots, \mathcal{R}_M^{\infty})$. Combining (4.37), (4.40) and (4.41) gives

$$\lim_{t\to\infty} \tilde{\boldsymbol{\xi}}(t) \in \boldsymbol{R}^{\infty}, \tag{4.42}$$

which implies that the MAS converges to a neighborhood of the consensus set. The proof is completed. □

It is shown that the sequence $c_i(t)$ generated by solving the online DMPC optimization problem converges to zero in **Lemma 4.3**. Then, we prove the consensus convergence of the constrained MAS with bounded time-varying delays controlled by the proposed consensus protocol in **Theorem 4.1**. It is worth mentioning that the results can be extended to the cases where the MAS is affected by unknown additive disturbances.

4.6 Numerical Examples

In this section, two numerical examples are conducted to verify the effectiveness of the developed theoretical results.

Example 1: *Linear MAS with semi-stable dynamics*

Consider an MAS consisting of five discrete-time linear systems and each agent i is described by [68]

$$x_i(t+1) = Ax_i(t) + Bu_i(t),\ i = 1, 2, \ldots, 5, \tag{4.43}$$

with

$$A = \begin{bmatrix} 0.8 & 0.1 & 0.1 & 0 & 0 \\ 0 & 0.9 & 0 & 0.1 & 0 \\ 0.1 & 0.1 & 0.6 & 0.1 & 0.1 \\ 0 & 0.1 & 0.1 & 0.8 & 0 \\ 0.1 & 0.1 & 0 & 0 & 0.8 \end{bmatrix},\ B = \begin{bmatrix} -0.1 & 0.1 \\ 0.1 & -0.2 \\ 0 & -0.3 \\ 0.08 & 0.1 \\ 0.2 & 0.08 \end{bmatrix}.$$

The control input constraints of five agents are all set as $\|u_i\|_{\infty} \leq 0.3$. The initial states of five agents are set as $x_1(0) = [0.94; 1.22; -1.12; 1.24; 0.40]$, $x_2(0) = [1.21; -0.66; 0.14; 1.37; 1.39]$, $x_3(0) = [-1.03; 1.41; 1.37; -0.04; 0.90]$, $x_4(0) = [-1.07; -0.23; 1.25; 0.88; 1.38]$ and $x_5(0) = [0.47; -1.39; 1.05; 1.30; 0.54]$, respectively. The maximum communication delay $\bar{\tau} = 3$. The communication network is described by

an undirected graph $\mathcal{G}$, and its Laplacian matrix is

$$\mathcal{L} = \begin{bmatrix} 1 & -0.5 & 0 & -0.5 & 0 \\ -0.5 & 1 & -0.5 & 0 & 0 \\ 0 & -0.5 & 1 & 0 & -0.5 \\ -0.5 & 0 & 0 & 1 & -0.5 \\ 0 & 0 & -0.5 & -0.5 & 1 \end{bmatrix}.$$

The predesigned consensus gain matrix is chosen as $K = [0.1258, -0.1015, 0.0542, 0.0071, -2.443; -0.0787, 0.1863, 0.0637, 0.0982, -0.1376]$ following the method in [68]. The prediction horizon is selected as $N = 10$, and the estimation error set $\Delta = \{\delta \mid \|\delta\| \leq 0.3\}$. Let $\epsilon = \sqrt{60}$. The weighting matrix $P_i = I_2$ and

$$S = \begin{bmatrix} 2.551 & -0.447 & 0.119 & -0.813 & -1.069 \\ -0.447 & 4.028 & 0.227 & 1.356 & -2.664 \\ 0.119 & 0.227 & 1.799 & 0.74 & -2.431 \\ -0.813 & 1.356 & 0.74 & 3.884 & -3.689 \\ -1.069 & -2.664 & -2.431 & -3.689 & 10.081 \end{bmatrix}$$

.

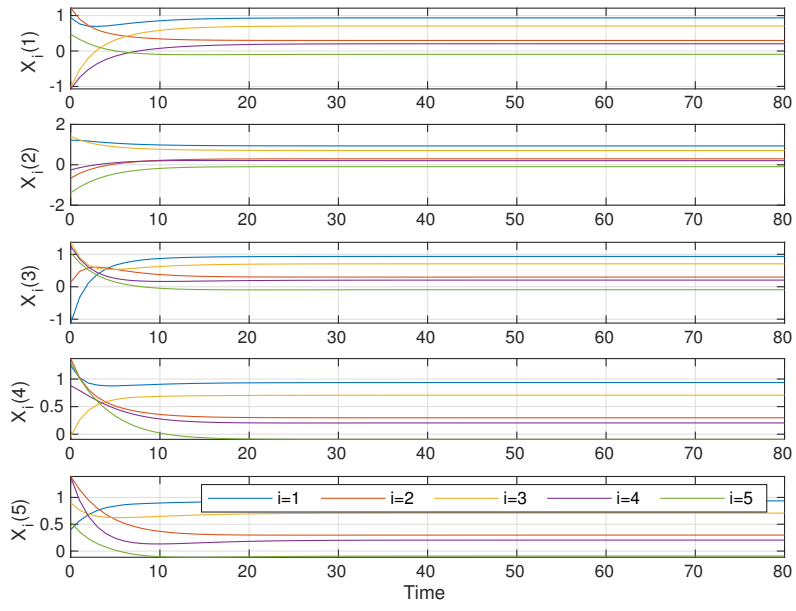

Figure 4.4: States of five agents under the consensus protocol in [68].

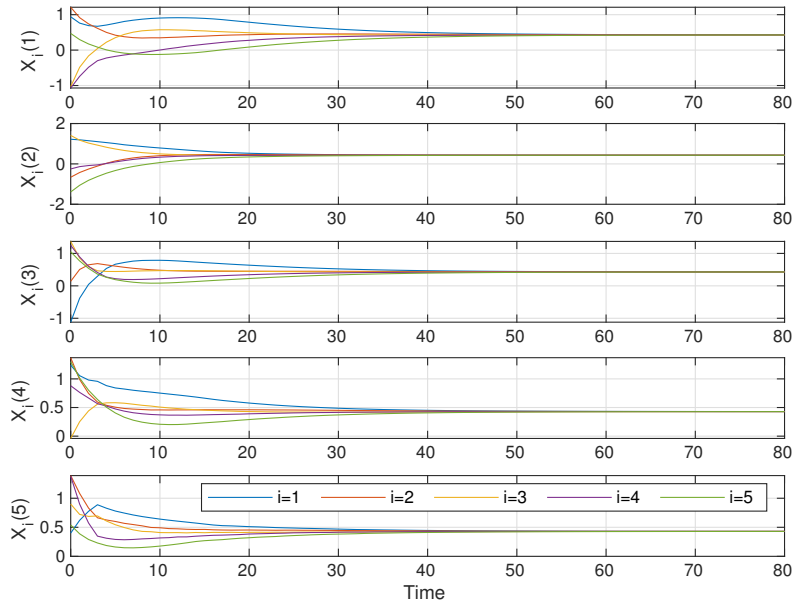

Figure 4.5: States of five agents under the proposed protocol.

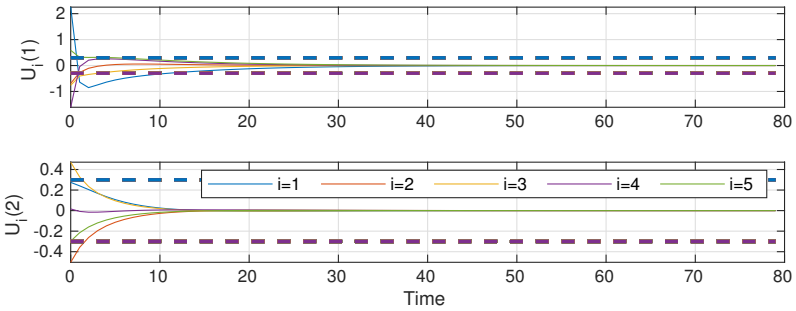

Figure 4.6: Control inputs of five agents under the predesigned consensus protocol.

Figures. 4.4 and 4.5 show the states of five agents with communication delays under the consensus protocol in [68] and the robust DMPC-based consensus protocol. Clearly, the consensus is not achieved under the protocol in [68], due to time-varying delays among agents. It can be seen from Figure 4.5 that five agents reach consensus under the proposed protocol.

On the other hand, the control inputs of all agents under the predesigned consensus protocol and the robust DMPC-based consensus protocol are shown in Figures. 4.6 and 4.7. It can be observed that the MAS only under the proposed consensus protocol satisfies control input constraints.

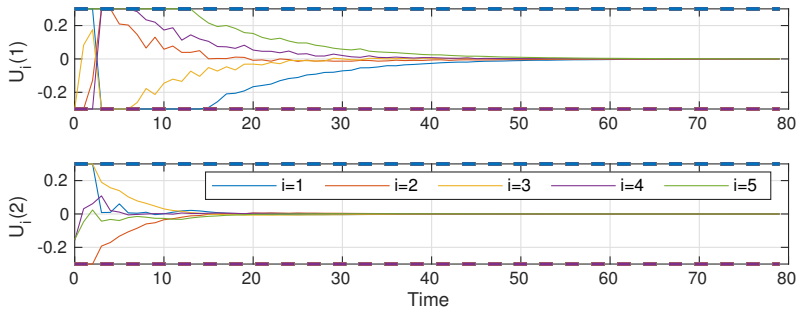

Figure 4.7: Control inputs of five agents under the robust DMPC-based consensus protocol.

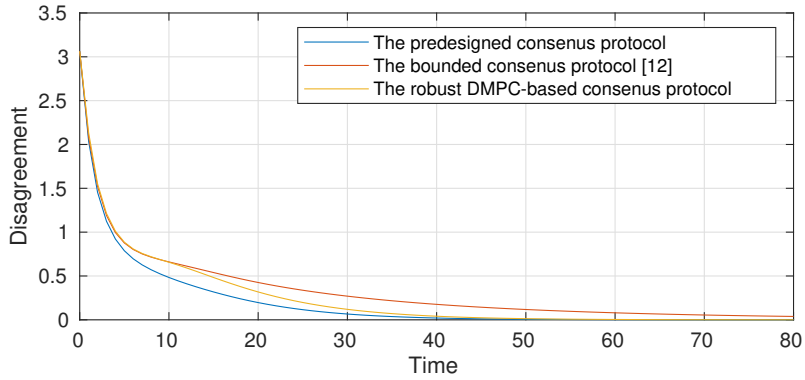

Figure 4.8: Consensus performance comparison of different consensus protocols.

To quantify the consensus performance, we define a disagreement function $D(t) = \sum_{i=1}^{M} \sum_{j \in \mathcal{N}_i} a_{ij} \|x_i(t) - x_j(t)\|/M$ for the MAS under different consensus protocols. The bounded consensus protocol from [169] is given as

$$u_i = \begin{cases} 0.3, & u_i \geq 0.3, \\ -0.3, & u_i \leq -0.3, \\ K' \sum\limits_{j \in \mathcal{N}_i} a_{ij}(x_i(t) - x_j(t)), & -0.3 < u_i < 0.3, \end{cases}$$

in which $K' = [0.0846, -0.1523, 0.0028, -0.1044, -0.2256; -0.0818, 0.2567, 0.2256, -0.0423, -0.0479]$. As illustrated in Figure 4.8, all disagreement trajectories monotonically decrease. The MAS under the predesigned consensus protocol converges at a faster rate than the proposed robust DMPC-based consensus protocol and the bounded consensus protocol in [169]. However, the control input constraints cannot be guaranteed under the predesigned consensus protocol as reported in Figure 4.6.

In contrast, the other two types of consensus protocols guarantee the satisfaction of control input constraints. In particular, the proposed DMPC-based consensus protocol achieves a faster consensus convergence rate than the bounded consensus protocol in [169].

Example 2: *Linear MAS with unstable dynamics*

Consider an MAS consisting of four discrete-time oscillators and each agent i is characterized by [105]

$$x_i(t+1) = Ax_i(t) + Bu_i(t),\ i = 1, 2, 3, 4, \tag{4.44}$$

with

$$A = \begin{bmatrix} 0 & 1 \\ -1.15 & 0 \end{bmatrix},\ B = \begin{bmatrix} 0.5 \\ 0.5 \end{bmatrix}.$$

The control input constraints of four agents are all set as $\|u_i\|_\infty \leq 0.1$. The initial states of four agents are set as $x_1(0) = [-0.18; 0.21]$, $x_2(0) = [0.32; -0.18]$, $x_3(0) = [-0.29; -0.14]$ and $x_4(0) = [-0.22; 0.24]$, respectively. The maximum communication delay $\bar{\tau} = 2$. The wireless communication network among the MAS is described by an undirected graph $\mathcal{G}$. The Laplacian matrix of $\mathcal{G}$ is

$$\mathcal{L} = \begin{bmatrix} 1 & -0.5 & 0 & -0.5 \\ -0.5 & 1 & -0.5 & 0 \\ 0 & -0.5 & 1 & -0.5 \\ -0.5 & 0 & -0.5 & 1 \end{bmatrix}.$$

The prediction horizon is $N = 7$ and the estimation error set is $\Delta = \{\delta \mid \|\delta\| \leq 0.1\}$. Let $\epsilon = \sqrt{0.96}$. The weighting matrix $P_i = 50$, the predesigned consensus gain matrix is designed as $K = [0.2748, -0.3148]$ and $S = \begin{bmatrix} 4.4733 & 0.8746 \\ 0.8746 & 3.3690 \end{bmatrix}$.

Figures. 4.9 and 4.10 show the states of four agents with communication delays using the consensus protocol in [68] and the proposed robust DMPC-based consensus protocol. It can be observed from Figure 4.9 that unstable agents with communication delays cannot reach consensus under the protocol in [68]. In contrast, as shown in Figure 4.10 four agents with communication delays asymptotically converge to consensus. The simulation results verify that the proposed consensus protocol applies to the general linear constrained MAS with semi-stable and unstable dynamics.

In addition, as shown in Figure 4.11, the control inputs of agents under the pre-

designed consensus protocol cannot satisfy control input constraints. In contrast, Figure 4.12 exhibits that all agents under the proposed consensus protocol satisfy control input constraints.

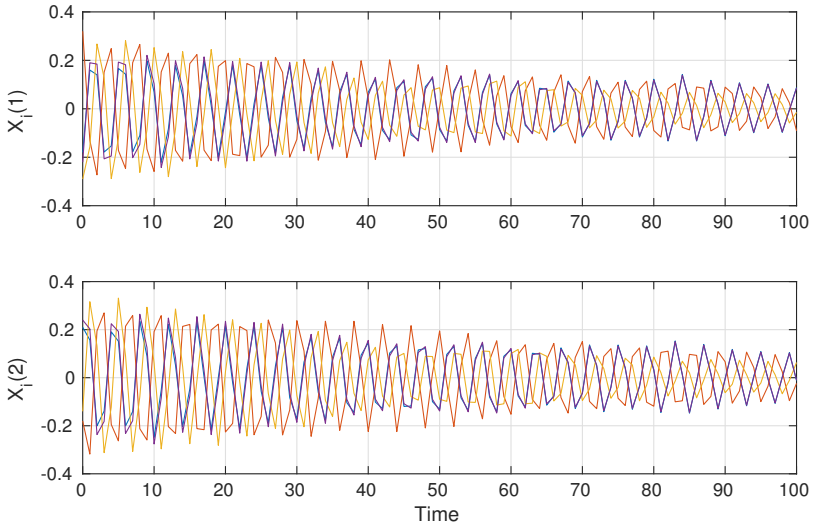

Figure 4.9: States of four agents under the consensus protocol in [68].

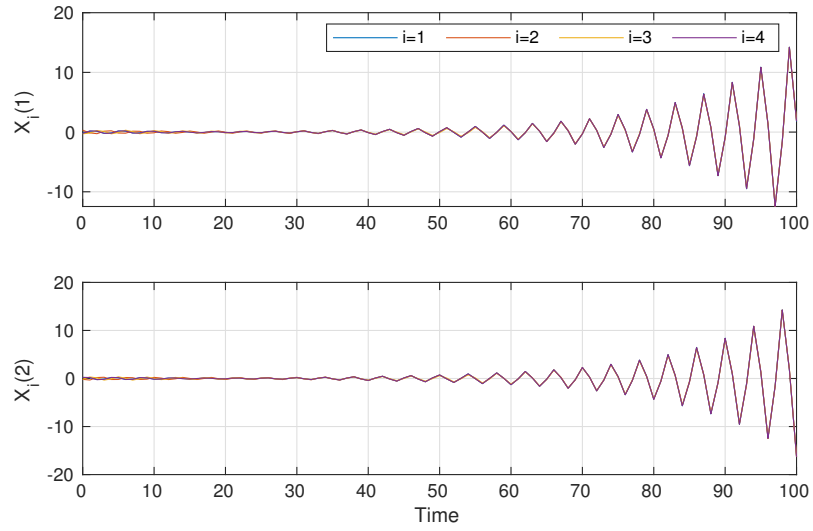

Figure 4.10: States of four agents under the proposed protocol.

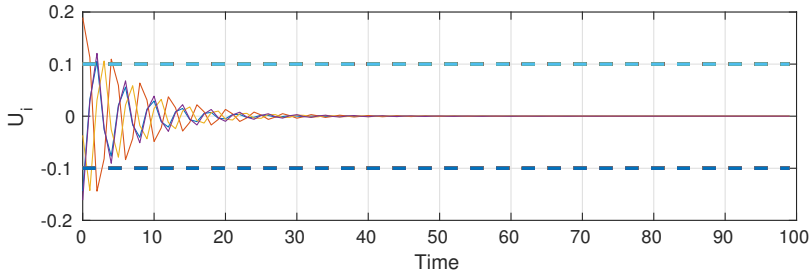

Figure 4.11: Control inputs of four agents under the predesigned consensus protocol.

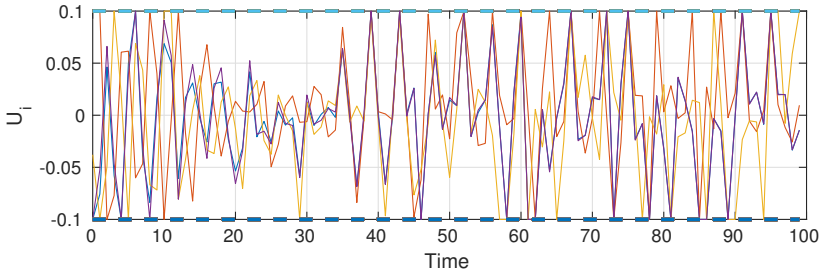

Figure 4.12: Control inputs of four agents under the robust DMPC-based consensus protocol.

4.7 Conclusion

In this chapter, we designed a robust DMPC-based consensus protocol for general the linear MAS with input constraints and time-varying communication delays. The proposed distributed consensus protocol, based on inverse optimal control and tube-based MPC techniques, achieved suboptimal consensus performance while satisfying control input constrains. Furthermore, the recursive feasibility of the DMPC optimization problem and the consensus convergence of the constrained MAS were rigorously analyzed. Two numerical examples were given to verify the proposed distributed consensus protocol.

Chapter 5

Distributed Lyapunov-Based Model Predictive Formation Tracking Control for Autonomous Underwater Vehicles Subject to Disturbances

5.1 Introduction

It is well known that the AUV plays an essential role in performing underwater tasks, such as deep-sea detection and oceanic rescue [133]. Compared with the single AUV, cooperative AUVs can perform more complicated underwater tasks. One fundamental problem of cooperative AUVs is the formation tracking control, which requires AUVs to keep a prescribed formation while simultaneously tracking a given reference trajectory. Some appealing methods have been developed to tackle this problem, e.g., the virtual structure control method [168], and the leader-follower method [12]. Unfortunately, these methods cannot optimize the control performance of cooperative AUVs with constraints. Alternatively, the DMPC method is an ingenious solution to this problem and is exploited for the cooperative AUVs [70]. The main challenge of applying DMPC for cooperative AUVs lies in guaranteeing closed-loop stability. The conventional MPC approach performs local linearization on the nonlinear system and then designs the additional terminal set and the terminal control law for the opti-

mization problem [4, 17]. However, the stability analysis by the local linearization is practically inefficient since AUVs have complex nonlinear system dynamics. To overcome this difficulty, the authors in [14, 82, 132] circumvent the local linearization by employing the Lyapunov-based MPC (LMPC), which combines the merits of the Lyapunov-based control with the MPC design, thereby inheriting the stability of the Lyapunov-based controller and the optimality of the MPC.

On the other hand, AUVs are exposed to unknown environmental disturbances induced by the ocean current in practice, which poses a significant challenge to the formation control task [1, 6]. For this reason, the formation control that ensures robustness against disturbances is highly appreciated. Compared with robust MPC, the ESO-based MPC method is more constructive and computationally tractable for cooperative AUVs with complex dynamics. Inspired by this attractive feature, we incorporate the ESO design into the DLMPC scheme, in which the ESO can estimate unknown ocean current disturbances. Regarding the safety of cooperative AUVs, collision avoidance is necessary to be considered in the distributed controller design. Several collision avoidance methods have been developed (see, e.g., [111, 153]). In [111], a class of control Lyapunov barrier functions is introduced to ensure collision avoidance, yielding the gradient-based control input. In [153], MPC is applied to solve this problem by imposing the collision avoidance constraint into the MPC optimization problem. In this chapter, we design a potential field-based cost term to account for collision avoidance and incorporate it into the overall cost function of the DLMPC optimization problem. The main contributions of this chapter are two-fold:

- A DLMPC method is proposed for the formation tracking problem of cooperative constrained AUVs, and an ESO is designed to estimate the unknown ocean current disturbances. In addition, a potential field-based collision cost term is designed to achieve inter-AUV collision avoidance. The control inputs of each AUV are determined by solving the local DMPC optimization problem based on its own and neighbors' information. The overall control performance and robustness of the AUVs are greatly enhanced.

- The recursive feasibility of the DLMPC algorithm is rigorously analyzed. Further, the closed-loop stability of cooperative AUVs is guaranteed by the stability constraint constructed by the ESO-based auxiliary controller and its associated Lyapunov function. The theoretical results provide a firm ground for practical cooperative AUVs' formation tracking control design.

5.2 Problem Formulation

5.2.1 AUV modeling

In this chapter, the 3-DOF horizontal motion of AUVs is considered under a reasonable assumption that the roll angle ϕ and the pitch angle θ are small [24]. Consider a team of M homogeneous AUVs, and the kinematics of AUV i, $i \in \mathcal{V}$ is described by

$$\dot{\eta}_i = R(\psi_i)\nu_i, \tag{5.1}$$

where $\eta_i = [x_i, y_i, \psi_i]^{\mathrm{T}}$ consists of the position $p_i = [x_i, y_i]^{\mathrm{T}}$ and the orientation ψ_i, $\nu_i = [u_i, v_i, r_i]^{\mathrm{T}}$ denotes the velocity, and the rotation matrix $R(\psi_i)$ is

$$R(\psi_i) = \begin{bmatrix} \cos\psi_i & -\sin\psi_i & 0 \\ \sin\psi_i & \cos\psi_i & 0 \\ 0 & 0 & 1 \end{bmatrix}.$$

The 3-DOF nonlinear dynamic motion equation of AUV i is expressed as

$$M_i\dot{\nu}_i + C_i(\nu_i)\nu_i + D_i(\nu_i)\nu_i + g_i(\eta_i) = \tau_i + \tau_{iw}, \tag{5.2}$$

where M_i is the inertia matrix including the added mass, $D_i(\nu_i)$ denotes the damping matrix, the restoring force is assumed by $g_i(\eta_i) = 0$, τ_i denotes the control input, $C_i(\nu_i)$ denotes the Coriolis-centripetal matrix, and $\tau_{iw} = M_i R^{\mathrm{T}}(\psi_i)w_i$, with w_i being the ocean current disturbances. Combining (5.1) and (5.2), we establish the system dynamics of AUV i

$$\dot{x}_i = \begin{bmatrix} R(\psi_i)\nu_i \\ M_i^{-1}(\tau_i + \tau_{iw} - C_i(\nu_i)\nu_i - D_i(\nu_i)\nu_i) \end{bmatrix} = f(x_i, \tau_i, w_i), \tag{5.3}$$

where $x_i = \mathrm{col}(\eta_i, \nu_i) \in \mathbb{R}^6$ and $\tau_i \in \mathbb{R}^3$ are the system state and the control input of AUV i, respectively.

The following essential properties of AUVs are exploited in the distributed controller design later.

P-1: The inertia matrix is symmetric, positive definite and upper bounded, i.e., $M_i = M_i^{\mathrm{T}} \succ 0$, $\|M_i\|_\infty = \bar{m}_i$, where $\bar{m}_i$ is a known constant.

P-2: The Coriolis matrix is skew-symmetric, i.e., $C_i(\nu_i) = -C_i^{\mathrm{T}}(\nu_i)$.

P-3: The rotation matrix satisfies that $R^{-1}(\psi_i) = R^{\mathrm{T}}(\psi_i)$ and $\|R^{\mathrm{T}}(\psi_i)\eta_i\| = \|\eta_i\|$.
P-4: The damping matrix is positive definite, i.e., $D_i(\nu_i) \succ 0$.

5.2.2 Problem formulation

To better describe the information exchange among AUVs, we introduce a directed graph $\mathcal{G}' = (\mathcal{V}, \mathcal{E})$. An assumption on the communication network $\mathcal{G}' = (\mathcal{V}, \mathcal{E})$ is presented as follows.

Assumption 5.1. *For cooperative AUVs, AUV i, $i \in \mathcal{V}$ can receive the information from the virtual leader and its neighbors. The AUVs are synchronized in the time clock, and the predicted system state sequences are available at sampling instants.*

We now formulate the formation tracking problem of cooperative AUVs. In order to maintain a prescribed formation shape and track the time-varying reference trajectory of the virtual leader $\eta_r(t) = \mathrm{col}(p_r(t), \psi_r(t))$, AUV i, $i \in \mathcal{V}$, is driven to satisfy: 1) Tracking control: $\lim_{t\to\infty}\{p_i(t) - p_r(t)\} = d_{ir}$, $\lim_{t\to\infty}\{\psi_i(t) - \psi_r(t)\} = 0$; 2) Formation control: $\lim_{t\to\infty}\{p_i(t) - p_j(t)\} = d_{ij}$; 3) Collision avoidance: $\|p_i(t) - p_j(t)\| \geq 2R$, where R is the safety radius of AUV i, $\lambda_i = d_{ir}$ is the configuration formation vector between AUV i and the reference trajectory, and $d_{ij} = p_i - p_j$ denotes the relative distance vector between AUV i and AUV j, $j \in \mathcal{V}, i \neq j$.

To avoid singularities of the reference trajectory, we make the following assumption.

Assumption 5.2. *The reference trajectory and its first-, second- and third-order derivatives are smooth and bounded, i.e.,* $0 \leq \underline{p} \leq \|p_r\|_\infty \leq \overline{p} < \infty, 0 \leq \underline{p_1} \leq \|\dot{p}_r\|_\infty \leq \overline{p}_1 < \infty, 0 \leq \underline{p_2} \leq \|\ddot{p}_r\|_\infty \leq \overline{p}_2 < \infty$ *and* $0 \leq \underline{p_3} \leq \|\dddot{p}_r\|_\infty \leq \overline{p}_3 < \infty$.

From the reference trajectory η_r, we make the following reference augmentation,

$$\begin{cases} \psi_r = \mathrm{atan2}(\dot{y}_r(t), \dot{x}_r(t)), \\ u_r = \sqrt{\dot{x}_r^2(t) + \dot{y}_r^2(t)}, \\ v_r = 0, \\ r_r = (\dot{x}_r(t)\ddot{y}_r(t) - \dot{y}_r(t)\ddot{x}_r(t))/(\dot{x}_r^2(t) + \dot{y}_r^2(t)), \end{cases}$$

where atan2 is the four-quadrant inverse tangent operator.

5.3 Distributed Lyapunov-Based Model Predictive Formation Tracking Control

In this section, we design the DLMPC method for the formation tracking problem of cooperative AUVs with unknown disturbances. First, an ESO-based auxiliary controller is designed using the backstepping technique [3]. Next, we present the distributed model predictive formation tracking optimization problem and the DLMPC algorithm. Finally, the algorithm's recursive feasibility and the closed-loop stability of AUVs are analyzed.

5.3.1 Design of the auxiliary control law

Let $\eta_i = [x_i, y_i, \psi_i]^{\mathrm{T}}$ denote the trajectory of AUV i and $\eta_{ir} = \eta_r - \lambda_i = [x_{ir}, y_{ir}, \psi_{ir}]^{\mathrm{T}}$ be the desired trajectory. Define a virtual reference trajectory

$$\begin{aligned} \dot{\eta}_{id} &= \dot{\eta}_{ir} - \Lambda_i \tilde{\eta}_i, \\ \nu_{id} &= R^{-1}(\psi_i)\dot{\eta}_{id}, \end{aligned} \tag{5.4}$$

where $\tilde{\eta}_i = \eta_i - \eta_{ir}$ denotes the tracking error of AUV i and Λ_i is a diagonal design matrix. And let

$$s_i = \dot{\eta}_i - \dot{\eta}_{id} = \dot{\tilde{\eta}}_i + \Lambda_i \tilde{\eta}_i, \tag{5.5}$$

where s_i is a new state variable. The error dynamics becomes

$$\begin{aligned} \dot{\tilde{\eta}}_i &= \dot{\eta}_i - \dot{\eta}_{ir} \\ &= R(\psi_i)(\nu_i - \nu_{ir}) \\ &= R(\psi_i)(R^{-1}(\psi_i)s_i + \alpha_i - \nu_{ir}) \\ &= -\Lambda_i \tilde{\eta}_i + s_i, \end{aligned} \tag{5.6}$$

where $\alpha_i = \nu_{id} = R^{-1}(\psi_i)(\dot{\eta}_{ir} - \Lambda_i \tilde{\eta}_i)$ is a stabilizing function. Further, we define

$$V_{i,1} = \frac{1}{2}\tilde{\eta}_i^{\mathrm{T}} K_{pi} \tilde{\eta}_i, \tag{5.7}$$

with $K_{pi} = \mathrm{diag}(k_{pi1}, k_{pi2}, k_{pi3})$, $k_{pi1} > 0, k_{pi2} > 0, k_{pi3} > 0$. Then the derivative of $V_{i,1}$ becomes

$$\dot{V}_{i,1} = \tilde{\eta}_i^{\mathrm{T}} K_{pi} \dot{\tilde{\eta}}_i = (-\tilde{\eta}_i^{\mathrm{T}} K_{pi} \Lambda_i \tilde{\eta}_i + s_i^{\mathrm{T}} K_{pi} \tilde{\eta}_i). \tag{5.8}$$

The dynamics of AUV i can be equivalently expressed as

$$M_i^*\ddot{\eta}_i + C_i^*\dot{\eta}_i + D_i^*\dot{\eta}_i = R(\psi_i)(\tau_i + \tau_{iw}), \tag{5.9}$$

where $M_i^* = R(\psi_i)M_iR^{\mathrm{T}}(\psi_i)$, $C_i^* = R(\psi_i)[C_i(\nu_i) - M_iS(\dot{\psi}_i)]R^{\mathrm{T}}(\psi_i)$, $D_i^* = R(\psi_i)D_i(\nu_i)R^{\mathrm{T}}(\psi_i)$ and $S(\dot{\psi}_i) = [0, -\dot{\psi}_i, 0; \dot{\psi}_i, 0, 0; 0, 0, 0]$.

In the next step, the Lyapunov function is defined as

$$V_{i,2} = V_{i,1} + \frac{1}{2}s_i^{\mathrm{T}}M_i^*s_i. \tag{5.10}$$

Taking the time derivative of $V_{i,2}$ results in

$$\begin{aligned}
\dot{V}_{i,2} =& \dot{V}_{i,1} + (s_i^{\mathrm{T}}M_i^*\dot{s}_i + \frac{1}{2}s_i^{\mathrm{T}}\dot{M}_i^*s_i) \\
=& s_i^{\mathrm{T}}(\frac{1}{2}\dot{M}_i^* - C_i^* - D_i^*)s_i - \tilde{\eta}_i^{\mathrm{T}}K_{pi}\Lambda_i\tilde{\eta}_i + s_i^{\mathrm{T}}K_{pi}\tilde{\eta}_i \\
&+ s_i^{\mathrm{T}}R(\psi_i)[\tau_i + \tau_{iw} - M_i\dot{\nu}_{id} - C_i(\nu_i)\nu_{id} - D_i(\nu_i)\nu_{id}] \\
=& s_i^{\mathrm{T}}R(\psi_i)[\tau_i + \tau_{iw} - M_i\dot{\nu}_{id} - C_i(\nu_i)\nu_{id} - D_i(\nu_i)\nu_{id} + R(\psi_i)^{\mathrm{T}}K_{pi}\tilde{\eta}_i] \\
&- \tilde{\eta}_i^{\mathrm{T}}K_{pi}\Lambda_i\tilde{\eta}_i - s_i^{\mathrm{T}}D_i^*s_i,
\end{aligned} \tag{5.11}$$

where $s_i^{\mathrm{T}}(\dot{M}_i^* - 2C_i^*)s_i = 0$ thanks to the property P-2.

The ideal auxiliary control law is then designed as

$$\tau_i^a = M_i\dot{\nu}_{id} + C_i(\nu_i)\nu_{id} + D_i(\nu_i)\nu_{id} - R^{\mathrm{T}}(\psi_i)K_{pi}\tilde{\eta}_i - R^{\mathrm{T}}(\psi_i)K_{di}s_i - \tau_{iw}, \tag{5.12}$$

in which $K_{di} = \mathrm{diag}(k_{di1}, k_{di2}, k_{di3})$, with $k_{di1} > 0, k_{di2} > 0, k_{di3} > 0$.

In practice, the accurate ocean current disturbances are not available. Since the ocean current has finite energy, we make the following assumption.

Assumption 5.3. *The ocean current disturbances w_i and its rate $\dot{w}_i$ are unknown but bounded by $\|w_i\| \leq \bar{w}_i$ and $\|\dot{w}_i\| \leq \bar{\dot{w}}_i$, respectively.*

In the following, an ESO is developed to estimate the unknown disturbances [27, 113]. To facilitate the ESO design, define $\mu_i = R(\psi_i)\nu_i$, then the system model (5.3) is transformed into

$$\begin{aligned}
\dot{\eta}_i =& \mu_i, \\
\dot{\mu}_i =& R(\psi_i)M_i^{-1}\tau_i + \phi_i(\eta_i, \mu_i) + w_i,
\end{aligned} \tag{5.13}$$

where $\phi_i(\eta_i, \mu_i) = S(\dot{\psi}_i)\mu_i - R(\psi_i)M_i^{-1}[C(\nu_i) + D(\nu_i)]R^{\mathrm{T}}(\psi_i)\mu_i$.

Let $\hat{\eta}_i$, $\hat{\mu}_i$ and $\hat{w}_i$ be the estimation of η_i, μ_i and w_i, respectively. Define the estimation errors $e_{1i} = \eta_i - \hat{\eta}_i$, $e_{2i} = \mu_i - \hat{\mu}_i$, $e_{3i} = w_i - \hat{w}_i$. Then, the ESO for AUV i, $i \in \mathcal{V}$ is designed as

$$\begin{cases} \dot{\hat{\eta}}_i = \hat{\mu}_i + K_1 e_{1i}, \\ \dot{\hat{\mu}}_i = R(\psi_i)M_i^{-1}\tau_i + \phi_i(\eta_i, \mu_i) + K_2 e_{1i} + \hat{w}_i, \\ \dot{\hat{w}}_i = K_3 e_{1i}, \end{cases} \tag{5.14}$$

where $K_1 = \mathrm{diag}(k_1, k_1, k_1)$, $K_2 = \mathrm{diag}(k_2, k_2, k_2)$ and $K_3 = \mathrm{diag}(k_3, k_3, k_3)$ are positive matrices. The estimation errors then become

$$\begin{cases} \dot{e}_{1i} = e_{2i} - K_1 e_{1i}, \\ \dot{e}_{2i} = e_{3i} - K_2 e_{1i}, \\ \dot{e}_{3i} = \dot{w}_i - K_3 e_{1i}. \end{cases} \tag{5.15}$$

Let $e_i = \mathrm{col}(e_{1i}, e_{2i}, e_{3i}) \in \mathbb{R}^9$, the estimation error dynamics (5.15) is expressed as

$$\dot{e}_i = Ae_i + B\dot{w}_i, \tag{5.16}$$

with

$$A = \begin{bmatrix} -K_1 & I_3 & 0_3 \\ -K_2 & 0_3 & I_3 \\ -K_3 & 0_3 & 0_3 \end{bmatrix}, \quad B = \begin{bmatrix} 0_3 \\ 0_3 \\ I_3 \end{bmatrix}.$$

The stability of error dynamic system in (5.16) is established if the following inequality,

$$A^{\mathrm{T}}P + PA \leq -\varrho I_9 \tag{5.17}$$

holds, where $P \succ 0$, $\varrho \geq 1$.

Based on the ESO (5.14), the auxiliary control law is designed as

$$\hat{\tau}_i^a = M_i\dot{\nu}_{id} + C_i(\nu_i)\nu_{id} + D_i(\nu_i)\nu_{id} - R^{\mathrm{T}}(\psi_i)K_{pi}\tilde{\eta}_i - R^{\mathrm{T}}(\psi_i)K_{di}s_i - \hat{\tau}_{iw}, \tag{5.18}$$

where $\hat{\tau}_{iw}(t_k)$ is the estimated disturbance.

The following lemma presents the stability of cooperative AUVs based on the auxiliary control law.

Lemma 5.1. *For a team of AUVs in* (5.3)*, if there exist a matrix* P *and a positive constant such that 1)* $\varrho-\theta_1-\theta_2>0$*, 2)* $\underline{\lambda}(K_{di}^*)-\bar{m}_i^2/2\theta_1>0$ *and the condition* (5.17) *hold, with the design parameters* $0<\theta_1<1$, $0<\theta_2<1$*. Then, the cooperative AUVs fulfill the formation tracking task under the ESO-based auxiliary control law* (5.18)*.*

Proof. The Lyapunov candidate function of the ESO is defined

$$V_{i,3}=\frac{1}{2}e_i^{\mathrm{T}}Pe_i, \tag{5.19}$$

which is bounded by $1/2\underline{\lambda}(P)\|e_i\|^2\leq V_{i,3}\leq 1/2\bar{\lambda}(P)\|e_i\|^2$.

The derivative of $V_{i,3}$ with respect to (5.16) satisfies

$$\dot{V}_{i,3}=\frac{1}{2}e_i^{\mathrm{T}}(A^{\mathrm{T}}P+PA)e_i+e_i^{\mathrm{T}}PB\dot{w}_i. \tag{5.20}$$

Consider the following Lyapunov function

$$V_i=V_{i,2}+V_{i,3},\ V=\sum_{i=1}^{M}V_i. \tag{5.21}$$

Note that the Lyapunov function (5.21) is continuously differentiable and radically unbounded. By Lyapunov theorems [50], there exist functions $\beta_i(\cdot), i=1,2$ which belong to class $\mathcal{K}_\infty$ such that the following inequality holds

$$\beta_1(\|\mathtt{x}_i\|)\leq V_i\leq\beta_2(\|\mathtt{x}_i\|),$$

where $\mathtt{x}_i=\mathrm{col}(\tilde{\eta}_i,s_i,e_i)$.

Under the ESO-based auxiliary control law (5.18), the derivative of the overall Lyapunov function becomes

$$\begin{aligned}
&\dot{V}|_{\hat{\tau}_i^a(t)}\\
=&\sum_{i=1}^{M}\Big\{-\tilde{\eta}_i^{\mathrm{T}}K_{pi}\Lambda_i\tilde{\eta}_i-s_i^{\mathrm{T}}K_{di}^*s_i+s_i^{\mathrm{T}}M_i^*e_{3i}+\frac{1}{2}e_i^{\mathrm{T}}(A^{\mathrm{T}}P+PA)e_i+e_i^{\mathrm{T}}PB\dot{w}_i\Big\}\\
\leq&\sum_{i=1}^{M}\Big\{-\tilde{\eta}_i^{\mathrm{T}}K_{pi}\Lambda_i\tilde{\eta}_i-(\underline{\lambda}(K_{di}^*)-\frac{\bar{m}_i^2}{2\theta_1})\|s_i\|^2-\frac{1}{2}(\varrho-\theta_1)\|e_i\|^2+\epsilon_1\Big\}\\
=&\sum_{i=1}^{M}\Big\{-\tilde{\eta}_i^{\mathrm{T}}K_{pi}\Lambda_i\tilde{\eta}_i-(\underline{\lambda}(K_{di}^*)-\frac{\bar{m}_i^2}{2\theta_1})\|s_i\|^2-\frac{1}{2}(\varrho-\theta_1-\theta_2)\|e_i\|^2-\frac{1}{2}\theta_2\|e_i\|^2+\epsilon_1\Big\}
\end{aligned}$$

where $\dot{V}|_{\hat{\tau}_i^a(t)}$ denotes the derivative of Lyapunov function under the control law $\hat{\tau}_i^a(t)$,

$K_{di}^* = D_i^* + K_{di}$, and $\epsilon_1 = \|e_i\|\|PB\|\bar{w}_i$. If $\|e_i\| \geq 2\|PB\|\bar{w}_i/\theta_2$ and the conditions 1) and 2) hold, then

$$\dot{V}_{i,3} \leq -\frac{1}{2}(\varrho - \theta_1 - \theta_2)\|e_i\|^2 < 0. \tag{5.22}$$

Therefore, the estimation errors converge to a compact set $\Omega_e = \{e_i \in \mathbb{R}^3 | \|e_i\| \leq \rho_{e_i}, \rho_{e_i} > 2\|PB\|\bar{w}_i/\theta_2\}$. In addition, $\dot{V}_i|_{\hat{\tau}_i^a(t)} < 0$, i.e., $\dot{V} < 0$. If the inequality $\|e_i\| > 2\|PB\|\bar{w}_i/\theta_2$ holds, then, cooperative AUVs fulfill the formation tracking task. □

5.3.2 Design of the DMPC optimization problem

5.3.2.1 Collision avoidance cost design

The potential field method is widely used for robots to avoid collisions [96,135]. Here a collision avoidance cost term is designed by using a potential field function that penalizes potential collisions among AUVs. The collision avoidance cost $J_{ij}^{ca}(t)$ is designed as

$$J_{ij}^{ca}(t) = \sum_{j \in \mathcal{N}_i} \frac{\Gamma}{1 + \exp(d_{ij}^{ca})} = \sum_{j \in \mathcal{N}_i} f_{pi}(t), \tag{5.23}$$

where $d_{ij}^{ca} = k_i(\|\tilde{d}_{ij}\| - 2R)$, $\|\tilde{d}_{ij}\|$ is the distance between AUV i and AUV j, $f_{pi}(t)$ is the collision avoidance function, $\Gamma > 0$ is a tuning parameter, and $k_i > 0$ is a parameter that defines the smoothness of the collision avoidance function.

5.3.2.2 The objective function design

To achieve the control objective, the cost function of AUV i at t_k is designed as

$$\begin{aligned} &J_i(x_i(t_k), \tilde{x}_j^a(s|t_k), \tau_i(s|t_k)) \\ &= \int_{t_k}^{t_k+T} \Big\{ \sum_{j \in \mathcal{N}_i} \|x_{ij}(s|t_k)\|_{Q_i}^2 + \|x_{ir}(s|t_k)\|_{Q_i'}^2 + J_{ij}^{ca}(s|t_k) + \|\tau_i(s|t_k)\|_{R_i}^2 \Big\} \, \mathrm{d}s, \end{aligned} \tag{5.24}$$

where t_k denotes the sampling time instant, $s \in [t_k, t_k + T]$, T denotes the prediction horizon, δ denotes the sampling period, i.e., $t_{k+1} = t_k + \delta$, $Q_i \succeq 0$, $Q_i' \succeq 0$, $R_i \succ 0$ are the weighting matrices, $x_{ir} = \tilde{x}_i + \Lambda_i - x_r$, $x_r = \mathrm{col}(\eta_r, \nu_r)$, and $x_{ij} = \tilde{x}_i + \Lambda_i - \tilde{x}_j^a - \Lambda_j$. $\Lambda_i = \mathrm{col}(\lambda_i, \dot{\lambda}_i)$, $J_{ij}^{ca}(s|t_k)$ is the collision avoidance cost. $\tilde{p}_i$ is the nominal position of AUV i and $\tilde{p}_j^a$ is the assumed position of AUV j. $\tilde{x}_i$ is the nominal state of AUV i, which is evaluated by $\dot{\tilde{x}}_i(s|t_k) = f(\tilde{x}_i(s|t_k), \tau_i(s|t_k), 0)$. The assumed state $\tilde{x}_j^a(s|t_k)$

of AUV j at t_k is generated by $\dot{\tilde{x}}_j^a(s|t_k) = f(\tilde{x}_j^a(s|t_k), \tilde{\tau}_j^a(s|t_k), 0)$, and the assumed control input $\tilde{\tau}_j^a(s|t_k)$, i.e.,

$$\tilde{\tau}_j^a(s|t_k) = \begin{cases} \tau_j^*(s|t_{k-1}), s \in [t_k, t_{k-1}+T), \\ \tau_j^*(t_{k-1}+T; t_{k-1}), s \in [t_{k-1}+T, t_k+T]. \end{cases}$$

5.3.2.3 The DMPC optimization problem

For AUV i, using the objective function (5.24), the DMPC optimization problem $\mathcal{P}_i$ is designed as

$$\begin{aligned} \min_{\tau_i \in S(\delta)} \quad & J_i(x_i(t_k), \tilde{x}_j^a(s|t_k), \tau_i(s|t_k)) && \text{(5.25a)} \\ \text{s.t.} \quad & \dot{\tilde{x}}_i(s|t_k) = f(\tilde{x}_i(s|t_k), \tau_i(s|t_k), 0), && \text{(5.25b)} \\ & \tilde{x}_i(t_k|t_k) = x_i(t_k), && \text{(5.25c)} \\ & \|\tau_i(s|t_k)\|_\infty \leq \tau^{\max}, && \text{(5.25d)} \\ & \dot{V}_i|_{\tau_i(t_k)} \leq \dot{V}_i|_{\hat{\tau}_i^a(t_k)}, && \text{(5.25e)} \end{aligned}$$

where $S(\delta)$ is a family of piece-wise constant function with the sampling period δ, $s \in [t_k, t_k+T]$, $\tau_i^*(t_k)$ is the optimal control input for AUV i at t_k. In addition, $\tau_i^*(s|t_k)$ denotes the optimal solution of the optimization problem $\mathcal{P}_i$. $x_i(t_k)$ and $x_i^*(s|t_k)$ denote the actual state and the optimal state, respectively. Furthermore, combining (5.11), (5.18) and the derivative of the associated Lyapunov function leads to the detailed expression of the stability constraint (5.25e) at time t_k

$$\begin{aligned} & s_i^{\mathrm{T}} R(\psi_i)(\tau_i(t_k) - M_i\dot{\nu}_{id} - C_i(\nu_i)\nu_{id} - D_i(\nu_i)\nu_{id} + R(\psi_i)^{\mathrm{T}} K_{pi}\tilde{\eta}_i) - \tilde{\eta}_i^{\mathrm{T}} K_{pi}\Lambda_i\tilde{\eta}_i - s_i^{\mathrm{T}} D_i^* s_i \\ & \leq -s_i^{\mathrm{T}} R(\psi_i)\hat{\tau}_{iw} - \tilde{\eta}_i^{\mathrm{T}} K_{pi}\Lambda_i\tilde{\eta}_i - s_i^{\mathrm{T}} K_{di}^* s_i, \end{aligned}$$

where $\tau_i(t_k)$ represents the optimization variable.

Note that (5.25b) is the nominal model of AUV $i, i \in \mathcal{V}$, which is used to predict the state trajectory. (5.25c) is the initial state condition at t_k. (5.25d) specifies the control input constraint. (5.25e) is the stability constraint that is constructed by the ESO-based auxiliary controller $\hat{\tau}_i^a(t_k)$ as well as the associated Lyapunov function V_i. The DLMPC controller inherits the stability and robustness of the ESO-based auxiliary controller [87].

Remark 5.1. *Conventional robust MPC techniques for the nonlinear systems, such*

as tube-based and min-max MPC, have a high requirement on the computation resource [78, 98]. In contrast, the proposed DLMPC method, where the ESO estimates the ocean current disturbances, does not introduce additional computational burden, thereby being more computationally efficient.

The distributed Lyapunov-based model predictive formation tracking algorithm is presented in **Algorithm 3**, and it is implemented in the receding horizon fashion.

Algorithm 3 DLMPC Algorithm

1: **Initialization**: For AUV $i, i \in \mathcal{V}$, choose the sampling period δ, the weighting matrix Q_i, Q_i', R_i, the safety radius R and other design parameters. Set $k = 0$;
Procedure
2: AUV i samples the system state $x_i(t_k)$;
3: AUV i receives the predicted state sequence of AUV j, i.e., $\tilde{x}_j^a(s|t_k)$, $j \in \mathcal{N}_i$, $s \in [t_k, t_k + T]$;
4: Generate the stability constraint (5.25e);
5: AUV i solves $\mathcal{P}_i$ (5.25), generating $\tau_i^*(s|t_k), s \in [t_k, t_k + T]$;
6: Apply the control input $\tau_i^*(s|t_k), s \in [t_k, t_k + \delta]$;
7: $k = k + 1$ and go to step 2.
end Procedure

5.3.3 Theoretical analysis

Two key lemmas [132] are introduced to guarantee the feasibility of the DMPC optimization problem.

Lemma 5.2. *Suppose that AUV i is controlled by the auxiliary control law* (5.18)*, then the Coriolis matrix $C_i(\nu_i)$ and the damping matrix $D_i(\nu_i)$ are bounded, i.e., $\|C_i(\nu_i)\|_\infty \leq \bar{c}_i$, $\|D_i(\nu_i)\|_\infty \leq \bar{d}_i$.*

Lemma 5.3. *Let $\bar{K}_p$ and $\bar{K}_d$ denote the largest entity in control gains $K_{pi}\Lambda_i$ and K_{di}, respectively. If the condition $\bar{m}_i\dot{\bar{\nu}}_{id} + (\bar{c}_i + \bar{d}_i)\bar{\nu}_{id} + (\bar{K}_p + \bar{K}_d)\|\Gamma_i(t_0)\| + \bar{m}_i(\hat{\bar{w}}_i) \leq \tau^{\max}$ holds, then the auxiliary control input $\|\hat{\tau}_i^a(t)\|_\infty \leq \tau^{\max}$.*

Proof. From the definition, it holds that $|\psi_r| \leq \pi$ and $\dot{\psi}_r = |r_r| \leq \bar{p}_1\bar{p}_2/(\underline{p}_1)^2 = \bar{\dot{\psi}}_r$. Here $\bar{\dot{\psi}}_r$ represents the maximum value of $\dot{\psi}_r$, other variables are defined in the similar way in the sequel. Then, $\ddot{\psi}_r$ is expressed as

$$|\ddot{\psi}_r| = |\frac{\dot{x}_r\dddot{y}_r - \dot{y}_r\dddot{x}_r}{\dot{x}_r^2 + \dot{y}_r^2} - \frac{2(\dot{x}_r\ddot{y}_r - \dot{y}_r\ddot{x}_r)(\dot{x}_r\ddot{x}_r + \dot{y}_r\ddot{y}_r)}{(\dot{x}_r^2 + \dot{y}_r^2)^2}| \leq \bar{p}_1\bar{p}_3/\underline{p}_1^2 + 2\bar{p}_1^2\bar{p}_2^2/\underline{p}_1^2 = \bar{\ddot{\psi}}_r,$$

with $0 < \bar{\ddot{\psi}}_r < \infty$. Hence, we obtain

$$\begin{aligned}\|\eta_r\|_\infty &= \bar{\eta}_r = \max\{\overline{p}, \pi\},\\ \|\dot{\eta}_r\|_\infty &= \bar{\dot{\eta}}_r = \max\{\overline{p}_1, \bar{\dot{\psi}}_r\},\\ \|\ddot{\eta}_r\|_\infty &= \bar{\ddot{\eta}}_r = \max\{\overline{p}_2, \bar{\ddot{\psi}}_r\}.\end{aligned}$$

Let $\Gamma_i = \mathrm{col}(\tilde{\eta}_i, R^{\mathrm{T}}(\psi_i)s_i, e_i)$, the Lyapunov function (5.21) is rewritten as $V_i = \frac{1}{2}\Gamma_i^{\mathrm{T}} S_i \Gamma_i$, where $S_i = \mathrm{diag}(K_p, M_i, P)$. From **Lemma 5.1**, one has $\dot{V}_i < 0$, $\|\Gamma_i\| \leq \|\Gamma_i(t_0)\|$. Furthermore, by $\|\tilde{\eta}_i\|_\infty \leq \|\tilde{\eta}_i\| \leq \|\Gamma_i\|$, $\|s_i\|_\infty \leq \|s_i\| \leq \|\Gamma_i\|$ and $\|e_i\|_\infty \leq \|e_i\| \leq \|\Gamma_i\|$, then we know that $\|\tilde{\eta}_i\|_\infty \leq \|\Gamma_i(t_0)\|$, $\|s_i\|_\infty \leq \|\Gamma_i(t_0)\|$ and $\|e_i\|_\infty \leq \|\Gamma_i(t_0)\|$. Therefore

$$\|\dot{\tilde{\eta}}_i\|_\infty = \|s_i - \tilde{\eta}_i\|_\infty \leq \|s_i\|_\infty + \|\tilde{\eta}_i\|_\infty \leq 2\|\Gamma_i(t_0)\|. \tag{5.26}$$

Note that $\dot{\eta}_{id} = \dot{\eta}_{ir} - \Lambda_i\tilde{\eta}_i$, $\nu_{id} = R^{\mathrm{T}}(\psi_i)\dot{\eta}_{id}$. Then, we have

$$\dot{\nu}_{id} = R^{\mathrm{T}}(\psi_i)\ddot{\eta}_{id} + R(\psi_i)S(\dot{\psi}_i)\dot{\eta}_{id}. \tag{5.27}$$

Since $\|s_i\|_\infty$ and $\|\tilde{\eta}_i\|_\infty$ are bounded, (5.5) and (5.26) imply $\dot{\eta}_{id}$, $\ddot{\eta}_{id}$ and $\dot{\tilde{\eta}}_i$ are bounded, i.e., $\|\dot{\eta}_{id}\|_\infty \leq \bar{\dot{\eta}}_{id}$ and $\|\ddot{\eta}_{id}\|_\infty \leq \bar{\ddot{\eta}}_{id}$. As a result, the upper bounds of $\|\nu_{id}\|_\infty$ and $\|\dot{\nu}_{id}\|_\infty$ are acquired and denoted as

$$\|\nu_{id}\|_\infty \leq \bar{\nu}_{id},\ \|\dot{\nu}_{id}\|_\infty \leq \bar{\dot{\nu}}_{id}. \tag{5.28}$$

Hence,

$$\begin{aligned}&\|\hat{\tau}_i^a(t)\|_\infty\\ \leq&\|M_i\dot{\nu}_{id}\|_\infty + \|(C_i(\nu_i) + D_i(\nu_i))\nu_{id}\|_\infty + \|R^{\mathrm{T}}(\psi_i)(K_{pi}\Lambda_i\tilde{\eta}_i + K_{di}s_i)\|_\infty + \|\hat{\tau}_{iw}\|_\infty\\ \leq&\bar{m}_i\|\dot{\nu}_{id}\|_\infty + (\bar{c}_i + \bar{d}_i)\|\nu_{id}\|_\infty + \bar{K}_p\|\tilde{\eta}_i\|_\infty + \bar{K}_d\|s_i\|_\infty + \|\hat{\tau}_{iw}\|_\infty\\ \leq&\bar{m}_i\bar{\dot{\nu}}_{id} + (\bar{c}_i + \bar{d}_i)\bar{\nu}_{id} + \bar{K}_p\|\Gamma_i(t_0)\| + \bar{K}_d\|\Gamma_i(t_0)\| + \bar{m}_i\bar{\hat{w}}_i\\ \leq&\tau^{\max},\end{aligned}$$

where $\bar{\hat{w}}_i = \bar{w}_i + \|\Gamma_i(t_0)\|$, which concludes the proof. □

In what follows, the recursive feasibility and stability of the cooperative AUVs under the DLMPC algorithm are presented in **Theorem 5.1**.

Theorem 5.1. *For the multi-AUV system described by* (5.3) *with unknown ocean current disturbances, AUV i solves the formation tracking optimization problem* $\mathcal{P}_i$ *at each sampling instant* t_k*.* 1) *If there exists a feasible solution at the initial instant* t_0*, then* ***Algorithm 3*** *is recursively feasible, i.e., the optimization problem* $\mathcal{P}_i$ *admits a solution for all* $t_k > t_0$*.* 2) *The formation tracking of the cooperative AUVs is achieved under* ***Algorithm 3****.*

Proof. 1) We first establish the recursive feasibility of **Algorithm 3** before the the stability proof. In order to guarantee the recursive feasibility of the optimization problem $\mathcal{P}_i$ of AUV i, $i \in \mathcal{V}$, we need to find a control input sequence that satisfies the constraint (5.25d) and (5.25e). Note that the auxiliary control input $\hat{\tau}_i^a(t_{k+1})$ is generated by the auxiliary controller for the cooperative AUVs at time t_{k+1}. Therefore, the constraint (5.25e) is satisfied if we choose the control input as the auxiliary control law, i.e., $\tau_i(t_{k+1}; t_{k+1}) = \hat{\tau}_i^a(t_{k+1})$. The optimization problem $\mathcal{P}_i$ is assumed to be feasible at t_k, and the optimal solution is $\tau_i^*(s; t_k), s \in [t_k, t_k + T]$. At time t_{k+1}, the feasible control inputs are chosen as

$$\tau_i(s; t_{k+1}) = \begin{cases} \hat{\tau}_i^a(t_{k+1}), s \in [t_{k+1}, t_{k+1} + \delta); \\ \tau_i^*(s; t_k), s \in [t_{k+1} + \delta, t_k + T); \\ \tau_i^*(t_k + T; t_k), s \in [t_k + T, t_{k+1} + T). \end{cases}$$

In the light of **Lemma 5.3**, the control input constraint (5.25d) is satisfied. Therefore, the recursive feasibility is guaranteed.
2) Upon using **Lemma 5.1**, we get $\dot{V}_i|_{\hat{\tau}_i^a(t_k)} < 0$. From (5.25e) and the optimal control input τ_i^* implemented at each sampling instant, we have

$$\dot{V}_i|_{\tau_i^*(t_k)} \leq \dot{V}_i|_{\hat{\tau}_i^a(t_k)} < 0. \tag{5.29}$$

The formation tracking of the cooperative AUVs under the control input generated by **Algorithm 3** is achieved. The stability of the cooperative AUVs is further ensured. This concludes the proof. □

5.4 Simulation Study

This section set up two simulation tests to verify the DLMPC algorithm for the cooperative AUVs. The inter-AUV collision avoidance is tested in the first test with and

without external disturbances. The second test illustrates the disturbance rejection by introducing external disturbances.

5.4.1 Simulation setup

A sinusoidal shape trajectory is chosen as the reference trajectory of the virtual leader

$$\begin{cases} x_r = 0.5t, \\ y_r = \sin(0.5t + \dfrac{\pi}{2}). \end{cases} \tag{5.30}$$

In the simulation, the time-varying disturbances induced by ocean current are simulated by

$$w_i = \begin{bmatrix} 0.5v_i^3 + 0.3\sin(0.7t) \\ 0.6u_i r_i + 0.3u_i + 0.2\sin(0.6t) \\ -0.5v_i^2 - u_i r_i - 0.2\sin(0.9t) \end{bmatrix}. \tag{5.31}$$

The system parameters of Falcon AUV are given as follows [129]: $m = 116\text{kg}$ and the moment of inertia with respect to the z-axis $I_z = 13.1\text{kg}\cdot\text{m}^2$. The hydrodynamic coefficients $X_{\dot{u}} = -167.6$, $Y_{\dot{v}} = -477.2$, $N_{\dot{r}} = -15.9$, $X_u = 26.9$, $Y_v = 35.8$, $N_r = 3.5$, $D_u = 241.3$, $D_v = 503.8$, and $D_r = 76.9$. $M_x = m - X_{\dot{u}}$, $M_y = m - Y_{\dot{v}}$, and $M_\psi = I_z - N_{\dot{r}}$, $D_i(\nu_i) = \text{diag}(X_u, Y_v, N_r) + \text{diag}(D_u|u_i|, D_v|v_i|, D_r|r_i|)$. $M_i = \text{diag}(M_x, M_y, M_\psi)$. $C_i(\nu_i) = [0, 0, -M_y v_i; 0, 0, M_x u_i; M_y v_i, -M_x u_i, 0]$.

The parameters of DLMPC are designed as follows: The sampling period $\delta = 0.1\text{s}$, the prediction horizon $T = 6\delta$. The safety radius $R = 0.25\text{m}$. The tuning parameter $\Gamma = 10^4$ and the smoothness parameter $k_i = 8$. The weighting matrices are chosen as $Q_i = \text{diag}(10^4, 10^4, 10^3, 10, 10, 10)$, $Q_i' = \text{diag}(10^4, 10^4, 10^3, 10^2, 10^2, 10^2)$ and $R_i = \text{diag}(10^{-3}, 10^{-3}, 10^{-3})$. The parameters of the ESO are selected as $K_1 = \text{diag}(5, 5, 5)$, $K_2 = \text{diag}(6, 6, 6)$ and $K_3 = \text{diag}(8, 8, 8)$. Let $K_{pi} = \text{diag}(1, 1, 1)$, $K_{di} = \text{diag}(1, 1, 1)$. The limit on control input is 1000N ($\text{N}\cdot\text{m}$). The desired formation and tracking vectors are $d_{1r} = [0, 1]^{\text{T}}$, $d_{2r} = [0, -1]^{\text{T}}$, $d_{3r} = [1, 0]^{\text{T}}$, $d_{12} = -d_{21} = [0, 2]^{\text{T}}$, $d_{13} = -d_{31} = [1, 1]^{\text{T}}$, $d_{23} = -d_{32} = [1, -1]^{\text{T}}$. The communication network $\mathcal{G}'$ is set up as $\mathcal{N}_1 = \{0, 3\}$, $\mathcal{N}_2 = \{0, 3\}$, $\mathcal{N}_3 = \{0, 1, 2\}$.

5.4.2 Formation tracking with collision avoidance

In the first test, the initial state conditions of three AUVs are $[0, 2, \pi/2, 0.4, 0, 0]^{\text{T}}$, $[-0.5, -0.5, 3\pi/4, 0.4, 0, 0]^{\text{T}}$, and $[-0.1, 0.1, -\pi/2, 0.4, 0, 0]^{\text{T}}$, respectively. In the first

two parts, the collision avoidance is considered for AUVs without disturbances, and AUVs are exposed to disturbances in the third part.

In the first part, the formation tracking of AUVs is considered without collision avoidance. The simulation results of DLMPC are illustrated in Figures 5.1 and 5.2. The trajectories of three AUVs in the X-Y plane are plotted in Figure 5.1, where the dash circles represent the safe radius of AUVs. During the period of $[0.6s, 0.7s]$, AUV2 and AUV3 collide. As shown in Figure 5.1, AUVs can track the reference trajectory but cannot avoid collisions. The control inputs of three AUVs are plotted in Figure 5.2. This simulation test provides a benchmark for the collision avoidance test.

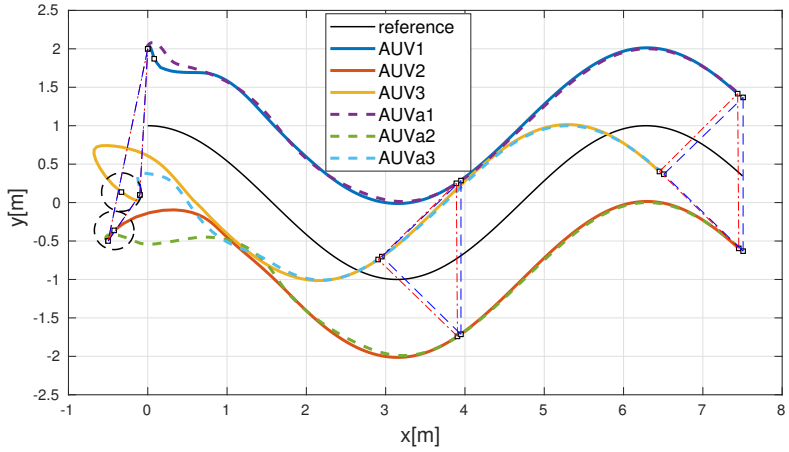

Figure 5.1: The trajectories of AUVs under DLMPC (without collision avoidance).

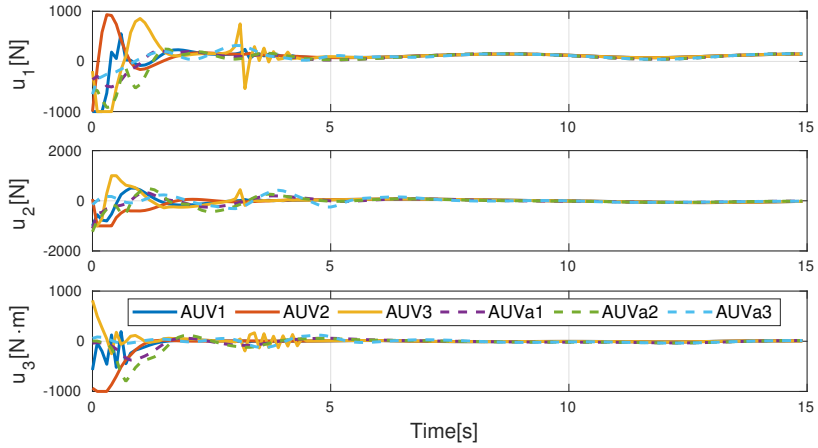

Figure 5.2: The control inputs of AUVs (without collision avoidance).

In the second part, the formation tracking task is reconsidered with the collision

avoidance guarantee, and the results are illustrated in Figures 5.3 and 5.4. The trajectories of three AUVs are plotted in Figure 5.3, in which the collision is avoided during the whole operational period. AUV1 denotes the first AUV controlled by DLMPC, and AUVa1 denotes the first AUV controlled by the auxiliary controller. It is observed that three AUVs track the reference trajectory with the prescribed geometric shape. Compared with the auxiliary control law, AUVs under DLMPC achieve faster and more accurate formation tracking performance. Figure 5.4 depicts the control inputs of three AUVs.

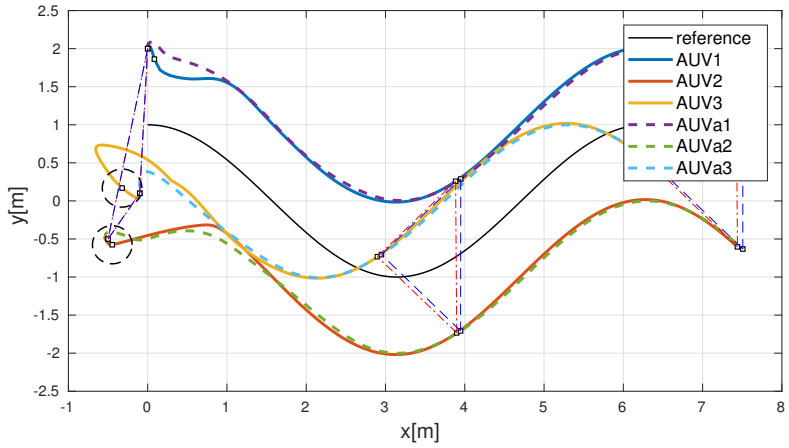

Figure 5.3: The trajectories of AUVs with collision avoidance.

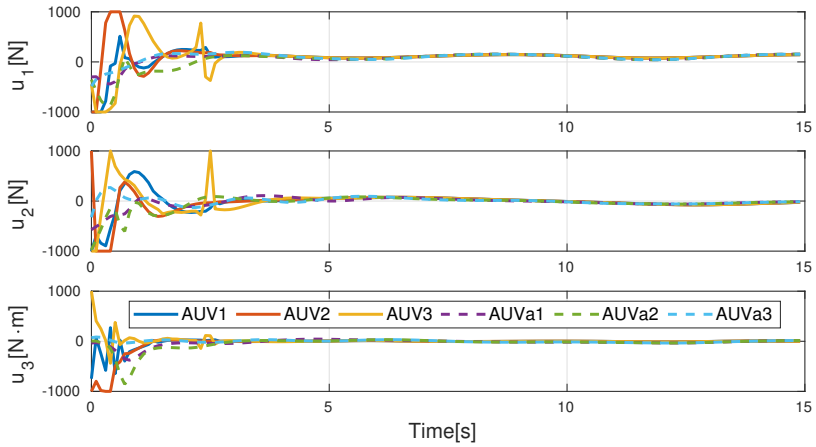

Figure 5.4: The control inputs of AUVs.

In the third part, the formation tracking of AUVs subject to disturbances is considered with collision avoidance, and the results are illustrated in Figures 5.5 and

5.6. The trajectories of AUVs are plotted in Figure 5.5, where the collision is avoided during the whole operational period for AUVs in the presence of disturbances. Figure 5.6 shows the corresponding control inputs of three AUVs. These simulation results verify that the proposed DLMPC algorithm is effective.

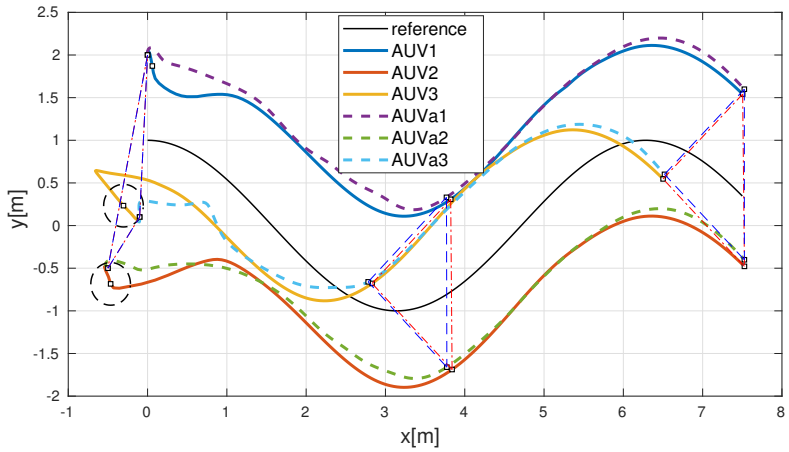

Figure 5.5: The trajectories of AUVs with disturbances.

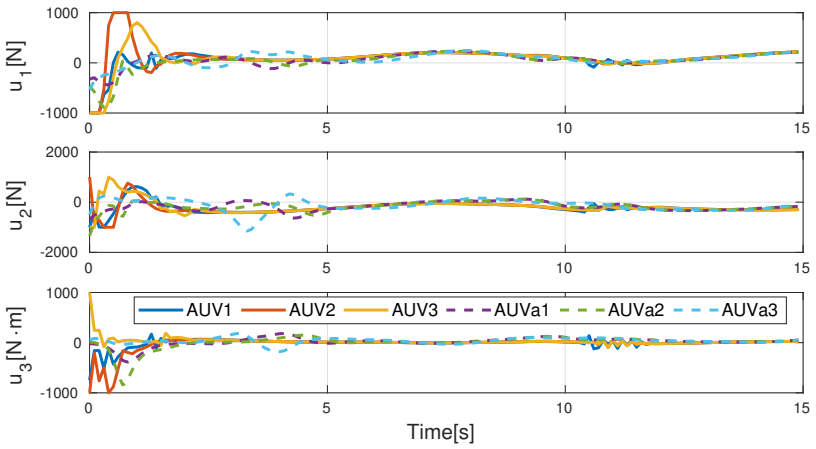

Figure 5.6: The control inputs of AUVs with disturbances.

5.4.3 Formation tracking of cooperative AUVs with disturbances

In the second test, AUVs are exposed to unknown ocean current disturbances as simulated in (5.31). The initial conditions of three AUVs are $[0, 2, \pi/2, 0.5, 0, 0]^{\mathrm{T}}$,

$[-0.5, -0.5, 3\pi/4, 0.5, 0, 0]^{\mathrm{T}}$, and $[-1.5, 1.1, -\pi/2, 0.5, 0, 0]^{\mathrm{T}}$, respectively. The formation tracking performance of the proposed algorithm and the auxiliary control law for the multi-AUV are illustrated in Figures 5.7–5.12.

In the first part of the second test, AUVs controlled by the DLMPC algorithm and the auxiliary control law without the ESO cannot accomplish the formation tracking task. In the second part, the results of AUVs controlled by the DLMPC algorithm and the ESO-based auxiliary control law are shown in Figures 5.7–5.9. As shown in Figure 5.7, AUVs under the DLMPC algorithm quickly converge to the reference trajectory with the predesigned formation. The formation tracking errors of three AUVs under the DLMPC algorithm are smaller than the ESO-based auxiliary control law in Figure 5.9. The control inputs under the DLMPC algorithm and the auxiliary controller are shown in Figure 5.10. The trajectories of the Lyapunov function with ESO-based auxiliary controller and DLMPC are illustrated in Figure 5.12. It illustrates that 1) DLMPC converges faster than the auxiliary control law from the perspective of evolutions of the Lyapunov function; 2) DLMPC improves the formation tracking performance of cooperative AUVs. The estimation errors of the disturbances are presented in Figure 5.11, and the estimation errors converge to a bounded region.

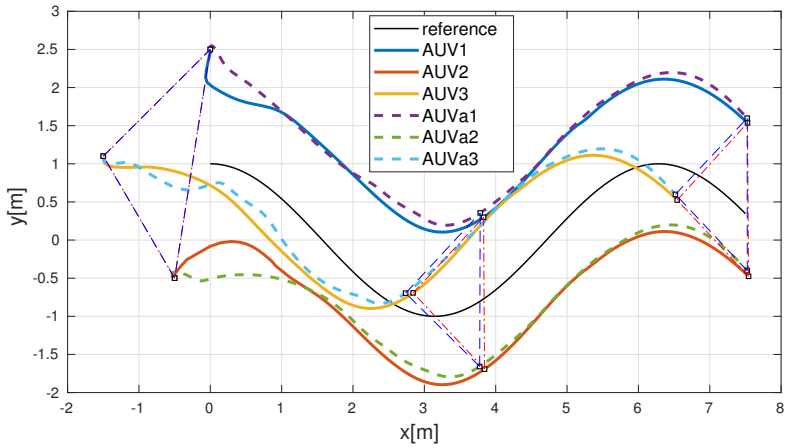

Figure 5.7: The trajectories of AUVs with disturbances (with the ESO).

Quantitatively, the mean square errors (MSEs) of the formation tracking using four different controllers are summarized in Table 5.1. The smaller MSEs value means better formation tracking performance. As can be seen, the proposed DLMPC with ESO achieves the smallest MSEs. The formation tracking performance is improved using DLMPC with ESO compared to the auxiliary controllers without the ESO. If

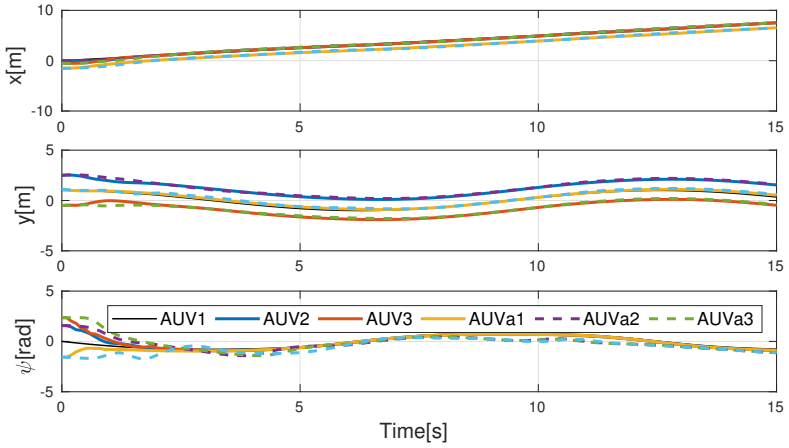

Figure 5.8: The states of AUVs with disturbances (with the ESO).

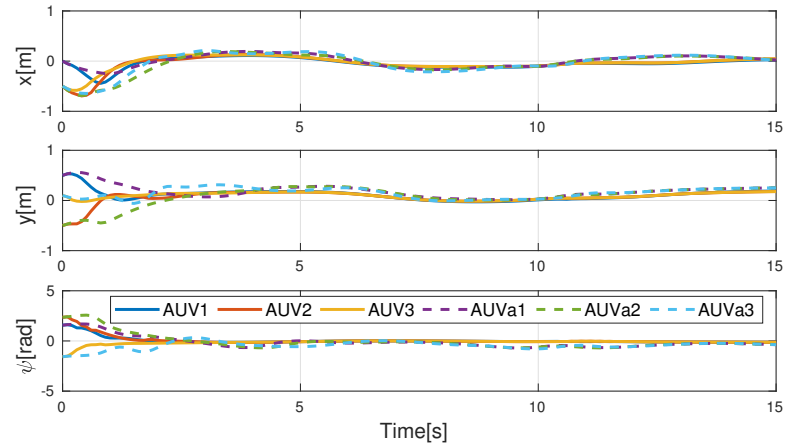

Figure 5.9: The formation tracking errors of AUVs with disturbances (with the ESO).

the AUVs are exposed to ocean current disturbances, the closed-loop stability cannot be ensured under the auxiliary controller and DLMPC without ESO.

Table 5.1: The MSEs under DLMPC and the auxiliary control law.

Method	$x[\mathrm{m}^2]$	$y[\mathrm{m}^2]$	$\psi[\mathrm{rad}^2]$
Auxiliary Controller (without ESO)	–	unstable	–
DLMPC (without ESO)	NaN	NaN	NaN
Auxiliary Controller (with ESO)	0.1063	0.1235	1.2374
DLMPC (with ESO)	**0.0611**	**0.0551**	**0.3650**

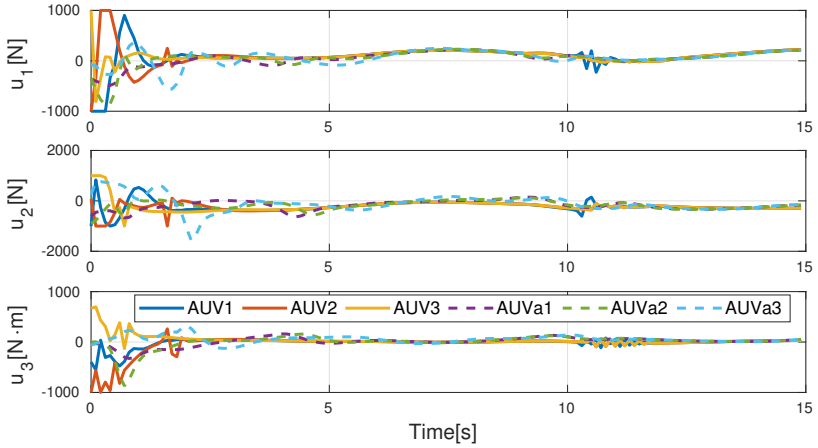

Figure 5.10: The control inputs of AUVs with disturbances (with the ESO).

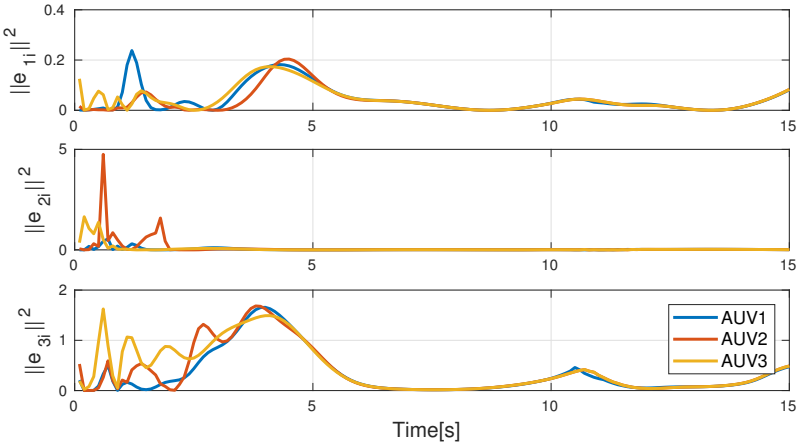

Figure 5.11: The estimation errors under the proposed ESO.

5.5 Conclusion

This chapter proposed a DLMPC algorithm for the formation tracking problem of constrained AUVs with unknown ocean current disturbances. The inter-AUV collision avoidance was achieved by designing a potential field-based cost term with well-tuned parameters integrated with the formation tracking cost function. The control performance and robustness could be effectively enhanced by incorporating a stability constraint generated by the ESO-based auxiliary controller and its associated Lyapunov function into the online MPC optimization problem. The algorithm's recursive feasibility and the cooperative AUVs' closed-loop stability were rigorously proved. The simulation results verified the effectiveness of the proposed distributed

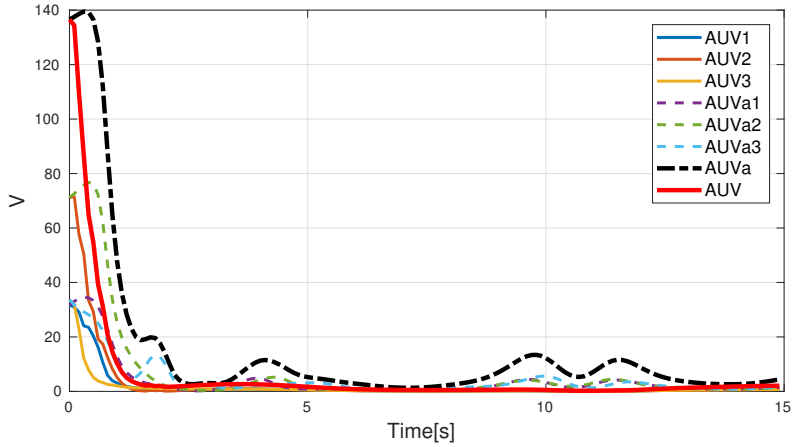

Figure 5.12: Comparison of the Lyapunov function trajectories under ESO-based auxiliary control law and DLMPC.

Lyapunov-based model predictive formation tracking control algorithm.

Chapter 6

Robust Distributed Model Predictive Platooning Control for Heterogeneous Autonomous Surface Vehicles

6.1 Introduction

The platooning control of connected vehicles has been widely studied in the intelligent transportation area owing to its potential to improve road capacity and efficiency [22]. In a similar vein, the platooning control of ASVs can also hugely improve waterborne transport efficiency and reduce labor costs [149]. Recently, some notable platooning control methods for connected vehicles have been reported in the literature, such as optimal control [46], sliding mode control [164], and delay-based spacing policy [2]. Compared with these methods, DMPC gains attention from platooning control researchers since it is computationally efficient and applicable to dynamically decoupled vehicle platoon systems [51, 89]. In [18], the authors present a DMPC algorithm for the homogeneous vehicle platoon and derive a sufficient condition to ensure the string stability. In [67], the platooning control input for each agent is generated by solving a local DMPC optimization problem with a neighboring γ-gain stability constraint. The string stability constraints suppress the spacing error at the price of the decreased feasibility, resulting in conservative and unsatisfactory control performance. To achieve better platooning coordination performance, the authors in [182] develop

a DMPC algorithm without the string stability constraint for the heterogeneous connected vehicles under four types of unidirectional communication networks.

However, the methods in [18, 67, 182] do not consider external disturbances that may destroy the stability of connected vehicles. Some robust DMPC methods have been developed to tackle this challenging problem [106, 146]. A recent paper [21] proposes a platooning control algorithm, which combines the tube-based DMPC with event-triggered feedforward control for homogeneous autonomous vehicles. However, the overall system is assumed to be synchronized, and inter-vehicle safety cannot be guaranteed. Inspired by these facts, a nonlinear tube-based DMPC approach for the constrained heterogeneous ASV platoon is proposed, where each ASV is assigned a local controller to calculate its local optimal control input. The main contributions of this chapter are summarized as follows:

- A nonlinear robust DMPC approach is developed for the heterogeneous ASV platoon with input constraints and bounded environmental disturbances. Compared with the collision avoidance method in [160], a coupled minimum safe following distance constraint is designed and incorporated into the optimization problem to ensure inter-vehicle safety.

- A novel cost term is introduced to suppress the error between the predicted and assumed state of each ASV, which does not require the overall system to be synchronized. The offline designed ancillary control law reduces the deviation between the actual system state and the optimal nominal system state, which is more computationally efficient in comparison with [98]. Moreover, the recursive feasibility of the robust distributed model predictive platooning control algorithm is analyzed, and the heterogeneous ASV platoon is proved to be ISS.

6.2 Problem Formulation

6.2.1 ASV modeling

Consider a group of $M+1$ heterogeneous ASVs [24], and the dynamics of ASV i satisfies

$$\begin{aligned} &\dot{\eta}_i = R(\psi_i)\nu_i, \\ &M_i\dot{\nu}_i + C_i(\nu_i)\nu_i + D_i(\nu_i)\nu_i = u_i + w_i, \end{aligned} \tag{6.1}$$

where $\eta_i = [x_i, y_i, \psi_i]^{\mathrm{T}}$ includes the surge displacement x_i, sway displacement y_i, and yaw angle ψ_i; $\nu_i = [\mu_i, v_i, r_i]^{\mathrm{T}}$ includes the surge velocity μ_i, sway velocity v_i and yaw velocity r_i. $u_i = [u_{ix}, u_{iy}, u_{i\psi}]^{\mathrm{T}}$ is the control input and $w_i = [w_{ix}, w_{iy}, w_{i\psi}]^{\mathrm{T}}$ is the external disturbance. $R(\psi_i) = [\cos\psi_i, -\sin\psi_i, 0; \sin\psi_i, \cos\psi_i, 0; 0, 0, 1]$ is the rotation matrix. The inertia matrix including the added mass is $M_i = \mathrm{diag}(M_{x_i}, M_{y_i}, M_{\psi_i})$ with $M_{x_i} = m_i - X_{\dot{\mu}_i}$, $M_{y_i} = m_i - Y_{\dot{v}_i}$, and $M_{\psi_i} = I_{z_i} - N_{\dot{r}_i}$. m_i and I_{z_i} are the ASV mass and the moment of inertia about the z-axis of the fixed body frame, respectively. The hydrodynamic damping matrix including the drag force and vortex-induced force is $D_i(\nu_i) = \mathrm{diag}(-X_{\mu_i}, -Y_{v_i}, -N_{r_i}) + \mathrm{diag}(-X_{\mu_i|\mu_i|}|\mu_i|, -Y_{v_i|v_i|}|v_i|, -N_{r_i|r_i|}|r_i|)$. The Coriolis and centripetal matrix is $C_i(\nu_i) = [0, 0, -M_{y_i}v_i; 0, 0, M_{x_i}\mu_i; M_{y_i}v_i, -M_{x_i}\mu_i, 0]$. Some notations of ASV i are introduced in Table 6.1

Table 6.1: Table of notations for ASV i.

x_i, μ_i	The actual position and the actual velocity.
$\bar{q}_i, q_i$	The nominal state and the actual state.
z_i	The actual error state.
x_i^e, μ_i^e	The actual error position and the actual error velocity.
$\bar{z}_i$	The nominal error state.
$\bar{x}_i^e, \bar{\mu}_i^e$	The nominal error position and the nominal error velocity.
$\bar{z}_{i,i-1}$	The nominal error state of ASV $i-1$ predicted by ASV i.
$\bar{u}_{i,i-1}$	The nominal control of ASV $i-1$ predicted by ASV i.
$\bar{u}_i^p, \bar{z}_i^p$	The control input candidate and its corresponding error state.
$\bar{z}_i^*, \bar{u}_i^*$	The optimal nominal error state and the optimal nominal control input.
π_i, u_i	The ancillary control law and the actual control input.
z_i^a, x_i^a	The assumed error state and the assumed position.
e_i	The deviation of the actual state from the nominal state.
$\mathbb{U}_i$	The control input constraint set.
$\bar{\mathbb{U}}_i$	The tightened control constraint set.
Ω_i	The terminal set.
$\check{o}$	The bound between the predicted and assumed error state.
d^x	The desired spacing between any two neighboring ASVs.
d_i^{safe}	The minimum safe following distance.

6.2.2 ASV platoon modeling

In this work, the platooning control of heterogeneous ASVs is studied in one-dimensional space, and the decoupled surge dynamics of ASV i is described by

$$\begin{aligned} &\dot{x}_i = \mu_i, \\ &M_{x_i}\dot{\mu}_i - X_{\mu_i}\mu_i - X_{\mu_i|\mu_i|}|\mu_i|\mu_i = u_{ix} + w_{ix}, \end{aligned} \tag{6.2}$$

with the system state $q_i(t) = [x_i(t), \mu_i(t)]^{\mathrm{T}} \in \mathbb{R}^2$. The predecessor-leader following communication topology is adopted, i.e., ASV i can receive the information from its preceding ASV $i-1$ and the lead ASV 0 [182]. Hence, the neighboring set of ASV i is denoted as $\mathcal{N}_i = \{0, i-1\}$, $i \in \mathcal{V}$. The state of lead ASV 0 is denoted as $q_0(t)$, and the follower ASV i tracks the following desired state

$$q_i^{\mathrm{des}}(t) = q_0(t) - \begin{bmatrix} id^x \\ 0 \end{bmatrix}, \ t \geq 0, \tag{6.3}$$

in which d^x denotes the desired spacing between ASV i and ASV $i-1$. For ASV i, $i \in \mathcal{V}^0$, the error state $z_i(t) = [x_i^e(t), \mu_i^e(t)]^{\mathrm{T}}$ is defined as

$$z_i(t) = q_i(t) - q_i^{\mathrm{des}}(t), \tag{6.4}$$

where $x_i^e(t)$ and $\mu_i^e(t)$ denote the error position and error velocity, respectively. Taking the time derivative of (6.4), the error dynamics of ASV i is described as

$$\begin{aligned} \dot{z}_i(t) =& f_i(z_i(t)) + B_i u_i(t) + B_i w_i(t) \\ =& \begin{bmatrix} \mu_i - \mu_0 \\ M_{x_i}^{-1}(X_{\mu_i}\mu_i + X_{\mu_i|\mu_i|}|\mu_i|\mu_i) - \dot{\mu}_0 \end{bmatrix} + B_i u_i(t) + B_i w_i(t), \end{aligned} \tag{6.5}$$

with $B_i = [0, M_{x_i}^{-1}]^{\mathrm{T}}$. By a slight abuse of notation, $u_i(t)$ and $w_i(t)$ are used to denote $u_{ix}(t)$ and $w_{ix}(t)$ in the sequel. Here ASV i is subject to the control input constraint $u_i(t) \in \mathbb{U}_i$. $w_i(t) \in \mathbb{W}_i := \{w_i \mid |w_i| \leq w_{i,\max}\}$ denotes the additive disturbance.

We make the following assumption for the error dynamics in (6.5).

Assumption 6.1. *1) The function $f_i(z_i) : \mathbb{R}^2 \to \mathbb{R}^2$ is continuously differentiable with $f_i(0) = 0$. 2) The system in (6.5) with any initial state $z_i(0)$ has a unique, absolutely continuous solution for the control input $u_i(t) \in \mathbb{U}_i$ and $w_i(t) \in \mathbb{W}_i$, $t \geq 0$.*

Without considering the disturbances $w_i(t)$, the nominal error dynamics of ASV

i can be written as

$$\dot{\bar{z}}_i(t) = f_i(\bar{z}_i(t)) + B_i\bar{u}_i(t), \tag{6.6}$$

where $\bar{z}_i$ and $\bar{u}_i$ are the nominal error state and nominal control input, respectively.

Note that a fixed graph, denoted by $\mathcal{G}'' = (\mathcal{V}^0, \mathcal{E})$, describes the information exchange among the heterogeneous ASVs, where $\mathcal{V}^0 = \{i \in \mathbb{N}_{\geq 0} \mid 0 \leq i \leq M\}$ is the set of the nodes representing a platoon of ASVs and $\mathcal{E} = \{(i,j) \subset \mathcal{V}^0 \times \mathcal{V}^0\}$ is the set of all directed edges denoting the communication from the ASV i to the ASV j. $\mathcal{N}_i := \{j \mid (i,j) \in \mathcal{E}\}$ denotes the set of ASV i's neighbors, i.e. ASV i receives the information from ASV j, $j \in \mathcal{N}_i$. $\mathcal{V} = \{i \in \mathbb{N}_{>0} \mid 1 \leq i \leq M\}$ denotes all follower ASVs.

6.2.3 Control objective

The main control objective of this work is to realize the platooning control of a group of heterogeneous ASVs subject to the input constraint and external disturbances. ASV i, $i \in \mathcal{V}$ maintains the desired spacing with its preceding ASV $i-1$ and tracks the speed of the lead ASV 0. Furthermore, in order to ensure the safety of the ASV platoon, the spacing between ASV i and ASV $i-1$ satisfies

$$x_i(t) - x_{i-1}(t) \leq -d_i^{\text{safe}}, \tag{6.7}$$

where $d_i^{\text{safe}} := (\mu_{i,\max} t_s + \mu_{i,\max}^2 / 2b_s)$ is the minimum safe following distance, t_s is the minimum reaction time, b_s is the maximum deceleration, and $\mu_{i,\max}$ is the maximum speed. From the definition of error state (6.4), the inequality (6.7) becomes

$$E(z_i(t) - z_{i-1}(t)) \leq -d_i^{\text{safe}} + d^x, \tag{6.8}$$

with $E = [1, 0]$ and $d_i^{\text{safe}} \leq d^x$. It is worth noting that ASV i only considers the minimum safe following distance d_i^{safe} between ASV i and its preceding ASV $i-1$, since the predecessor-leader following communication topology is adopted.

In this work, a robust DMPC method is proposed to achieve the control objective of the heterogeneous ASV platoon. As shown in Figure 6.1, the control input applied to ASV i consists of two components: 1) the nominal control $\bar{u}_i^*(t)$ generated by solving the DMPC problem steers the nominal error state $\bar{z}_i(t)$ towards the origin, and 2) the offline ancillary control law $\pi_i(z_i(t), \bar{z}_i(t))$ keeps the actual error state $z_i(t)$

in a specific set centered along the nominal error state $\bar{z}_i(t)$.

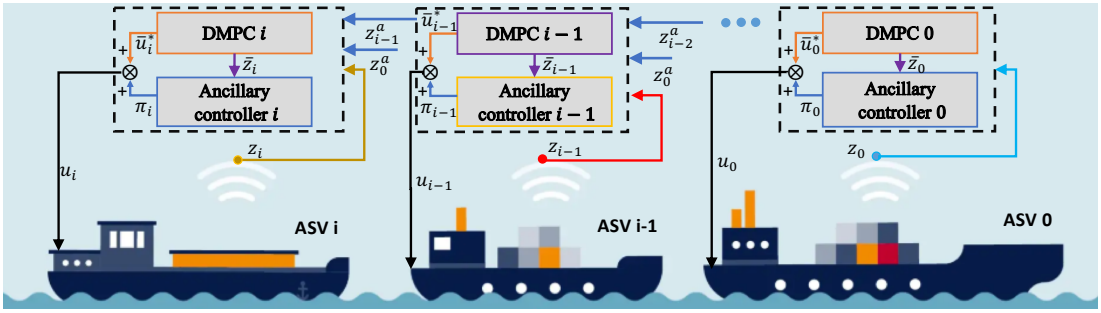

Figure 6.1: The proposed control diagram for the ASV platoon.

It is assumed that the DMPC problem of each ASV has the same prediction horizon T and the sampling period $\delta \in (0, T]$. Let t_k be the sampling time instant, with $k \in \mathbb{N}_{\geq 0}$ and $t_{k+1} = t_k + \delta$. We define $\bar{z}_i(\cdot|t_k)$ as the nominal error state of ASV i, $\bar{z}_{i,i-1}(\cdot|t_k)$ as the nominal error state of ASV $i-1$ predicted by ASV i, $\bar{z}_i^*(\cdot|t_k)$ as the optimal nominal error state, $\bar{z}_{i,i-1}^*(\cdot|t_k)$ as the optimal nominal error state of ASV $i-1$ predicted by ASV i, $z_i^a(\cdot|t_k)$ as the assumed error state, and $\bar{z}_i^p(\cdot|t_k)$ as the predicted error state. The corresponding control inputs are denoted likewise.

As depicted in Figure 6.1, ASV i receives the assumed error states $z_{i-1}^a(s|t_k), s \in [t_k, t_k + T]$ from its preceding ASV $i-1$, since the optimal nominal error states $\bar{z}_{i-1}^*(s|t_k), s \in [t_k, t_k + T]$ of the preceding ASV $i-1$ are not available for ASV i at t_k. The assumed nominal error state $z_i^a(\cdot|t_k)$ of ASV i at t_k is defined by

$$z_i^a(s|t_k) = \begin{cases} \bar{z}_i^*(s|t_{k-1}), & s \in [t_k, t_{k-1} + T], \\ 0, & s \in (t_{k-1} + T, t_k + T]. \end{cases} \tag{6.9}$$

Similarly, the assumed control $u_i^a(\cdot|t_k)$ is constructed as

$$u_i^a(s|t_k) = \begin{cases} \bar{u}_i^*(s|t_{k-1}), & s \in [t_k, t_{k-1} + T], \\ 0, & s \in (t_{k-1} + T, t_k + T]. \end{cases}$$

With these notations, the cost function at t_k is designed as

$$\begin{aligned} & J_i\left(\bar{\mathbf{z}}_i(t_k), z_{i-1}^a(\cdot|t_k), \bar{\mathbf{u}}_i(\cdot|t_k)\right) \\ = & \int_{t_k}^{t_k+T} L_i\left(\bar{\mathbf{z}}_i(s|t_k), z_{i-1}^a(s|t_k), \bar{\mathbf{u}}_i(s|t_k)\right) \mathrm{d}s + F_i\left(\bar{\mathbf{z}}_i(t_k + T|t_k)\right), \end{aligned}$$

in which $\bar{\mathbf{z}}_i(t_k) = [\bar{z}_i(t_k), \bar{z}_{i,i-1}(t_k)]^{\mathrm{T}}$, $\bar{z}_i(t_k)$ is the initial nominal error state and

$\bar{z}_{i,i-1}(t_k) = z^a_{i-1}(t_k|t_k)$ is the initial nominal error state of ASV $i-1$, $\bar{\mathbf{z}}_i(s|t_k) = [\bar{z}_i(s|t_k), \bar{z}_{i,i-1}(s|t_k)]^{\mathrm{T}}$ and $\bar{\mathbf{u}}_i(s|t_k) = [\bar{u}_i(s|t_k), \bar{u}_{i,i-1}(s|t_k)]^{\mathrm{T}}$.

The terminal cost function is designed as

$$F_i\left(\bar{\mathbf{z}}_i(t_k+T|t_k)\right) = \|\bar{z}_i(t_k+T|t_k)\|_{P_i} + \|\bar{z}_{i,i-1}(t_k+T|t_k)\|_{P_{i,i-1}}$$

and the stage cost is defined as

$$\begin{aligned} &L_i\left(\bar{\mathbf{z}}_i(s|t_k), z^a_{i-1}(s|t_k), \bar{\mathbf{u}}_i(s|t_k)\right) \\ =&\|\bar{z}_i(s|t_k)\|_{Q_i} + \|\bar{z}_i(s|t_k) - z^a_{i-1}(s|t_k)\|_{H_i} + \|\bar{u}_i(s|t_k)\|_{R_i} \\ &+ \|\bar{z}_i(s|t_k) - z^a_i(s|t_k)\|_{F_i} + \|\bar{z}_{i,i-1}(s|t_k)\|_{Q_{i,i-1}} + \|\bar{u}_{i,i-1}(s|t_k)\|_{R_{i,i-1}}, \end{aligned} \tag{6.10}$$

with $P_i \succeq 0$, $P_{i,i-1} \succeq 0$, $Q_i \succeq 0$, $Q_{i,i-1} \succeq 0$, $R_{i,i-1} \succ 0$, $H_i \succeq 0$, $F_i \succeq 0$, $R_i \succ 0$, and $H_{-1} = H_0 = Q_{0,-1} = R_{0,-1} = 0$.

Remark 6.1. *The cost term $\|\bar{z}_i(s|t_k) - z^a_{i-1}(s|t_k)\|_{H_i}$ in* (6.10) *aims to minimize the predecessor-follower spacing error (i.e., $x_i - x_{i-1} + d^x = z_i - z_{i-1}$), and also maintains the same velocity as its preceding ASV $i-1$. The cost term $\|\bar{z}_i(s|t_k) - z^a_i(s|t_k)\|_{F_i}$ in* (6.10) *is introduced to suppress the deviation between the nominal error state $\bar{z}_i(s|t_k)$ and the assumed error state $z^a_i(s|t_k)$. The cost term $\|\bar{z}_{i,i-1}(s|t_k)\|_{Q_{i,i-1}}$ is designed to approximate the error state of ASV $i-1$.*

The following assumption is given for the nominal error system in (6.6).

Assumption 6.2. *For the nominal error system of ASV i, there exist an admissible terminal control law $\kappa_i(\cdot) \in \bar{\mathbb{U}}_i$ and a terminal invariant set $\Omega_i(\epsilon_i)$ with a constant $\epsilon_i > 0$, such that: 1) $\forall \bar{z}_i(t_k) \in \Omega_i(\epsilon_i)$, and by implementing $\kappa_i(\cdot)$, $\bar{z}_i(t) \in \Omega_i(\epsilon_i)$ with $t > t_k$; 2) $\forall \bar{z}_i(t) \in \Omega_i(\epsilon_i), i \in \mathcal{V}^0$, $\dot{F}_i\left(\bar{\mathbf{z}}_i(t)\right) + L_i\left(\bar{\mathbf{z}}_i(t), z^a_{i-1}(t), \bar{\mathbf{u}}_i(t)\right) \leq 0$.*

6.3 Robust Distributed Model Predictive Platooning Control

The DMPC optimization problem and the ancillary control law are first presented in this section. A robust control invariant set is then provided in **Lemma 6.1**. Finally, the robust DMPC algorithm is given.

6.3.1 DMPC optimization problem

The DMPC optimization problem $\mathcal{P}_i$ for ASV i, $i \in \mathcal{V}^0$ at time t_k is designed as

$$\min_{\bar{\mathbf{u}}_i(\cdot|t_k)} J_i\left(\bar{\mathbf{z}}_i(t_k), z_{i-1}^a(\cdot|t_k), \bar{\mathbf{u}}_i(\cdot|t_k)\right)$$

$$\begin{aligned}
\text{s.t.}\quad & \bar{z}_i(t_k|t_k) = \bar{z}_i(t_k), && \text{(6.11a)}\\
& \dot{\bar{z}}_i(s|t_k) = f_i(\bar{z}_i(s|t_k)) + B_i\bar{u}_i(s|t_k), && \text{(6.11b)}\\
& \bar{u}_i(s|t_k) \in \bar{\mathbb{U}}_i, && \text{(6.11c)}\\
& \|\bar{z}_i(s|t_k) - z_i^a(s|t_k)\| \leq \check{o}, && \text{(6.11d)}\\
& \bar{z}_i(t_k+T|t_k) \in \Omega_i(\epsilon_i), && \text{(6.11e)}\\
& \bar{z}_{i,i-1}(t_k|t_k) = z_{i-1}^a(t_k|t_k), && \text{(6.11f)}\\
& \dot{\bar{z}}_{i,i-1}(s|t_k) = f_{i-1}(\bar{z}_{i,i-1}(s|t_k)) + B_{i-1}\bar{u}_{i,i-1}(s|t_k), && \text{(6.11g)}\\
& \bar{u}_{i,i-1}(s|t_k) = u_{i-1}^a(s|t_k), s \in [t_k, t_{k+1}), && \text{(6.11h)}\\
& \bar{u}_{i,i-1}(s|t_k) \in \bar{\mathbb{U}}_{i-1}, && \text{(6.11i)}\\
& \bar{z}_{i,i-1}(t_k+T|t_k) \in \Omega_{i-1}(\epsilon_{i-1}), && \text{(6.11j)}\\
& E(\bar{z}_i(s|t_k) - \bar{z}_{i,i-1}(s|t_k)) \leq d^x - \hat{d}_i^{\text{safe}}, && \text{(6.11k)}
\end{aligned}$$

where $s \in [t_k, t_k+T)$, the tightened control input constraint is defined as $\bar{\mathbb{U}}_i = \mathbb{U}_i \ominus K_i\mathbb{E}_i \neq \emptyset$, with K_i being the control gain of the ancillary controller and $\mathbb{E}_i$ being the robust control invariant set, and $\hat{d}_i^{\text{safe}} := d_i^{\text{safe}} + e_{i,\max}^x + e_{i-1,\max}^x + \check{o}$. $e_{i,\max}^x$ is the maximum position error between the nominal position and the actual position, which will be given in Section 6.3.2. Based on the assumed state $z_{i-1}^a(t_k|t_k)$ broadcast from ASV $i-1$, the states of ASV $i-1$ are locally estimated by ASV i. The terminal constraint is defined as $\Omega_i(\epsilon_i) = \{\bar{z}_i \mid \|\bar{z}_i\| \leq \epsilon_i\}$, with $\epsilon_i < \check{o}$ and $\epsilon_i + \epsilon_{i-1} < d^x - \hat{d}_i^{\text{safe}}$.

Remark 6.2. *The collision avoidance safety of cooperative AUVs in [160] is achieved by incorporating a coupled collision avoidance cost term into the overall cost function. Instead, the inter-vehicle safety of the ASV platoon in this work is guaranteed via the coupled constraint in* (6.11k)*. The presence of coupled constraints makes the DMPC optimization problem more challenging concerning the recursive feasibility analysis. Following the similar approximation strategy in [123, 147], the nominal error dynamics and constraints of ASV $i-1$ are assumed to be known by the local ASV i in the optimization problem $\mathcal{P}_i$. Hence, ASV i can approximate the error states of its pre-*

ceding ASV $i-1$, which will not be broadcast among ASVs. In this way, the coupled constraint (6.8) *can be decoupled as a local constraint* (6.11k).

6.3.2 The ancillary controller

The control input applied to ASV i is designed as

$$u_i(s) = \bar{u}_i^*(s|t_k) + \pi_i(z_i(s), \bar{z}_i^*(s|t_k)),\ s \in [t_k, t_{k+1}), \tag{6.12}$$

for the sake of simplicity, $\bar{u}_i^*(s)$ denotes the optimal nominal control $\bar{u}_i^*(s|t_k)$ and $\pi_i(s)$ denotes the ancillary control law $\pi_i(z_i(s), \bar{z}_i^*(s|t_k))$ in the sequel. The deviation between the actual and nominal error system state is defined as $e_i(s) = z_i(s) - \bar{z}_i(s|t_k)$, $s \geq t_k$, with $e_i(s) = [e_{xi}(s), e_{\mu i}(s)]^{\mathrm{T}}$. Next, the robust control invariant set $\mathbb{E}_i$ is derived. The set $\mathbb{E}_i$ centers along the reference state (i.e., the nominal error state $\bar{z}_i(s|t_k)$) and the ancillary control law $\pi_i(s)$ ensures that $e_i(s) \in \mathbb{E}_i$.

The following lemma presents the ancillary controller design and the robust control invariant set $\mathbb{E}_i$.

Lemma 6.1. *Suppose that* ***Assumption 6.1*** *holds. Let $S_i(e_i(s)) : \mathbb{R}^2 \to [0, \infty)$ be a continuously differentiable function with $0 < S_i(e_i(s)) \leq \alpha_2(\|e_i(s)\|)$, where $\alpha_2(\cdot)$ is a $\mathcal{K}_\infty$ function. Let $\bar{z}_i(s|t_k)$, $s \geq t_k$ be the reference state, and the feedback control law is defined as*

$$\pi_i(s) = -K_i e_i(s), \tag{6.13}$$

with $K_i = [k_{pi} + k_{di} + d_i,\ M_{x_i} + k_{di}]$, $d_i = -X_{\mu_i} - X_{\mu_i|\mu_i|}|\mu_i|$. If there exist K_i, $\rho_i > 0$, and $\sigma_i > 0$, such that

$$\frac{\mathrm{d}}{\mathrm{d}s} S_i(e_i(s)) + \rho_i S_i(e_i(s)) - \sigma_i w_i^2(s) \leq 0, \forall w_i(s) \in \mathbb{W}_i, \tag{6.14}$$

with $S_i(e_i(s)) = \frac{1}{2} e_i^{\mathrm{T}}(s) \Gamma_i e_i(s)$ and $\Gamma_i = [k_{pi}, M_{x_i}; M_{x_i}, M_{x_i}]$. Then, $\forall e_i(t_k) \in \mathbb{E}_i$, $e_i(s) \in \mathbb{E}_i$, for all $s > t_k$, where

$$\mathbb{E}_i := \left\{ e_i(s) \mid S_i(e_i(s)) \leq \frac{\sigma_i w_{i,\max}^2}{\rho_i} \right\}. \tag{6.15}$$

Proof. The proof can be obtained by employing the argument in [172, Lemma 1]. Also, it implies that the deviations $|e_i^x(s)|$ and $|e_i^\mu(s)|$ are bounded, i.e., $|e_i^x(s)| \leq e_{i,\max}^x$, $|e_i^\mu(s)| \leq e_{i,\max}^\mu$, with $e_{i,\max}^x > 0$ and $e_{i,\max}^\mu > 0$. □

6.3.3 Robust DMPC algorithm

The robust DMPC algorithm is implemented in a receding horizon fashion and is presented in **Algorithm 4**.

Algorithm 4 Robust DMPC algorithm for ASV i, $i \in \mathcal{V}$

1: **Initialization**: Set $k = 0$. For ASV $i, i \in \mathcal{V}^0$, give the desired states $q_i^{\text{des}}(\cdot|t_k)$ at t_k. Set $\bar{z}_0(t_k) = 0$ and $\bar{z}_i(s|t_k) = z_i^a(s|t_k) = 0, s \in [t_k, t_k + T]$;
2: ASV 0 samples $z_0(t_k)$, solves $\mathcal{P}_0$ without (6.11f) – (6.11k) and broadcasts $z_0^a(\cdot|t_k)$ to ASV $j, j \in \mathcal{V}$;
3: ASV i receives $z_\ell^a(\cdot|t_k), \ell \in \mathcal{N}_i$;
4: ASV i samples $z_i(t_k)$, solves $\mathcal{P}_i$ in (6.11), and further generates control inputs $u_i(s)$ via (6.12);
5: ASV i applies $u_i(s), s \in [t_k, t_k + \delta)$, and transmits $z_i^a(\cdot|t_k)$ to ASV $i + 1$.
6: $k = k + 1$. Go to Step 2 until the control is finished.

6.4 Theoretical Analysis

This section presents the theoretical analysis, including the recursive feasibility of the proposed algorithm and the closed-loop robust stability of the heterogeneous ASV platoon in the presence of external disturbances.

Theorem 6.1. *Suppose that **Assumptions 6.1** and **6.2** hold. For the heterogeneous ASV platoon, if the optimization problem $\mathcal{P}_i$ is feasible at t_0, then, 1) It is recursively feasible at time t_k, $t_k > t_0$ under **Algorithm 4** if the conditions $\epsilon_i < \check{o}$ and $\epsilon_i + \epsilon_{i-1} < d^x - \hat{d}_i^{safe}$ hold. 2) The inter-vehicle safety is ensured for all admissible disturbances $w_i \in \mathbb{W}_i$. 3) The ASVs under the robust DMPC algorithm is ISS if $F_i \succeq H_{i+1}$ holds.*

Proof. 1) The recursive feasibility of the DMPC algorithm is proved by induction. The optimal nominal control inputs obtained at t_k are denoted as $\bar{u}_i^*(s|t_k), \bar{u}_{i,i-1}^*(s|t_k), s \in [t_k, t_k + T)$, which drive the nominal error systems of ASV i and ASV $i - 1$ into the terminal region $\Omega_i(\epsilon_i)$ and $\Omega_{i-1}(\epsilon_{i-1})$, respectively. The optimal nominal error states with control inputs $\bar{u}_i^*(s|t_k), s \in [t_k, t_k + T)$ are given by $\dot{\bar{z}}_i^*(s|t_k) = f_i(\bar{z}_i^*(s|t_k)) + B_i\bar{u}_i^*(s|t_k), s \in [t_k, t_k + T)$. At t_{k+1}, based on the optimal nominal control inputs at t_k and **Assumption 6.2**, a feasible control input candidate $\bar{u}_i^p(\cdot|t_{k+1})$ for the problem

$\mathcal{P}_i$ is given as

$$\bar{u}_i^p(s|t_{k+1}) = \begin{cases} \bar{u}_i^*(s|t_k), & s \in [t_{k+1}, t_k + T)\,, \\ \kappa_i(\bar{z}_i(s|t_k)), & s \in [t_k + T, t_{k+1} + T)\,, \end{cases} \tag{6.16}$$

where $\kappa_i(\cdot)$ is the terminal controller for ASV i. The corresponding states are computed as

$$\bar{z}_i^p(s|t_{k+1}) = \begin{cases} \bar{z}_i^*(s|t_k), & s \in [t_{k+1}, t_k + T)\,, \\ z_i^\kappa(s|t_k), & s \in [t_k + T, t_{k+1} + T)\,. \end{cases} \tag{6.17}$$

The control input candidate and the corresponding states of locally approximated ASV $i-1$ are constructed similarly.

According to **Assumption 6.2**, $\kappa_i(\bar{z}_i(s|t_k)) \in \bar{\mathbb{U}}_i, s \in [t_k + T, t_{k+1} + T)$. In addition, $\bar{u}_i^p(s|t_{k+1}) = \bar{u}_i^*(s|t_k) \in \bar{\mathbb{U}}_i, s \in [t_{k+1}, t_k + T)$. Hence, the control input constraint (6.11c) is satisfied. Further, since the terminal region $\Omega_i(\epsilon_i)$ is invariant with the terminal control law $\kappa_i(\bar{z}_i(s|t_k)), s \in [t_k + T, t_{k+1} + T)$, it has $\bar{z}_i^p(t_{k+1} + T|t_{k+1}) \in \Omega_i(\epsilon_i)$. Therefore, the terminal state constraint (6.11e) holds. Due to the assumed states in (6.9) and the states in (6.17) coincide, i.e., $\bar{z}_i^p(s|t_{k+1}) = z_i^a(s|t_{k+1}), s \in [t_{k+1}, t_k + T]$. In addition, $z_i^a(s|t_k) = 0, s \in (t_k + T, t_{k+1} + T]$ and $\epsilon_i \leq \check{o}$, thus $\|\bar{z}_i^p(s|t_{k+1}) - z_i^a(s|t_{k+1})\| \leq \check{o}, s \in (t_k + T, t_{k+1} + T]$ holds. Hence, the constraint (6.11d) is fulfilled. The constraints (6.11i) and (6.11j) of ASV $i-1$ can be proved following the same logic of (6.11c) and (6.11e). Next, for $s \in [t_{k+1}, t_k + T]$,

$$E(\bar{z}_i^p(s|t_{k+1}) - \bar{z}_{i,i-1}^p(s|t_{k+1})) = E(\bar{z}_i^*(s|t_k) - \bar{z}_{i,i-1}^*(s|t_k)) \leq d^x - \hat{d}_i^{\text{safe}}.$$

And for $s \in (t_k + T, t_{k+1} + T]$, since the inequality $\epsilon_i + \epsilon_{i-1} < d^x - \hat{d}_i^{\text{safe}}$ holds, and the terminal constraint implies that (6.11k) is ensured. Thus, the minimum safe following distance constraint (6.11k) is satisfied.

2) At time t_k, from **Lemma 6.1**, it can be obtained $z_i(s) \in \bar{z}_i^*(s|t_k) \oplus \mathbb{E}_i$, $s \in [t_k, t_k + \delta]$, $z_{i-1}(s) \in \bar{z}_{i-1}^*(s|t_k) \oplus \mathbb{E}_{i-1}, s \in [t_k, t_k + \delta]$. Since $z_{i-1}^a(t_k|t_k) = \bar{z}_{i,i-1}(t_k|t_k) = \bar{z}_{i-1}(t_k|t_k)$, and $\bar{u}_{i,i-1}^*(s|t_k) = u_{i-1}^a(s|t_k)$, then $\bar{z}_{i,i-1}(s|t_k) = z_{i-1}^a(s|t_k), s \in [t_k, t_k + \delta]$. In addition, by the constraint (6.11d), it can be obtained

$$z_{i-1}(s) \in \bar{z}_{i,i-1}^*(s|t_k) \oplus \mathbb{E}_{i-1} \oplus \check{\mathbb{O}},$$

with $s \in [t_k, t_k + \delta], \check{\mathbb{O}} := \{\bar{z}_i \mid \|\bar{z}_i - z_i^a\| \leq \check{o}\}$. Therefore, the actual inter-ASV safety in (6.8) is ensured since the constraint (6.11k) holds.

3) For the overall ASV system, the Lyapunov function is chosen as the sum of the distributed optimal cost function

$$V(t_k) = \sum_{i\in\mathcal{V}^0} J_i\left(\bar{\mathbf{z}}_i(t_k), z^a_{i-1}(\cdot|t_k), \bar{\mathbf{u}}^*_i(\cdot|t_k)\right). \tag{6.18}$$

At time t_k, the calculated optimal control input $\bar{u}^*_i(s|t_k)$,$s \in [t_k, t_k+\delta)$ is applied. At t_{k+1}, applying the feasible control inputs (6.16) yields

$$\begin{aligned}
V(t_{k+1}) &= \sum_{i\in\mathcal{V}^0} J_i\left(\bar{\mathbf{z}}_i(t_{k+1}), z^a_{i-1}(\cdot|t_{k+1}), \bar{\mathbf{u}}^*_i(\cdot|t_{k+1})\right)\\
&\le \sum_{i\in\mathcal{V}^0} J_i\left(\bar{\mathbf{z}}_i(t_{k+1}), z^a_{i-1}(\cdot|t_{k+1}), \bar{\mathbf{u}}^p_i(\cdot|t_{k+1})\right)\\
&= \sum_{i\in\mathcal{V}^0} \Big\{ \int_{t_{k+1}}^{t_{k+1}+T} L_i\Big(\bar{\mathbf{z}}^p_i(s|t_{k+1}), z^a_{i-1}(s|t_{k+1}), \bar{\mathbf{u}}^p_i(s|t_{k+1})\Big)\,\mathrm{d}s\\
&\quad + F_i(\bar{\mathbf{z}}^p_i(t_{k+1}+T|t_{k+1}))\Big\}.
\end{aligned}$$

Hence, the difference of the Lyapunov function (6.18) at t_{k+1} and t_k becomes

$$\begin{aligned}
&V(t_{k+1}) - V(t_k)\\
&\le \sum_{i\in\mathcal{V}^0} J_i\left(\bar{\mathbf{z}}_i(t_{k+1}), z^a_{i-1}(\cdot|t_{k+1}), \bar{\mathbf{u}}^p_i(\cdot|t_{k+1})\right) - V(t_k)\\
&= \sum_{i\in\mathcal{V}^0} (\Delta^i_1 + \Delta^i_2 + \Delta^i_3),
\end{aligned}$$

where

$$\begin{aligned}
\Delta^i_1 =& -\int_{t_k}^{t_{k+1}} \Big\{\|\bar{z}^*_i(s|t_k) - z^a_{i-1}(s|t_k)\|_{H_i} + \|\bar{z}^*_i(s|t_k) - z^a_i(s|t_k)\|_{F_i}\\
&+ \|\bar{z}^*_i(s|t_k)\|_{Q_i} + \|\bar{u}^*_i(s|t_k)\|_{R_i} + \|\bar{z}^*_{i,i-1}(s|t_k)\|_{Q_{i,i-1}} + \|\bar{u}^*_{i,i-1}(s|t_k)\|_{R_{i,i-1}}\Big\}\,\mathrm{d}s,\\
\Delta^i_2 =& \int_{t_{k+1}}^{t_k+T} \Big\{L_i(\bar{\mathbf{z}}^p_i(s|t_{k+1}), z^a_{i-1}(s|t_{k+1}), \bar{\mathbf{u}}^p_i(s|t_{k+1}))\\
&- L_i(\bar{\mathbf{z}}^*_i(s|t_k), z^a_{i-1}(s|t_k), \bar{\mathbf{u}}^*_i(s|t_k))\Big\}\,\mathrm{d}s,\\
\Delta^i_3 =& \int_{t_k+T}^{t_{k+1}+T} \Big\{\|\bar{z}^p_i(s|t_{k+1})\|_{Q_i} + \|\bar{u}^p_i(s|t_{k+1})\|_{R_i} + \|\bar{u}^p_{i,i-1}(s|t_{k+1})\|_{R_{i,i-1}}\\
&+ \|\bar{z}^p_{i,i-1}(s|t_{k+1})\|_{Q_{i,i-1}} + \|\bar{z}^p_i(s|t_{k+1})\|_{F_i} + \|\bar{z}^p_i(s|t_{k+1})\|_{H_i}\Big\}\,\mathrm{d}s\\
&+ \|\bar{z}^p_i(t_{k+1}+T|t_{k+1})\|_{P_i} - \|\bar{z}^*_{i,i-1}(t_k+T|t_k)\|_{P_{i,i-1}}\\
&+ \|\bar{z}^p_{i,i-1}(t_{k+1}+T|t_{k+1})\|_{P_{i,i-1}} - \|\bar{z}^*_i(t_k+T|t_k)\|_{P_i}.
\end{aligned}$$

It is easy to find that the inequality $\Delta_1^i < 0$ always holds. Since the assumed states in (6.9) and the states in (6.17) coincide, that is, $\bar{z}_i^p(s|t_{k+1}) = z_i^a(s|t_{k+1}), s \in [t_{k+1}, t_k + T]$. Then, it can be obtained

$$\begin{aligned}
&\|\bar{z}_i^p(s|t_{k+1}) - z_i^a(s|t_{k+1})\|_{F_i} - \|\bar{z}_i^*(s|t_k) - z_{i-1}^a(s|t_k)\|_{H_i} \\
&\quad + \|\bar{z}_i^p(s|t_{k+1}) - z_{i-1}^a(s|t_{k+1})\|_{H_i} - \|\bar{z}_i^*(s|t_k) - z_i^a(s|t_k)\|_{F_i} \\
=&\|\bar{z}_i^p(s|t_{k+1}) - z_{i-1}^a(s|t_{k+1})\|_{H_i} - \|\bar{z}_i^*(s|t_k) - z_i^a(s|t_k)\|_{F_i} \\
&\quad - \|\bar{z}_i^*(s|t_k) - z_{i-1}^a(s|t_k)\|_{H_i} \\
\leq&\|\bar{z}_i^*(s|t_k) - z_{i-1}^a(s|t_k)\|_{H_i} + \|\bar{z}_{i-1}^*(s|t_k) - z_{i-1}^a(s|t_k)\|_{H_i} \\
&\quad - \|\bar{z}_i^*(s|t_k) - z_i^a(s|t_k)\|_{F_i} - \|\bar{z}_i^*(s|t_k) - z_{i-1}^a(s|t_k)\|_{H_i} \\
=&\|\bar{z}_{i-1}^*(s|t_k) - z_{i-1}^a(s|t_k)\|_{H_i} - \|\bar{z}_i^*(s|t_k) - z_i^a(s|t_k)\|_{F_i}.
\end{aligned} \tag{6.19}$$

Next, from $H_0 = H_{-1} = 0$, $F_i \succeq H_{i+1}$ and (6.19), we obtain

$$\begin{aligned}
&\sum_{i\in\mathcal{V}^0} \Delta_2^i \\
=&\sum_{i\in\mathcal{V}^0} \Big\{ \int_{t_{k+1}}^{t_k+T} \{-\|\bar{z}_i^*(s|t_k) - z_i^a(s|t_k)\|_{F_i} \\
&+ \|\bar{z}_i^p(s|t_{k+1}) - z_{i-1}^a(s|t_{k+1})\|_{H_i} - \|\bar{z}_i^*(s|t_k) - z_{i-1}^a(s|t_k)\|_{H_i}\} \,\mathrm{d}s\Big\} \\
\leq&\sum_{i\in\mathcal{V}^0} \int_{t_{k+1}}^{t_k+T} \{\|\bar{z}_{i-1}^*(s|t_k) - z_{i-1}^a(s|t_k)\|_{H_i} - \|\bar{z}_i^*(s|t_k) - z_i^a(s|t_k)\|_{F_i}\} \,\mathrm{d}s \\
\leq&\int_{t_{k+1}}^{t_k+T} -\|\bar{z}_M^*(s|t_k) - z_M^a(s|t_k)\|_{F_M} \,\mathrm{d}s \leq 0.
\end{aligned} \tag{6.20}$$

With the terminal control law $\kappa_i(\cdot)$ and $\kappa_{i-1}(\cdot)$, the system states will be $\bar{z}_i^p(s|t_{k+1})$ and $\bar{z}_{i,i-1}^p(s|t_{k+1})$, $s \in [t_k + T, t_{k+1} + T]$, respectively. By **Assumption 6.2**, one has

$$\begin{aligned}
&\sum_{i\in\mathcal{V}^0} \Delta_3^i \\
=&\sum_{i\in\mathcal{V}^0} \Big\{ \int_{t_k+T}^{t_{k+1}+T} \{\|\bar{z}_i^p(s|t_{k+1})\|_{Q_i} + \|\bar{u}_i^p(s|t_{k+1})\|_{R_i} + \|\bar{z}_i^p(s|t_{k+1})\|_{F_i} \\
&+ \|\bar{z}_{i,i-1}^p(s|t_{k+1})\|_{Q_{i,i-1}} + \|\bar{z}_i^p(s|t_{k+1})\|_{H_i} + \|\bar{u}_{i,i-1}^p(s|t_{k+1})\|_{R_{i,i-1}}\} \,\mathrm{d}s \\
&+ \|\bar{z}_i^p(t_{k+1} + T|t_{k+1})\|_{P_i} - \|\bar{z}_{i,i-1}^*(t_k + T|t_k)\|_{P_{i,i-1}} \\
&+ \|\bar{z}_{i,i-1}^p(t_{k+1} + T|t_{k+1})\|_{P_{i,i-1}} - \|\bar{z}_i^*(t_k + T|t_k)\|_{P_i}\Big\} \\
\leq&0.
\end{aligned} \tag{6.21}$$

According to (6.19), (6.20) and (6.21), we have

$$V(t_{k+1}) - V(t_k) \leq \sum_{i \in \mathcal{V}^0} (\Delta_1^i + \Delta_2^i + \Delta_3^i) < 0, \tag{6.22}$$

which implies that the nominal error systems are asymptotically stable.

Then, we define $\bar{Z}^*(t) = [\bar{z}_0^{*\mathrm{T}}(t), \ldots, \bar{z}_M^{*\mathrm{T}}(t)]^{\mathrm{T}}$, $Z(t) = [z_0^{\mathrm{T}}(t), \ldots, z_M^{\mathrm{T}}(t)]^{\mathrm{T}}$, $E(t) = [e_0^{\mathrm{T}}(t), \ldots, e_M^{\mathrm{T}}(t)]^{\mathrm{T}}$, $U(t) = [u_0(t), \ldots, u_M(t)]^{\mathrm{T}}$ and $\bar{U}^*(t) = [\bar{u}_0^*(t), \ldots, \bar{u}_M^*(t)]^{\mathrm{T}}$, $W(t) = [w_0(t), \ldots, w_M(t)]^{\mathrm{T}}$. Further, the overall closed-loop nominal system and the overall closed-loop actual system are given by

$$\dot{\bar{Z}}^*(t) = F(\bar{Z}^*(t)) + B\bar{U}^*(t), \tag{6.23a}$$

$$\dot{Z}(t) = F(Z(t)) + BU(t) + BW(t), \tag{6.23b}$$

where $F(\cdot) = \mathrm{col}(f_0(z_0(t)), \ldots, f_M(z_M(t))) \in \mathbb{R}^{2(M+1)\times 1}$ and $B = \mathrm{diag}(B_0, \ldots, B_M) \in \mathbb{R}^{2(M+1)\times M}$.

Following the result in [50, Lemma 4.5], if the overall nominal error system in (6.23a) is asymptotically stable, then there exists a $\mathcal{KL}$ function $\alpha_3(\cdot,\cdot)$, such that

$$\|\bar{Z}^*(t)\| \leq \alpha_3(\|\bar{Z}^*(t_0)\|, t - t_0), t \geq t_0. \tag{6.24}$$

By **Lemma 6.1**, if $e_i(t_k) \in \mathbb{E}_i$, then $e_i(t) \in \mathbb{E}_i, t \geq t_k$ always holds. The inequality $\frac{1}{2}e_i(t)^{\mathrm{T}}\Gamma_i e_i(t) \leq \sigma_i w_{i,\max}^2/\rho_i$ results in $\|e_i(t)\| \leq c_i w_{i,\max}$, where $c_i = \sqrt{2\sigma_i/\rho_i\lambda_{\min}(\Gamma_i)}$. By defining a $\mathcal{K}$ function $\gamma_i(\|w_i\|_{[t_0,t]}) = c_i w_{i,\max}$, we know $\|e_i(t)\| \leq \gamma_i(\|w_i\|_{[t_0,t]})$. Note that if the actual error state $z_i(t)$ satisfies $z_i(t) \in \bar{z}_i(t) \oplus \mathbb{E}_i$ for all admissible disturbance sequences. This implies that $\|z_i(t)\| \leq \|\bar{z}_i(t)\| + c_i w_{i,\max}$ holds. Since $z_i(t) = \bar{z}_i^*(t) + e_i(t)$, thus one gets $Z(t) = \bar{Z}^*(t) + E(t)$. By defining a $\mathcal{K}$ function $\gamma(\|W\|_{[t_0,t]}) = c\sqrt{M+1}\|W_{\max}\|$ for the overall closed-loop system, it is easy to obtain $\|E(t)\| \leq \sqrt{\sum_{i\in\mathcal{V}^0} c_i^2 w_{i,\max}^2} \leq \gamma(\|W\|_{[t_0,t]})$, where $c = \max_{i\in\mathcal{V}^0}\{c_i\}$ and $W_{\max} = [w_{0,\max}, \ldots, w_{M,\max}]^{\mathrm{T}}$. Therefore, it follows from (6.24) that

$$\|Z(t)\| \leq \|\bar{Z}^*(t)\| + \|E(t)\| \overset{(6.24)}{\leq} \alpha_3(\|\bar{Z}^*(t_0)\|, t - t_0) + \gamma(\|W\|_{[t_0,t]}). \tag{6.25}$$

From **Definition 2.7**, the overall closed-loop system in (6.23b) is proved to be ISS. □

6.5 Simulation Study

In this section, the simulation of the heterogeneous ASV platoon is presented to verify the effectiveness of the proposed robust distributed model predictive platooning control strategy. The simulated ASV platoon consists of seven Cybership II with different configuration parameters [136], which are selected and shown in Table 6.2. The control input constraint is $|u_i| \leq 40\text{N}$. The desired spacing is chosen as $d^x = 2.5\text{m}$, and the minimum safe following distance is given as $d_i^{\text{safe}} = 0.5\text{m}$.

Table 6.2: Parameters of the ASVs in the platoon.

ASV i	mass m_i	added mass $X_{\dot{\mu}_i}$	surge linear drag X_{μ_i}	surge quadratic drag $X_{\mu_i\|\mu_i\|}$
0	15.0kg	−2.00kg	−0.72kg/s	−2.05kg/m
1	18.0kg	−2.00kg	−0.80kg/s	−2.00kg/m
2	12.0kg	−3.00kg	−1.30kg/s	−1.60kg/m
3	14.0kg	−1.60kg	−1.70kg/s	−2.30kg/m
4	13.7kg	−2.60kg	−1.35kg/s	−1.80kg/m
5	13.0kg	−1.30kg	−1.00kg/s	−1.30kg/m
6	14.0kg	−3.60kg	−1.20kg/s	−1.30kg/m

The speed $\mu_0(t)$ of the desired state is given by

$$\mu_0(t) = \begin{cases} 1 \text{ m/s}, & 0\text{s} \leq t < 1.6\text{s}, \\ 1 + 1.4t \text{ m/s}, & 1.6\text{s} < t \leq 2\text{s}, \\ 1.56 \text{ m/s}, & 2\text{s} < t \leq 3.9\text{s}, \\ 1.56 - 1.6t \text{ m/s}, & 3.9\text{s} < t \leq 4.4\text{s}, \\ 0.76 \text{ m/s}, & 4.4\text{s} < t \leq 6\text{s}. \end{cases} \tag{6.26}$$

In the simulation, time-varying disturbances are simulated by $w_i(t) = A_i \sin(b_i t + c_i)$, where A_i, b_i and $c_i, i \in \mathcal{V}^0$ are given in Table 6.3.

Table 6.3: Disturbance parameters of the ASV platoon.

i	0	1	2	3	4	5	6
A_i	4.5	5.0	5.5	5.3	6.1	5.89	6.0
b_i	0.5π	0.7π	0.8π	0.75π	0.9π	0.8π	0.65π
c_i	$\pi/2$	0	$\pi/3$	$-\pi/4$	$\pi/5$	$2\pi/3$	$-\pi/6$

The parameters for the DMPC optimization problem $\mathcal{P}_i$ are designed as follows: The sampling period $\delta = 0.1$s, the prediction horizon $T = 5\delta$. The weighting matrices are chosen as $Q_i = Q_{i,i-1} = \text{diag}(10^3, 10^2)$, $P_i = P_{i,i-1} = \text{diag}(10^4, 10^3)$, $H_i = \text{diag}(10^2, 10)$, and $F_i = \text{diag}(10^2, 10^2)$. Note that the weighting matrix $R_i = R_{i,i-1} = 10^{-4}$ is chosen so that the control penalty is comparable to the cost terms of Q_i, F_i and H_i. The terminal set level is $\epsilon_i = 0.2$ and the upper bound of the predicted and assumed error state is chosen as $\check{o} = 0.5$.

The robust control invariant set $\mathbb{E}_i$ in (6.15) is constructed based on the conditions in **Lemma 6.1**. In addition, the ancillary controller should be designed to guarantee that the tightened control input constraint set is not empty, i.e. $\bar{\mathbb{U}}_i = \mathbb{U}_i \ominus K_i\mathbb{E}_i \neq \emptyset$. Intuitively, a smaller robust control invariant set leads to a larger admissible control input domain of the DMPC problem $\mathcal{P}_i$. The control gains k_{pi}, k_{di} and the variables σ_i and ρ_i for ASV $i, i \in \mathcal{V}^0$ are shown in Table 6.4. Then, the tightened control input constraint sets are: $|\bar{u}_0| \leq 20.67$N, $|\bar{u}_1| \leq 22.16$N, $|\bar{u}_2| \leq 21.32$N, $|\bar{u}_3| \leq 22.93$N, $|\bar{u}_4| \leq 26.24$N, $|\bar{u}_5| \leq 26.02$N, and $|\bar{u}_6| \leq 21.38$N.

Table 6.4: The ancillary control gain K_i of the ASVs.

ASV i	0	1	2	3	4	5	6
k_{pi}	6.0	7.0	9.0	4.0	9.0	10.0	8.0
k_{di}	6.0	8.0	6.0	4.0	8.0	8.0	7.0
ρ_i	0.92	0.85	1.32	1.13	0.75	1.0	0.76
σ_i	0.20	0.10	0.25	0.15	0.05	0.08	0.09

The simulation results of the heterogeneous ASV platoon using the proposed robust DMPC strategy are demonstrated in Figure 6.2 – Figure 6.4. The proposed strategy demonstrates a good platooning control performance as illustrated in Figure 6.2. The dash line represents the nominal position of the ASV platoon, the solid line represents the actual position, and the shading area represents a hyper-tube whose center is the nominal state. As shown in Figure 6.3, the error $e_i(t)$ between the nominal error state $\bar{z}_i(t)$ and the actual error state $z_i(t)$ stays within a small bounded set and the nominal error state $\bar{z}_i(t)$ approximately converges to zero. Figure 6.4 shows the control inputs of seven heterogeneous ASVs. It is observed that the control input constraints of each ASV are always satisfied.

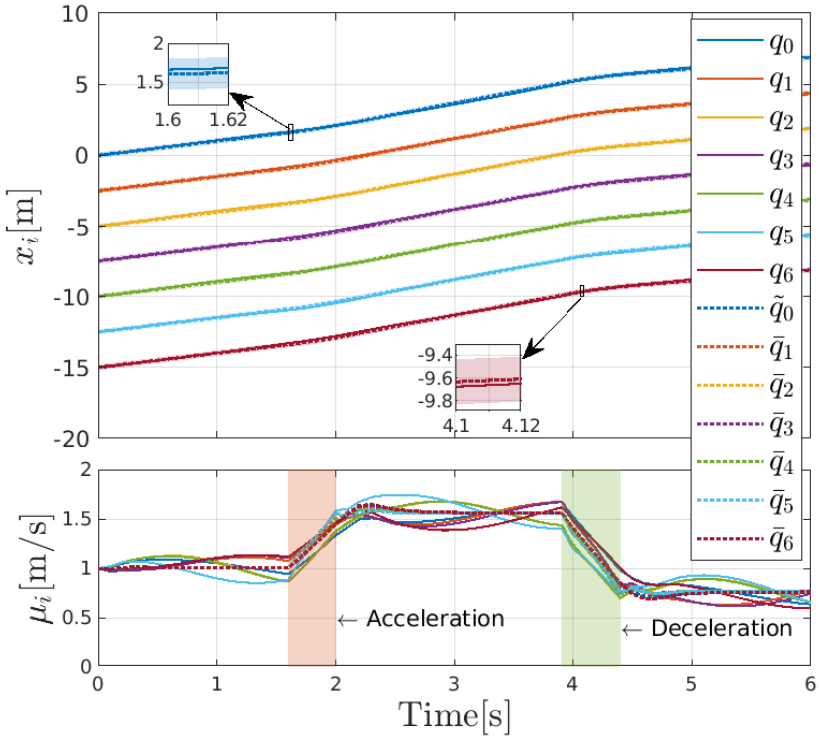

Figure 6.2: States q_i and $\bar{q}_i$ of ASVs under the proposed robust DMPC.

6.6 Conclusion

In this chapter, a robust DMPC approach has been designed for the heterogeneous ASV platoon with external disturbances over the predecessor-leader following communication topology. Each ASV received the assumed predicted state sequences from its predecessor and the lead ASV, measured its system states, and broadcast its assumed predicted state sequences to its follower ASV. Further, by incorporating a coupled minimum safe following distance constraint into the DMPC optimization problem, the local safe control input was generated for each ASV. The proposed platooning algorithm's recursive feasibility and the closed-loop stability of the heterogeneous ASVs were rigorously analyzed. Simulation studies have been performed to verify the effectiveness of the proposed platooning control method.

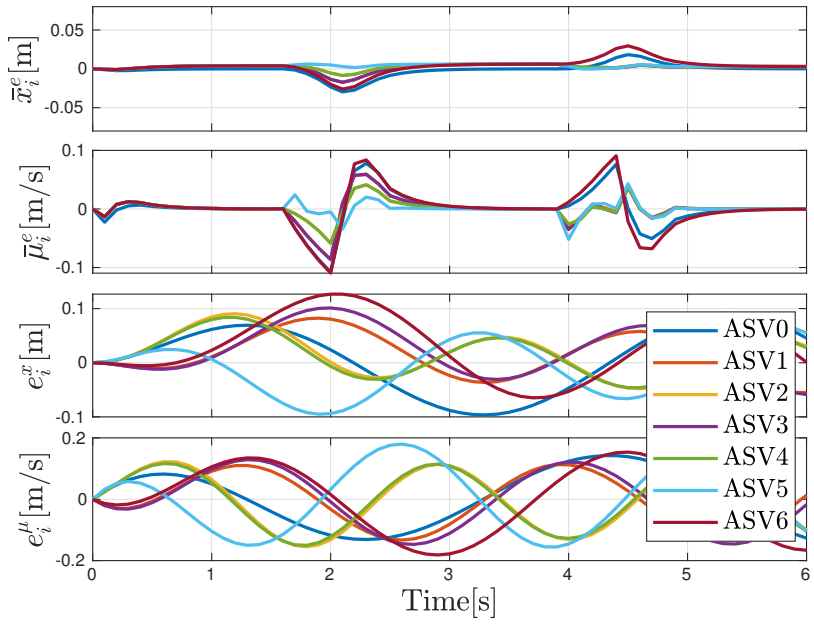

Figure 6.3: States $\bar{z}_i$ and e_i of ASVs under the proposed robust DMPC.

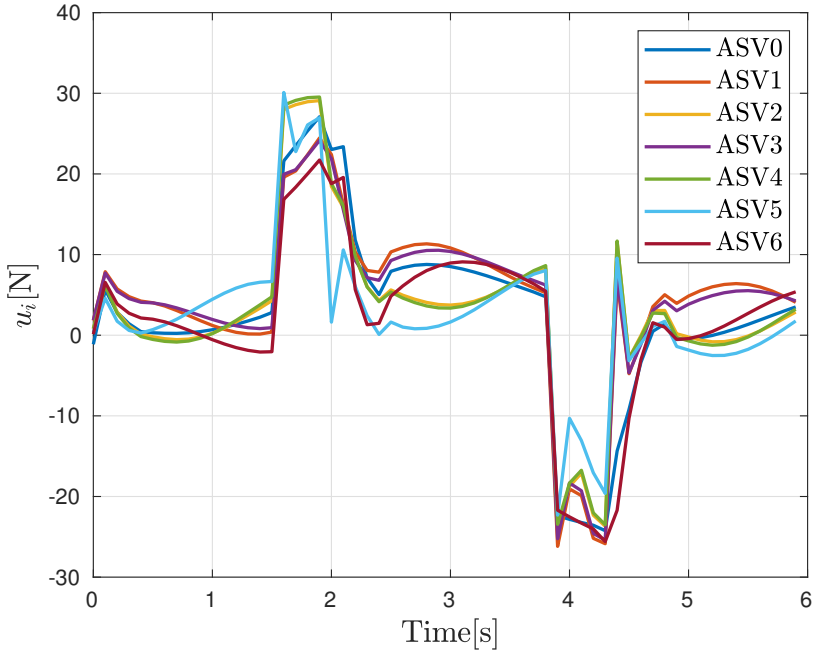

Figure 6.4: Control inputs u_i of ASVs under the proposed robust DMPC.

Chapter 7

Conclusion and Future Directions

This dissertation studied distributed coordination problems of the constrained MAS under uncertainties, including a) *theoretical study:* the formation stabilization problem of the nonlinear MAS with two types of uncertainties and the consensus problem of the general linear MAS with communication delays (**Chapter 3** and **Chapter 4**); b) *application study:* the formation tracking problem of cooperative AUVs and the platooning control problem of heterogeneous ASVs (**Chapter 5** and **Chapter 6**). We have designed robust DMPC algorithms to solve these problems and provided the rigorous theoretical analysis of the recursive feasibility and closed-loop stability.

7.1 Conclusion

Chapter 3 studied the formation stabilization control problem of the dynamically decoupled asynchronous nonlinear MAS with parametric uncertainties, external disturbances, heavy communication burden, and bounded time-varying communication delays. We have proposed a self-triggered min-max DMPC to tackle this challenging problem. A new constraint was incorporated into the local DMPC optimization problem, which provided an upper bound for the deviation between the newest and the previously predicted states. We have shown that the closed-loop MAS was ISpS provided that this constraint was satisfied. Notably, the communication load was significantly reduced while achieving desired control performance. Simulations were carried out to verify the effectiveness and superiority of the proposed algorithm concerning the control performance and communication load.

Chapter 4 investigated the consensus problem of the general linear MAS with in-

put constraints and bounded time-varying communication delays. The delay-induced estimation errors regarded as external disturbances were tackled by exploiting the tube-based MPC scheme. We have developed a robust DMPC-based consensus protocol based on the inverse optimal control and robust MPC technique, which only depended on the information of its immediate neighbors. We have proved the recursive feasibility and consensus convergence for the constrained MAS in the presence of bounded varying delays. Two numerical examples have been provided for illustrative validations.

Chapter 5 has tackled the formation tracking control problem of cooperative AUVs with unknown ocean current disturbances. We proposed a DLMPC algorithm to address this challenging problem. Furthermore, a coupled cost term was designed based on the artificial potential field method to guarantee the inter-AUV collision avoidance. The stability and robustness were further enhanced by incorporating a stability constraint generated by an ESO-based auxiliary controller and the associated Lyapunov function into the DMPC optimization problem without adding a terminal cost and a terminal constraint. The recursive feasibility and closed-loop stability of AUVs were rigorously proved. Simulation results have verified the effectiveness of the proposed algorithm.

In **Chapter 6**, a robust DMPC approach was designed for the heterogeneous ASV platoon with external disturbances over the fixed predecessor-leader following communication topology. Each follower ASV received the assumed predicted state trajectories from its predecessor and the lead ASV, sampled the local states, and broadcast the assumed predicted state trajectory to its following ASV. The local safe control input was calculated for each ASV by incorporating the coupled minimum safe following distance constraint into the DMPC optimization problem. We have rigorously proved the proposed algorithm's recursive feasibility and the ASV platoon's closed-loop stability. Simulation studies were presented to demonstrate the effectiveness of the proposed distributed platooning control method.

7.2 Future Work

7.2.1 Resilient DMPC for constrained consensus of the MAS under adversarial attacks

Typically, the information is exchanged in a distributed fashion for the MAS without the central collection and process. Potential malicious intrusions and adversarial attacks may exist in the communication networks, leading to vulnerability or damage. Resilient consensus becomes critical when some malicious agents in the network do not obey the predefined communication rule and try to mislead the other agents. The objective is to achieve the consensus of normal agents, depending on the reliable information of their neighbors. There has been a growing interest in studying the resilient consensus problem of the MAS under cyber-attacks. Conventional consensus protocols are not applicable for the security-critical MAS with constraints. To systematically address this problem, a distributed attack detection algorithm will be developed and incorporated into the DMPC-based consensus algorithm in **Chapter 4**.

7.2.2 DMPC of the MAS over time-varying networks: A distributed optimization approach

The study of DMPC for the MAS has received considerable attention recently from the control and system communities; see [17, 19] and the references therein. In the literature, a fixed communication graph is often adopted to describe the information exchange among the MAS. The fixed network communication topology is, without any question, the core mechanism that enables agents to cooperate based on the information exchange among agents. In practice, a time-varying communication graph is more suitable for practical MAS applications due to packet drops, node failures, and link failures. Hence, it becomes essential to generate distributed optimal control policy by solving the optimization problem over the time-varying graph. Moreover, it is desirable to improve the control performance while maximizing the convergence rate and minimizing energy consumption. This work will investigate DMPC for constrained linear systems over the time-varying communication networks and also exploit the distributed optimization techniques to accelerate the convergence of the DMPC optimization problem, e.g., [84].

7.2.3 Scalable distributed model platooning control of connected vehicles: A plug-and-play scenario

The platooning control problem of connected vehicles has been regarded as an appealing solution to reduce fuel consumption and increase traffic efficiency. The plug-and-play capability further improves the capacity of the road and enables the cooperation between autonomous vehicles to be more flexible. However, deploying the plug-and-play DMPC algorithms on the connected vehicle systems remains challenging. First, the vehicle platoon has to change its formation, and a feasible controller for transitioning between two formations is needed. Second, the collision-free guarantee and the closed-loop stability of the connected vehicles are necessary. Third, the connectivity of the connected vehicles should be maintained since each vehicle suffers from a limited communication range. To cope with these difficulties, we will develop the scalable DMPC for the plug-and-play platooning control problem of connected vehicles with constraints.

Appendix A

Publications

- **Journal papers**

  1. **Henglai Wei**, Chao Shen and Yang Shi. Distributed Lyapunov-based model predictive formation tracking control for autonomous underwater vehicles subject to disturbances. *IEEE Transactions on Systems, Man, and Cybernetics: Systems*, 51(8), pp. 5198-5208, 2021.
     (This work is presented in Chapter 5.)
  2. **Henglai Wei**, Qi Sun, Jicheng Chen and Yang Shi. Robust distributed model predictive platooning control for heterogeneous autonomous surface vehicles. *Control Engineering Practice*, 107, p. 104655, 2021.
     (This work is presented in Chapter 6.)
  3. **Henglai Wei**, Kunwu Zhang and Yang Shi. Self-triggered min-max DMPC for asynchronous multi-agent systems with communication delays. *IEEE Transactions on Industrial Informatics*, doi: 10.1109/TII.2021.3127197.
     (This work is presented in Chapter 3.)

- **Journal paper under review**

  1. **Henglai Wei**, Changxin Liu and Yang Shi. A robust distributed model predictive control framework for consensus of multi-agent systems with varying delays and input constraints. Submitted.
     (This work is presented in Chapter 4.)

- **Conference paper**

  1. **Henglai Wei**, Kunwu Zhang and Yang Shi. Distributed min-max MPC for dynamically coupled nonlinear systems: A self-triggered approach. *IFAC-*

PapersOnLine, 53(2), pp.6037-6042, 2020.

- **Book**

1. Yang Shi, Chao Shen, **Henglai Wei** and Kunwu Zhang. *Advanced Model Predictive Control for Autonomous Marine Vehicles*, Springer.

Bibliography

[1] Aras Adhami-Mirhosseini, Mohammad J Yazdanpanah, and A Pedro Aguiar. Automatic bottom-following for underwater robotic vehicles. *Automatica*, 50(8):2155–2162, 2014.

[2] Bart Besselink and Karl Henrik Johansson. String stability and a delay-based spacing policy for vehicle platoons subject to disturbances. *IEEE Transactions on Automatic Control*, 62(9):4376–4391, 2017.

[3] CL Philip Chen, Guo-Xing Wen, Yan-Jun Liu, and Zhi Liu. Observer-based adaptive backstepping consensus tracking control for high-order nonlinear semi-strict-feedback multi-agent systems. *IEEE Transactions on Cybernetics*, 46(7):1591–1601, 2015.

[4] Hong Chen and Frank Allgöwer. A quasi-infinite horizon nonlinear model predictive control scheme with guaranteed stability. *Automatica*, 34(10):1205–1217, 1998.

[5] Linying Chen, Hans Hopman, and Rudy R Negenborn. Distributed model predictive control for vessel train formations of cooperative multi-vessel systems. *Transportation Research Part C: Emerging Technologies*, 92:101–118, 2018.

[6] Mou Chen, Shuzhi Sam Ge, Bernard Voon Ee How, and Yoo Sang Choo. Robust adaptive position mooring control for marine vessels. *IEEE Transactions on Control Systems Technology*, 21(2):395–409, 2013.

[7] Zhaomeng Cheng, Hai-Tao Zhang, Ming-Can Fan, and Guanrong Chen. Distributed consensus of multi-agent systems with input constraints: A model predictive control approach. *IEEE Transactions on Circuits and Systems I: Regular Papers*, 62(3):825–834, 2015.

[8] Luigi Chisci, J Anthony Rossiter, and Giovanni Zappa. Systems with persistent disturbances: Predictive control with restricted constraints. *Automatica*, 37(7):1019–1028, 2001.

[9] Panagiotis D Christofides, Riccardo Scattolini, David Munoz de la Pena, and Jinfeng Liu. Distributed model predictive control: A tutorial review and future research directions. *Computers & Chemical Engineering*, 51:21–41, 2013.

[10] Christian Conte, Niklaus R Voellmy, Melanie N Zeilinger, Manfred Morari, and Colin N Jones. Distributed synthesis and control of constrained linear systems. In *Proceedings of the 2012 American Control Conference (ACC)*, pages 6017–6022, June 2012.

[11] David A Copp, Kyriakos G Vamvoudakis, and João P Hespanha. Distributed output-feedback model predictive control for multi-agent consensus. *Systems & Control Letters*, 127:52–59, 2019.

[12] Rongxin Cui, Shuzhi Sam Ge, Bernard Voon Ee How, and Yoo Sang Choo. Leader-follower formation control of underactuated autonomous underwater vehicles. *Ocean Engineering*, 37(17-18):1491–1502, 2010.

[13] Georgios Darivianakis, Annika Eichler, and John Lygeros. Distributed model predictive control for linear systems with adaptive terminal sets. *IEEE Transactions on Automatic Control*, 65(3):1044–1056, 2019.

[14] David Munoz de la Pena and Panagiotis D Christofides. Lyapunov-based model predictive control of nonlinear systems subject to data losses. *IEEE Transactions on Automatic Control*, 53(9):2076–2089, 2008.

[15] Dimos Dimarogonas, Emilio Frazzoli, and Karl Henrik Johansson. Distributed event-triggered control for multi-agent systems. *IEEE Transactions on Automatic Control*, 57(5):1291–1297, 2011.

[16] Allan Andre do Nascimento, Hamid Reza Feyzmahdavian, Mikael Johansson, Winston Garcia-Gabin, and Kalevi Tervo. Tube-based model predictive control for dynamic positioning of marine vessels. *IFAC-PapersOnLine*, 52(21):33–38, 2019.

[17] William B Dunbar. Distributed receding horizon control of dynamically coupled nonlinear systems. *IEEE Transactions on Automatic Control*, 52(7):1249–1263, 2007.

[18] William B Dunbar and Derek S Caveney. Distributed receding horizon control of vehicle platoons: Stability and string stability. *IEEE Transactions on Automatic Control*, 57(3):620–633, 2012.

[19] William B Dunbar and Richard M Murray. Distributed receding horizon control for multi-vehicle formation stabilization. *Automatica*, 42(4):549–558, 2006.

[20] Sami El-Ferik, Bilal A Siddiqui, and Frank L Lewis. Distributed nonlinear MPC of multi-agent systems with data compression and random delays. *IEEE Transactions on Automatic Control*, 61(3):817–822, 2015.

[21] Shuo Feng, Haowei Sun, Yi Zhang, Jianfeng Zheng, Henry X Liu, and Li Li. Tube-based discrete controller design for vehicle platoons subject to disturbances and saturation constraints. *IEEE Transactions on Control Systems Technology*, 28(3):1066–1073, 2020.

[22] Shuo Feng, Yi Zhang, Shengbo Eben Li, Zhong Cao, Henry X Liu, and Li Li. String stability for vehicular platoon control: Definitions and analysis methods. *Annual Reviews in Control*, 47:81–97, 2019.

[23] Giancarlo Ferrari-Trecate, Luca Galbusera, Marco Pietro Enrico Marciandi, and Riccardo Scattolini. Model predictive control schemes for consensus in multi-agent systems with single-and double-integrator dynamics. *IEEE Transactions on Automatic Control*, 54(11):2560–2572, 2009.

[24] Thor I Fossen. *Marine Control Systems: Guidance, Navigation and Control of Ships, Rigs and Underwater Vehicles*. Marine Cybernetics, 2002.

[25] Thor I Fossen. *Handbook of Marine Craft Hydrodynamics and Motion Control*. John Wiley & Sons, 2011.

[26] Elisa Franco, Lalo Magni, Thomas Parisini, Marios M Polycarpou, and Davide M Raimondo. Cooperative constrained control of distributed agents with nonlinear dynamics and delayed information exchange: A stabilizing receding-horizon approach. *IEEE Transactions on Automatic Control*, 53(1):324–338, 2008.

[27] Mingyu Fu and Lingling Yu. Finite-time extended state observer-based distributed formation control for marine surface vehicles with input saturation and disturbances. *Ocean Engineering*, 159:219–227, 2018.

[28] Yulong Gao, Li Dai, Yuanqing Xia, and Yuwei Liu. Distributed model predictive control for consensus of nonlinear second-order multi-agent systems. *International Journal of Robust and Nonlinear Control*, 27(5):830–842, 2017.

[29] Pontus Giselsson, Minh Dang Doan, Tamás Keviczky, Bart De Schutter, and Anders Rantzer. Accelerated gradient methods and dual decomposition in distributed model predictive control. *Automatica*, 49(3):829–833, 2013.

[30] Paul J Goulart, Eric C Kerrigan, and Jan M Maciejowski. Optimization over state feedback policies for robust control with constraints. *Automatica*, 42(4):523–533, 2006.

[31] Gene Grimm, Michael J Messina, Sezai E Tuna, and Andrew R Teel. Nominally robust model predictive control with state constraints. *IEEE Transactions on Automatic Control*, 52(10):1856–1870, 2007.

[32] Dominic Groß and Olaf Stursberg. A cooperative distributed MPC algorithm with event-based communication and parallel optimization. *IEEE Transactions on Control of Network Systems*, 3(3):275–285, 2015.

[33] Bruno J Guerreiro, Carlos Silvestre, Rita Cunha, and António Pascoal. Trajectory tracking nonlinear model predictive control for autonomous surface craft. *IEEE Transactions on Control Systems Technology*, 22(6):2160–2175, 2014.

[34] Christian A Hans, Philipp Braun, Jörg Raisch, Lars Grüne, and Carsten Reincke-Collon. Hierarchical distributed model predictive control of interconnected microgrids. *IEEE Transactions on Sustainable Energy*, 10(1):407–416, 2018.

[35] Shahab Heshmati-Alamdari, George C Karras, Panos Marantos, and Kostas J Kyriakopoulos. A robust predictive control approach for underwater robotic vehicles. *IEEE Transactions on Control Systems Technology*, 28(6):2352–2363, 2020.

[36] Shahab Heshmati-Alamdari, Alexandros Nikou, and Dimos Dimarogonas. Robust trajectory tracking control for underactuated autonomous underwater vehicles in uncertain environments. *IEEE Transactions on Automation Science and Engineering*, 18(3):1288–1301, 2021.

[37] Matthias Hirche, Philipp N Köhler, Matthias A Müller, and Frank Allgöwer. Distributed model predictive control for consensus of constrained heterogeneous linear systems. In *Proceedings of the 59th IEEE Conference on Decision and Control (CDC)*, pages 1248–1253. IEEE, 2020.

[38] Yu-Chi Ho. On centralized optimal control. *IEEE Transactions on Automatic Control*, 50(4):537–538, 2005.

[39] Qing Hui and Wassim M Haddad. $\mathcal{H}_2$ optimal semistable stabilisation for linear discrete-time dynamical systems with applications to network consensus. *International Journal of Control*, 82(3):456–469, 2009.

[40] Nguyen T Hung, Antonio M Pascoal, and Tor A Johansen. Cooperative path following of constrained autonomous vehicles with model predictive control and event-triggered communications. *International Journal of Robust and Nonlinear Control*, 30(7):2644–2670, 2020.

[41] Gian Paolo Incremona, Antonella Ferrara, and Lalo Magni. Asynchronous networked MPC with ISM for uncertain nonlinear systems. *IEEE Transactions on Automatic Control*, 62(9):4305–4317, 2017.

[42] Rawand E Jalal and Bryan P Rasmussen. Limited-communication distributed model predictive control for coupled and constrained subsystems. *IEEE Transactions on Control Systems Technology*, 25(5):1807–1815, 2016.

[43] Zhong-Ping Jiang and Yuan Wang. Input-to-state stability for discrete-time nonlinear systems. *Automatica*, 37(6):857–869, 2001.

[44] Zhong-Ping Jiang and Yuan Wang. A converse Lyapunov theorem for discrete-time systems with disturbances. *Systems & Control Letters*, 45(1):49–58, 2002.

[45] Bo Jin, Huiping Li, Weisheng Yan, and Ming Cao. Distributed model predictive control and optimization for linear systems with global constraints and time-varying communication. *IEEE Transactions on Automatic Control*, 66(7):3393–3400, 2021.

[46] I Ge Jin and Gábor Orosz. Optimal control of connected vehicle systems with communication delay and driver reaction time. *IEEE Transactions on Intelligent Transportation Systems*, 18(8):2056–2070, 2016.

[47] Björn Johansson, Alberto Speranzon, Mikael Johansson, and Karl Henrik Johansson. Distributed model predictive consensus. In *International Symposium on Mathematical Theory of Networks and Systems, Kyoto, Japan, July 24-28*, pages 2438–2444, 2006.

[48] Nadir Kapetanović, Marco Bibuli, Nikola Mišković, and Massimo Caccia. Real-time model predictive line following control for underactuated marine vehicles. *IFAC-PapersOnLine*, 50(1):12374–12379, 2017.

[49] Tamás Keviczky and Karl Henrik Johansson. A study on distributed model predictive consensus. *IFAC Proceedings Volumes*, 41(2):1516–1521, 2008.

[50] Hassan K Khalil. *Nonlinear Systems*. Upper Saddle River, NJ, USA: Prentice-Hall, 2002.

[51] Roozbeh Kianfar, Paolo Falcone, and Jonas Fredriksson. A control matching model predictive control approach to string stable vehicle platooning. *Control Engineering Practice*, 45:163–173, 2015.

[52] Johannes Köhler, Matthias A Müller, and Frank Allgöwer. A novel constraint tightening approach for nonlinear robust model predictive control. In *Proceedings of 2018 American Control Conference (ACC)*, pages 728–734, June 2018.

[53] Arman Sharifi Kolarijani, Sander Christian Bregman, Peyman Mohajerin Esfahani, and Tamás Keviczky. A decentralized event-based approach for robust model predictive control. *IEEE Transactions on Automatic Control*, 65(8):3517–3529, 2020.

[54] Wilbur Langson, Ioannis Chryssochoos, SV Raković, and David Q Mayne. Robust model predictive control using tubes. *Automatica*, 40(1):125–133, 2004.

[55] Mircea Lazar, D Muñoz De La Peña, WPMH Heemels, and Teodoro Alamo. On input-to-state stability of min–max nonlinear model predictive control. *Systems & Control Letters*, 57(1):39–48, 2008.

[56] Mircea Lazar and WPMH Heemels. Predictive control of hybrid systems: Input-to-state stability results for sub-optimal solutions. *Automatica*, 45(1):180–185, 2009.

[57] Jay H Lee and Zhenghong Yu. Worst-case formulations of model predictive control for systems with bounded parameters. *Automatica*, 33(5):763–781, 1997.

[58] Lei Fang and P. J. Antsaklis. Information consensus of asynchronous discrete-time multi-agent systems. In *Proceedings of the 2005 American Control Conference (ACC)*, pages 1883–1888, 2005.

[59] Huiping Li, Bo Jin, and Weisheng Yan. Distributed model predictive control for linear systems under communication noise: Algorithm, theory and implementation. *Automatica*, 125:109422, 2021.

[60] Huiping Li and Yang Shi. Networked min–max model predictive control of constrained nonlinear systems with delays and packet dropouts. *International Journal of Control*, 86(4):610–624, 2013.

[61] Huiping Li and Yang Shi. Robust distributed model predictive control of constrained continuous-time nonlinear systems: A robustness constraint approach. *IEEE Transactions on Automatic Control*, 59(6):1673–1678, 2013.

[62] Huiping Li and Yang Shi. Distributed receding horizon control of large-scale nonlinear systems: Handling communication delays and disturbances. *Automatica*, 50(4):1264–1271, 2014.

[63] Huiping Li and Yang Shi. Network-based predictive control for constrained nonlinear systems with two-channel packet dropouts. *IEEE Transactions on Industrial Electronics*, 61(3):1574–1582, 2014.

[64] Huiping Li and Yang Shi. Robust distributed model predictive control of constrained continuous-time nonlinear systems: A robustness constraint approach. *IEEE Transactions on Automatic Control*, 59(6):1673–1678, 2014.

[65] Huiping Li and Yang Shi. *Robust Receding Horizon Control for Networked and Distributed Nonlinear Systems*. New York, NY, USA: Springer, 2017.

[66] Huiping Li, Yang Shi, and Weisheng Yan. On neighbor information utilization in distributed receding horizon control for consensus-seeking. *IEEE Transactions on Cybernetics*, 46(9):2019–2027, 2015.

[67] Huiping Li, Yang Shi, and Weisheng Yan. Distributed receding horizon control of constrained nonlinear vehicle formations with guaranteed γ-gain stability. *Automatica*, 68:148–154, 2016.

[68] Huiping Li, Yang Shi, Weisheng Yan, and Fuqiang Liu. Receding horizon consensus of general linear multi-agent systems with input constraints: An inverse optimality approach. *Automatica*, 91:10–16, 2018.

[69] Huiping Li, Pan Xie, and Weisheng Yan. Receding horizon formation tracking control of constrained underactuated autonomous underwater vehicles. *IEEE Transactions on Industrial Electronics*, 64(6):5004–5013, 2016.

[70] Huiping Li, Pan Xie, and Weisheng Yan. Receding horizon formation tracking control of constrained underactuated autonomous underwater vehicles. *IEEE Transactions on Industrial Electronics*, 64(6):5004–5013, 2017.

[71] Huiping Li and Weisheng Yan. Receding horizon control based consensus scheme in general linear multi-agent systems. *Automatica*, 56:12–18, 2015.

[72] Huiping Li and Weisheng Yan. Model predictive stabilization of constrained underactuated autonomous underwater vehicles with guaranteed feasibility and stability. *IEEE/ASME Transactions on Mechatronics*, 22(3):1185–1194, 2016.

[73] Huiping Li, Weisheng Yan, Yang Shi, and Yintao Wang. Periodic event-triggering in distributed receding horizon control of nonlinear systems. *Systems & Control Letters*, 86:16–23, 2015.

[74] Zhen Li and Jing Sun. Disturbance compensating model predictive control with application to ship heading control. *IEEE Transactions on Control Systems Technology*, 20(1):257–265, 2011.

[75] Zhen Li, Jing Sun, and Soryeok Oh. Path following for marine surface vessels with rudder and roll constraints: An MPC approach. In *Proceedings of the 2009 American Control Conference (ACC)*, pages 3611–3616. IEEE, 2009.

[76] Zhongkui Li, Zhisheng Duan, Guanrong Chen, and Lin Huang. Consensus of multiagent systems and synchronization of complex networks: A unified viewpoint. *IEEE Transactions on Circuits and Systems I: Regular Papers*, 57(1):213–224, 2009.

[77] Haojiao Liang, Huiping Li, and Demin Xu. Nonlinear model predictive trajectory tracking control of underactuated marine vehicles: Theory and experiment. *IEEE Transactions on Industrial Electronics*, 68(5):4238–4248, 2021.

[78] Daniel Limón, T Alamo, Francisco Salas, and Eduardo F Camacho. Input to state stability of min-max MPC controllers for nonlinear systems with bounded uncertainties. *Automatica*, 42(5):797–803, 2006.

[79] Daniel Limón, Ignacio Alvarado, Teodoro Alamo, and Eduardo F Camacho. MPC for tracking piecewise constant references for constrained linear systems. *Automatica*, 44(9):2382–2387, 2008.

[80] Peng Lin and Wei Ren. Constrained consensus in unbalanced networks with communication delays. *IEEE Transactions on Automatic Control*, 59(3):775–781, 2013.

[81] Peng Lin, Wei Ren, and Huijun Gao. Distributed velocity-constrained consensus of discrete-time multi-agent systems with nonconvex constraints, switching topologies, and delays. *IEEE Transactions on Automatic Control*, 62(11):5788–5794, 2016.

[82] Changxin Liu, Jian Gao, and Demin Xu. Lyapunov-based model predictive control for tracking of nonholonomic mobile robots under input constraints. *International Journal of Control, Automation and Systems*, 15(5):2313–2319, 2017.

[83] Changxin Liu, Huiping Li, Jian Gao, and Demin Xu. Robust self-triggered min–max model predictive control for discrete-time nonlinear systems. *Automatica*, 89:333–339, 2018.

[84] Changxin Liu, Huiping Li, and Yang Shi. A unitary distributed subgradient method for multi-agent optimization with different coupling sources. *Automatica*, 114:108834, 2020.

[85] Changxin Liu, Huiping Li, Yang Shi, and Demin Xu. Distributed event-triggered model predictive control of coupled nonlinear systems. *SIAM Journal on Control and Optimization*, 58(2):714–734, 2020.

[86] Jinfeng Liu, Xianzhong Chen, David Muñoz de la Peña, and Panagiotis D Christofides. Iterative distributed model predictive control of nonlinear systems: Handling asynchronous, delayed measurements. *IEEE Transactions on Automatic Control*, 57(2):528–534, 2011.

[87] Jinfeng Liu, David Muñoz de la Peña, and Panagiotis D Christofides. Distributed model predictive control of nonlinear systems subject to asynchronous and delayed measurements. *Automatica*, 46(1):52–61, 2010.

[88] Jinfeng Liu, David Muñoz de la Peña, and Panagiotis D Christofides. Distributed model predictive control of nonlinear process systems. *AIChE Journal*, 55(5):1171–1184, 2009.

[89] Peng Liu, Arda Kurt, and Umit Ozguner. Distributed model predictive control for cooperative and flexible vehicle platooning. *IEEE Transactions on Control Systems Technology*, (99):1–14, 2018.

[90] Xiaotao Liu, Yang Shi, and Daniela Constantinescu. Distributed model predictive control of constrained weakly coupled nonlinear systems. *Systems & Control Letters*, 74:41–49, 2014.

[91] Zhixiang Liu, Youmin Zhang, Xiang Yu, and Chi Yuan. Unmanned surface vehicles: An overview of developments and challenges. *Annual Reviews in Control*, 41:71–93, 2016.

[92] Matthias Lorenzen, Fabrizio Dabbene, Roberto Tempo, and Frank Allgöwer. Constraint-tightening and stability in stochastic model predictive control. *IEEE Transactions on Automatic Control*, 62(7):3165–3177, 2016.

[93] JM Maestre, D Munoz De La Pena, EF Camacho, and T Alamo. Distributed model predictive control based on agent negotiation. *Journal of Process Control*, 21(5):685–697, 2011.

[94] Lalo Magni, Davide Martino Raimondo, and Riccardo Scattolini. Regional input-to-state stability for nonlinear model predictive control. *IEEE Transactions on Automatic Control*, 51(9):1548–1553, 2006.

[95] D Limon Marruedo, T Alamo, and EF Camacho. Input-to-state stable MPC for constrained discrete-time nonlinear systems with bounded additive uncertainties. In *Proceedings of the 41st IEEE Conference on Decision and Control (CDC)*, volume 4, pages 4619–4624. IEEE, 2002.

[96] Silvia Mastellone, Dušan M Stipanović, Christopher R Graunke, Koji A Intlekofer, and Mark W Spong. Formation control and collision avoidance for multi-agent non-holonomic systems: Theory and experiments. *The International Journal of Robotics Research*, 27(1):107–126, 2008.

[97] David Q Mayne. Model predictive control: Recent developments and future promise. *Automatica*, 50(12):2967–2986, 2014.

[98] David Q Mayne, Erric C Kerrigan, EJ Van Wyk, and P Falugi. Tube-based robust nonlinear model predictive control. *International Journal of Robust and Nonlinear Control*, 21(11):1341–1353, 2011.

[99] David Q Mayne, Maria M Seron, and SV Raković. Robust model predictive control of constrained linear systems with bounded disturbances. *Automatica*, 41(2):219–224, 2005.

[100] Xiaoxiao Mi, Yuanyuan Zou, Shaoyuan Li, and Hamid Reza Karimi. Self-triggered DMPC design for cooperative multi-agent systems. *IEEE Transactions on Industrial Electronics*, 67(1):512–520, 2020.

[101] Pablo Rodolfo Baldivieso Monasterios and Paul Anthony Trodden. Model predictive control of linear systems with preview information: Feasibility, stability and inherent robustness. *IEEE Transactions on Automatic Control*, 2018.

[102] Matthias A Müller, Marcus Reble, and Frank Allgöwer. Cooperative control of dynamically decoupled systems via distributed model predictive control. *International Journal of Robust and Nonlinear Control*, 22(12):1376–1397, 2012.

[103] Angelia Nedic, Asuman Ozdaglar, and Pablo A Parrilo. Constrained consensus and optimization in multi-agent networks. *IEEE Transactions on Automatic Control*, 55(4):922–938, 2010.

[104] Rudy R Negenborn and Jose Maria Maestre. Distributed model predictive control: An overview and roadmap of future research opportunities. *IEEE Control Systems Magazine*, 34(4):87–97, 2014.

[105] Dinh Hoa Nguyen. A sub-optimal consensus design for multi-agent systems based on hierarchical LQR. *Automatica*, 55:88–94, 2015.

[106] Alexandros Nikou and Dimos Dimarogonas. Decentralized tube-based model predictive control of uncertain nonlinear multiagent systems. *International Journal of Robust and Nonlinear Control*, 29(10):2799–2818, 2019.

[107] So-Ryeok Oh and Jing Sun. Path following of underactuated marine surface vessels using line-of-sight based model predictive control. *Ocean Engineering*, 37(2-3):289–295, 2010.

[108] Reza Olfati-Saber, J Alex Fax, and Richard M Murray. Consensus and cooperation in networked multi-agent systems. *Proceedings of the IEEE*, 95(1):215–233, 2007.

[109] Reza Olfati-Saber and Richard M Murray. Consensus problems in networks of agents with switching topology and time-delays. *IEEE Transactions on Automatic Control*, 49(9):1520–1533, 2004.

[110] Chong-Jin Ong and Bonan Hou. Consensus of heterogeneous multi-agent system with input constraints. *Automatica*, 134:109895, 2021.

[111] Dimitra Panagou, Dušan M Stipanović, and Petros G Voulgaris. Distributed coordination control for multi-robot networks using Lyapunov-like barrier functions. *IEEE Transactions on Automatic Control*, 61(3):617–632, 2016.

[112] Alexey Pavlov, Håvard Nordahl, and Morten Breivik. MPC-based optimal path following for underactuated vessels. *IFAC Proceedings Volumes*, 42(18):340–345, 2009.

[113] Zhouhua Peng and Jun Wang. Output-feedback path-following control of autonomous underwater vehicles based on an extended state observer and projection neural networks. *IEEE Transactions on Systems, Man, and Cybernetics: Systems*, 48(4):535–544, 2018.

[114] Tristan Perez, Ching-Yaw Tzeng, and Graham C Goodwin. Model predictive rudder roll stabilization control for ships. *IFAC Proceedings Volumes*, 33(21):45–50, 2000.

[115] Bruno Picasso, Delia Desiderio, and Riccardo Scattolini. Robust stability analysis of nonlinear discrete-time systems with application to MPC. *IEEE Transactions on Automatic Control*, 57(1):185–191, 2011.

[116] Davide Martino Raimondo, Daniel Limon, Mircea Lazar, Lalo Magni, and Eduardo Ferná ndez Camacho. Min-max model predictive control of nonlinear systems: A unifying overview on stability. *European Journal of Control*, 15(1):5–21, 2009.

[117] Saša V Raković, Basil Kouvaritakis, Rolf Findeisen, and Mark Cannon. Homothetic tube model predictive control. *Automatica*, 48(8):1631–1638, 2012.

[118] Saša V Raković, William S Levine, and Behçet Açıkmeşe. Elastic tube model predictive control. In *Proceedings of the 2016 American Control Conference (ACC)*, pages 3594–3599, July 2016.

[119] James Blake Rawlings and David Q Mayne. *Model predictive control: Theory and Design*. Nob Hill Pub., 2009.

[120] Wei Ren. Consensus algorithms for double-integrator dynamics. *IEEE Transactions on Automatic Control*, 53(6):1503–1509, 2008.

[121] Wei Ren and Randal W Beard. Consensus seeking in multiagent systems under dynamically changing interaction topologies. *IEEE Transactions on Automatic Control*, 50(5):655–661, 2005.

[122] Arthur Richards and Jonathan How. Robust stable model predictive control with constraint tightening. In *Proceedings of the 2006 American Control Conference (ACC)*, pages 1557–1562, June 2006.

[123] Arthur Richards and Jonathan P How. Robust distributed model predictive control. *International Journal of Control*, 80(9):1517–1531, 2007.

[124] Stefano Riverso, Marcello Farina, and Giancarlo Ferrari-Trecate. Plug-and-play decentralized model predictive control for linear systems. *IEEE Transactions on Automatic Control*, 58(10):2608–2614, 2013.

[125] Riccardo Scattolini. Architectures for distributed and hierarchical model predictive control– A review. *Journal of Process Control*, 19(5):723–731, 2009.

[126] Pierre OM Scokaert, James B Rawlings, and Edward S Meadows. Discrete-time stability with perturbations: Application to model predictive control. *Automatica*, 33(3):463–470, 1997.

[127] Chao Shen, Brad Buckham, and Yang Shi. Modified C/GMRES algorithm for fast nonlinear model predictive tracking control of AUVs. *IEEE Transactions on Control Systems Technology*, 25(5):1896–1904, 2016.

[128] Chao Shen and Yang Shi. Distributed implementation of nonlinear model predictive control for AUV trajectory tracking. *Automatica*, 115:108863, 2020.

[129] Chao Shen, Yang Shi, and Brad Buckham. Integrated path planning and tracking control of an auv: A unified receding horizon optimization approach. *IEEE/ASME Transactions on Mechatronics*, 22(3):1163–1173, 2017.

[130] Chao Shen, Yang Shi, and Brad Buckham. Lyapunov-based model predictive control for dynamic positioning of autonomous underwater vehicles. In *Proceedings of the 2017 International Conference on Unmanned Systems (ICUS)*, pages 588–593. IEEE, 2017.

[131] Chao Shen, Yang Shi, and Brad Buckham. Path-following control of an AUV: A multiobjective model predictive control approach. *IEEE Transactions on Control Systems Technology*, 27(3):1334–1342, 2018.

[132] Chao Shen, Yang Shi, and Brad Buckham. Trajectory tracking control of an autonomous underwater vehicle using Lyapunov-based model predictive control. *IEEE Transactions on Industrial Electronics*, 65(7):5796–5805, 2018.

[133] Yang Shi, Chao Shen, Huazhen Fang, and Huiping Li. Advanced control in marine mechatronic systems: A survey. *IEEE/ASME Transactions on Mechatronics*, 22(3):1121–1131, 2017.

[134] Yang Shi and Kunwu Zhang. Advanced model predictive control framework for autonomous intelligent mechatronic systems: A tutorial overview and perspectives. *Annual Reviews in Control*, 52:170–196, 2021.

[135] David H Shim, H Jin Kim, and Shankar Sastry. Decentralized nonlinear model predictive control of multiple flying robots. In *Proceedings of the 42nd IEEE Conference on Decision and Control (CDC)*, pages 3621–3626. IEEE, 2003.

[136] Roger Skjetne, Thor I Fossen, and Petar V Kokotović. Adaptive maneuvering, with experiments, for a model ship in a marine control laboratory. *Automatica*, 41(2):289–298, 2005.

[137] Eduardo D Sontag and Yuan Wang. New characterizations of input-to-state stability. *IEEE Transactions on Automatic Control*, 41(9):1283–1294, 1996.

[138] Asgeir J Sørensen. A survey of dynamic positioning control systems. *Annual reviews in control*, 35(1):123–136, 2011.

[139] Brett T Stewart, Aswin N Venkat, James B Rawlings, Stephen J Wright, and Gabriele Pannocchia. Cooperative distributed model predictive control. *Systems & Control Letters*, 59(8):460–469, 2010.

[140] Yanxu Su, Yang Shi, and Changyin Sun. Distributed model predictive control for tracking consensus of linear multiagent systems with additive disturbances and time-varying communication delays. *IEEE Transactions on Cybernetics*, 51(7):3813–3823, 2021.

[141] Qi Sun, Kunwu Zhang, and Yang Shi. Resilient model predictive control of cyber–physical systems under DoS attacks. *IEEE Transactions on Industrial Informatics*, 16(7):4920–4927, 2019.

[142] Yuan Gong Sun and Long Wang. Consensus of multi-agent systems in directed networks with nonuniform time-varying delays. *IEEE Transactions on Automatic Control*, 54(7):1607–1613, 2009.

[143] Zhongqi Sun, Li Dai, Kun Liu, Yuanqing Xia, and Karl Henrik Johansson. Robust MPC for tracking constrained unicycle robots with additive disturbances. *Automatica*, 90:172–184, 2018.

[144] Kuan Tak Tan, XY Peng, Ping Lam So, Yun Chung Chu, and Michael ZQ Chen. Centralized control for parallel operation of distributed generation inverters in microgrids. *IEEE Transactions on Smart Grid*, 3(4):1977–1987, 2012.

[145] Paul Trodden. Feasible parallel-update distributed MPC for uncertain linear systems sharing convex constraints. *Systems & Control Letters*, 74:98–107, 2014.

[146] Paul Trodden and Arthur Richards. Distributed model predictive control of linear systems with persistent disturbances. *International Journal of Control*, 83(8):1653–1663, 2010.

[147] Paul Trodden and Arthur Richards. Cooperative distributed MPC of linear systems with coupled constraints. *Automatica*, 49(2):479–487, 2013.

[148] Aleksander Veksler, Tor Arne Johansen, Francesco Borrelli, and Bjørnar Realfsen. Dynamic positioning with model predictive control. *IEEE Transactions on Control Systems Technology*, 24(4):1340–1353, 2016.

[149] Christophe Viel, Ulysse Vautier, Jian Wan, and Luc Jaulin. Platooning control for heterogeneous sailboats based on constant time headway. *IEEE Transactions on Intelligent Transportation Systems*, 21(5):2078–2089, 2020.

[150] Mario E Villanueva, Rien Quirynen, Moritz Diehl, Benoît Chachuat, and Boris Houska. Robust MPC via min–max differential inequalities. *Automatica*, 77:311–321, 2017.

[151] Anja Wahl and Ernst-Dieter Gilles. Track-keeping on waterways using model predictive control. *IFAC Proceedings Volumes*, 31(30):149–154, 1998.

[152] Chen Wang and Chong-Jin Ong. Distributed model predictive control of dynamically decoupled systems with coupled cost. *Automatica*, 46(12):2053–2058, 2010.

[153] Peng Wang and Baocang Ding. Distributed RHC for tracking and formation of nonholonomic multi-vehicle systems. *IEEE Transactions on Automatic Control*, 59(6):1439–1453, 2014.

[154] Qishao Wang, Zhisheng Duan, Yuezu Lv, Qingyun Wang, and Guanrong Chen. Distributed model predictive control for linear-quadratic performance and consensus state optimization of multiagent systems. *IEEE Transactions on Cybernetics*, 51(6):2905–2915, 2021.

[155] Qishao Wang, Zhisheng Duan, Yuezu Lv, Qingyun Wang, and Guanrong Chen. Linear quadratic optimal consensus of discrete-time multi-agent systems with optimal steady state: A distributed model predictive control approach. *Automatica*, 127:109505, 2021.

[156] Wanqing Wang, Huiping Li, Weisheng Yan, and Yang Shi. Self-triggered distributed model predictive control of nonholonomic systems. In *Proceedings of the 11th Asian Control Conference (ASCC)*, pages 280–285. IEEE, 2017.

[157] Zheming Wang and Chong-Jin Ong. Distributed MPC of constrained linear systems with time-varying terminal sets. *Systems & Control Letters*, 88:14–23, 2016.

[158] Zheming Wang and Chong Jin Ong. Distributed model predictive control of linear discrete-time systems with local and global constraints. *Automatica*, 81:184–195, 2017.

[159] Zheming Wang and Chong-Jin Ong. Accelerated distributed MPC of linear discrete-time systems with coupled constraints. *IEEE Transactions on Automatic Control*, 63(11):3838–3849, 2018.

[160] Henglai Wei, Chao Shen, and Yang Shi. Distributed Lyapunov-based model predictive formation tracking control for autonomous underwater vehicles subject to disturbances. *IEEE Transactions on Systems, Man, and Cybernetics: Systems*, 51(8):5198–5208, 2021.

[161] Henglai Wei, Qi Sun, Jicheng Chen, and Yang Shi. Robust distributed model predictive platooning control for heterogeneous autonomous surface vehicles. *Control Engineering Practice*, 107:104655, 2021.

[162] Henglai Wei, Kunwu Zhang, and Yang Shi. Distributed min-max MPC for dynamically coupled nonlinear systems: A self-triggered approach. *IFAC-PapersOnLine*, 53(2):6037–6042, 2020.

[163] Henglai Wei, Kunwu Zhang, and Yang Shi. Self-triggered min-max DMPC for asynchronous multi-agent systems with communication delays. *IEEE Transactions on Industrial Informatics*, 2021.

[164] Yujia Wu, Shengbo Eben Li, Jorge Cortés, and Kameshwar Poolla. Distributed sliding mode control for nonlinear heterogeneous platoon systems with positive definite topologies. *IEEE Transactions on Control Systems Technology*, 28(4):1272–1283, 2020.

[165] Feng Xiao and Long Wang. Asynchronous consensus in continuous-time multi-agent systems with switching topology and time-varying delays. *IEEE Transactions on Automatic Control*, 53(8):1804–1816, 2008.

[166] Yijing Xie and Zongli Lin. Global optimal consensus for higher-order multi-agent systems with bounded controls. *Automatica*, 99:301–307, 2019.

[167] Zheng Yan and Jun Wang. Model predictive control for tracking of underactuated vessels based on recurrent neural networks. *IEEE Journal of Oceanic Engineering*, 37(4):717–726, 2012.

[168] Erfu Yang and Dongbing Gu. Nonlinear formation-keeping and mooring control of multiple autonomous underwater vehicles. *IEEE/ASME Transactions on Mechatronics*, 12(2):164–178, 2007.

[169] Tao Yang, Ziyang Meng, Dimos Dimarogonas, and Karl Henrik Johansson. Global consensus for discrete-time multi-agent systems with input saturation constraints. *Automatica*, 50(2):499–506, 2014.

[170] Tao Yang, Xinlei Yi, Junfeng Wu, Ye Yuan, Di Wu, Ziyang Meng, Yiguang Hong, Hong Wang, Zongli Lin, and Karl Henrik Johansson. A survey of distributed optimization. *Annual Reviews in Control*, 47:278–305, 2019.

[171] Keyou You and Lihua Xie. Network topology and communication data rate for consensusability of discrete-time multi-agent systems. *IEEE Transactions on Automatic Control*, 56(10):2262–2275, 2011.

[172] Shuyou Yu, Christoph Maier, Hong Chen, and Frank Allgöwer. Tube MPC scheme based on robust control invariant set with application to Lipschitz nonlinear systems. *Systems & Control Letters*, 62(2):194–200, 2013.

[173] Shuyou Yu, Marcus Reble, Hong Chen, and Frank Allgöwer. Inherent robustness properties of quasi-infinite horizon nonlinear model predictive control. *Automatica*, 50(9):2269–2280, 2014.

[174] Jingyuan Zhan, Zhong-Ping Jiang, Yebin Wang, and Xiang Li. Distributed model predictive consensus with self-triggered mechanism in general linear multiagent systems. *IEEE Transactions on Industrial Informatics*, 15(7):3987–3997, 2019.

[175] Jingyuan Zhan and Xiang Li. Consensus of sampled-data multi-agent networking systems via model predictive control. *Automatica*, 49(8):2502–2507, 2013.

[176] Jun Zhang, Tairen Sun, and Zhilin Liu. Robust model predictive control for path-following of underactuated surface vessels with roll constraints. *Ocean Engineering*, 143:125–132, 2017.

[177] Ridong Zhang, Sheng Wu, Zhixing Cao, Jingyi Lu, and Furong Gao. A systematic min–max optimization design of constrained model predictive tracking control for industrial processes against uncertainty. *IEEE Transactions on Control Systems Technology*, 26(6):2157–2164, 2017.

[178] Yongding Zhang, Xiaofeng Liu, Minzhou Luo, and Chenguang Yang. MPC-based 3-D trajectory tracking for an autonomous underwater vehicle with constraints in complex ocean environments. *Ocean Engineering*, 189:106309, 2019.

[179] Zhiyun Zhao and Zongli Lin. Global leader-following consensus of a group of general linear systems using bounded controls. *Automatica*, 68:294–304, 2016.

[180] Huarong Zheng, Rudy R Negenborn, and Gabriël Lodewijks. Fast ADMM for distributed model predictive control of cooperative waterborne AGVs. *IEEE Transactions on Control Systems Technology*, 25(4):1406–1413, 2016.

[181] Huarong Zheng, Jun Wu, Weimin Wu, and Yifeng Zhang. Robust dynamic positioning of autonomous surface vessels with tube-based model predictive control. *Ocean Engineering*, 199:106820, 2020.

[182] Yang Zheng, Shengbo Eben Li, Keqiang Li, Francesco Borrelli, and J Karl Hedrick. Distributed model predictive control for heterogeneous vehicle platoons under unidirectional topologies. *IEEE Transactions on Control Systems Technology*, 25(3):899–910, 2017.

[183] Yuanyuan Zou, Xu Su, Shaoyuan Li, Yugang Niu, and Dewei Li. Event-triggered distributed predictive control for asynchronous coordination of multi-agent systems. *Automatica*, 99:92–98, 2019.